Hepatobiliary Transport of Arsenic

by

Barbara Anne Roggenbeck

A thesis submitted in partial fulfillment of the requirements for the degree of

Doctor of Philosophy

Department of Physiology
University of Alberta

Abstract

Arsenic is a proven human carcinogen and associated with a myriad of other adverse health effects. This metalloid is methylated in human liver to monomethylarsonic acid (MMA^V), monomethylarsonous acid (MMA^{III}), dimethylarsinic acid (DMA^V), and dimethylarsinous acid (DMA^{III}) and eliminated predominantly in urine. Hepatic basolateral transport of As species is ultimately critical for urinary elimination; however, these pathways are not fully elucidated in humans. Based on rodent studies it appears that the ATP binding-cassette (ABC) transporters in subfamily, multidrug resistance proteins (MRPs/ABCCs), are likely to play a role in efflux of As out of the hepatocyte. The current studies use several techniques to identify MRPs that may be important for hepatobiliary transport of As. Sandwich cultured human hepatocytes (SCHH) were used as a physiological model to characterize hepatic efflux of As. Cytotoxicity assays were used to screen the basolateral MRP candidate proteins MRP3 (ABCC3) and MRP5 (ABCC5) for their ability to transport As^{III}, As^V, MMA^{III}, MMA^V, DMA^{III}, and DMA^V. The data obtained from the SCHH studies, the cytotoxicity studies, and studies done with MRP4 (ABCC4) by other members of the lab led us to use RNA silencing to further investigate the role of MRP4 in the basolateral efflux of As. The SCHH model showed that basolateral transport of As was temperature- and GSH-dependent and inhibited by the MRP inhibitor MK-571. Canalicular efflux was completely lost after GSH depletion suggesting MRP2 (ABCC2)-dependence. Treatment of SCHH with As^{III} (0.1-1 μM) dose-dependently increased MRP2 and MRP4 levels, but not MRP1 (ABCC1), MRP6 (ABCC6), or aquaglyceroporin 9. Treatment of SCHH with oltipraz (Nrf2 activator) increased MRP4 levels and basolateral efflux of As. In contrast, oltipraz increased MRP2 levels without increasing biliary excretion. These results suggest As basolateral transport

prevails over biliary excretion and is mediated at least in part by an MRP. Candidate MRP proteins at the basolateral surface of the hepatocytes include MRP3, MRP4, MRP5, and MRP6. HEK293 cells overexpressing MRP3 or MRP5 did not confer resistance to As^{III}, As^{V}, MMA^{III}, MMA^{V}, DMA^{III}, or DMA^{V} in cytotoxicity assays and provided evidence that MRP3 and MRP5 do not provide cellular protection against arsenicals. The role of MRP6 is under investigation. MRP4/*ABCC4* is a high affinity transporter of DMA^{V} and the diglutathione conjugate of MMA^{III} ($MMA(GS)_2$), therefore, its role in As efflux was further investigated using RNA silencing in SCHH. Knockdown of MRP4 using shRNA containing lentiviral particles did not decrease the levels of any arsenicals in the efflux media of two SCHH preparations under the conditions tested. Non-specific effects of the lentivirus made interpretation of the RNA silencing experiments difficult however, we conclude that other transport proteins localized to the basolateral membrane of hepatocytes should be considered for their contribution to the efflux of As into blood for eventual urinary elimination.

Preface

Chapter 3: Characterization of arsenic using sandwich cultured human hepatocytes

This thesis chapter was published as: *Roggenbeck, B.A., Carew, M.W., Charrois, G.J., Douglas, D.N., Kneteman, N.M., Lu, X., Le, X.C., and Leslie*, *E.M.*, Characterization of arsenic hepatobiliary transport using sandwich cultured human hepatocytes, Toxicol Sci. 2015 Jun;145(2):307-20. doi: 10.1093/toxsci/kfv051. Epub 2015 Mar 9. Barbara A. Roggenbeck completed all experiments with SCHH preparations 5-26. Elaine M. Leslie and Gregory J. Charrois completed experiments with SCHH preparations 1-4. Michael W. Carew assisted with hepatocyte isolations and experiments for SCHH preparations 5-19. Norman M. Kneteman and Donna N. Douglas provided hepatocytes for preparations 21-26. X. Chris Le and Xiufen Lu completed the arsenic speciation analysis on SCHH efflux samples in Fig. 3.9.

Chapter 4: MRP3 and MRP5 do not protect HEK293 cells from inorganic, monomethylated, or dimethlyated species

Barbara A. Roggenbeck completed all experiments except Fig. 4.5, 4.6, and Table 4.3, which were completed by Michael W. Carew and Mayukh Banerjee. Table 4.1, 4.2, 4.3 and data from Fig. 4.5 and 4.6 of this chapter were published in *Banerjee, M., Carew, M.W., Roggenbeck, B.A., Whitlock, B.D., Naranmandura, H., Le, X.C., and Leslie, E.M.*, A Novel

Pathway for Arsenic Elimination: Human Multidrug Resistance Protein 4 (MRP4/ABCC4) Mediates Cellular Export of Dimethylarsinic Acid (DMA^{V}) and the Diglutathione Conjugate of Monomethylarsonous acid (MMA^{III}), Molecular Pharmacol. 2014 Aug; 86(2):168-79. doi: 10.1124/mol.113.091314. Epub 2014 May 28. Anaida Osoria Perez assisted with the confocal imaging. Diane P. Swanlund assisted with the MRP5 stable cell line cloning and performed the FACS analysis on the MRP5 stable cell line.

Chapter 5: Knockdown of MRP4 in SCHH using shRNA

Barbara A. Roggenbeck completed all experiments in this chapter. Hepatocytes were provided by Norman M. Kneteman and Donna N. Douglas. X.Chris Le and Xiufen Lu assisted with the speciation analysis on the SCHH efflux media.

Dedication

For my dad.

Acknowledgements

I would like to thank my supervisor Dr. Elaine Leslie for giving me the opportunity to do research in her lab, teaching me everything she knows, keeping her door open, and being not only an outstanding supervisor, but a genuinely compassionate and caring mentor.

I would also like to thank the members of my supervisory committee and candidacy examination: Drs. James Young, Xing-Fang Li, Emmanuelle Cordat, and Chris Cheeseman. I appreciate all of your time, support, suggestions, and insightful discussions. Also, many thanks to the external examiners on my defense committee, Drs. Qingcheng Mao and Arno Siraki for their time.

I thank Dr. Mike Carew for being a great friend and my sanity through many long days in the lab. Second, thanks to Dr. Caley Shukalek for smiling every day and baking me gluten free pies. Also many thanks to Dr. Sohail Qazi, Vanessa Marensi, Gurnit Kaur, Dr. Mayukh Banerjee, Detective Brayden Whitlock, and Diane Swanlund for all the scientific discussions, support, laughs, and coffee breaks. Last but not least, I must thank my dear friend and colleague, Dr. Kate Witkowska, for being my friend, for the birthday parties, tea parties, and of course, the dance parties.

To my parents, Victoria Roggenbeck and the late David Roggenbeck; I would not be who I am or where I am today without you. To Jerry and Sheila Pogue, for your love, support, and countless last minute drives to Edmonton.

To my husband, Jason, your encouragement, positive attitude, and love inspires me daily to strive to be a better person. I could not ask for a more supportive partner in life.

To my son, David, for being my sunshine.

Table of Contents

List of Tables

List of Figures

List of Abbreviations

6-MP (6-mercaptopurine)

6-TG (6-thioguanine)

ABC (ATP-binding cassette)

AchR (Aryl hydrocarbon receptor)

ADP (Adenosine diphosphate)

AQP (Aquaglyceroporin)

As (Arsenic)

As^{III} (Arsenite)

As^{V} (Arsenate)

AS3MT (Arsenic (+3 oxidation state) methyltransferase)

$As(GS)_3$ (Arsenic triglutathione)

ATP (Adenosine triphosphate)

ARE (Antioxidant response element)

BCA (Bicinchoninic acid assay)

BCRP (Breast cancer resistance protein)

BHA (Butylated hydroxyanisole)

BSA (Bovine serum albumin)

BSO (Buthionine sulfoxamine)

CaCo (Human epithelial colorectal adenocarcinoma)

cAMP (Cyclic adenosine monophosphate)

CDFDA (5 (and 6)- carboxy 2',7'dichlorofluorescein-diacetate)

CFTR (Cystic fibrosis transmembrane regulator)

cGMP (Cyclic guanosine monophosphate)

CK (Creatine kinase)

CP (Creatine phosphatase)

DEM (Diethyl maleate)

DMA^{III} (Dimethylarsinous acid)

DMA^{V} (Dimethylarsinic acid)

DMA(GS) (Dimethyl arsenic glutathione)

DMSO (Dimethyl sulfoxide)

DNA (Deoxyribonucleic acid)

DNP (dinitrophenyl)

$E_2$17βG (Estradiol-17β-glucuronide)

EDTA (Ethylenediaminetetraacetic acid)

EGTA (Ethylene glycol tetraacetic acid)

FBS (Fetal bovine serum)

G418 (Geneticin)

GLUT (Glucose transporter)

$[GS_2AsSe]^-$ (Seleno- bis (*S*-glutathionyl) arsinium ion)

GSSG (Glutathione disulfide)

GSH (Glutathione)

GST (Glutathione S-transferase)

GSTO (Glutathione S-transferase omega)

H69AR (Human small cell lung cancer, acquired resistance)

HEK293 (Human embryonic kidney)

HepG2 (Hepatocellular carcinoma)

HNE (Hydroxynonenal)

IARC (International Agency for Research on Cancer)

ITS (Insulin, transferrin, selenium)

LDH (Lactate dehydrogenase)

LLC-PK1 (Porcine kidney)

LTC_4 (Leukotriene C_4)

LTD_4 (Leukotriene D_4)

MCF-10A (Human mammary epithelial)

MDCK (Madin-Darby canine kidney)

Mdm2 (Mouse double minute 2)

MDR (Multidrug resistance)

miRNA (micro RNA)

MMA^{III} (Monomethylarsonous acid)

MMA^{V} (Monomethylarsonic acid)

$MMA(GS)_2$ (Monomethyl arsenic diglutathione)

MOI (Multiplicity of infection)

MRP (Multidrug resistance protein)

MSD (Membrane spanning domain)

MTS (3-(4,5-dimethylthiazol-2yl)-5-(3-carboxymethoxyphenyl)-2-(4-sulfophenyl)-2H-tetrazolium, inner salt)

NADPH (Nicotinamide adenine dinucleotide)

Nox2 (NADPH oxidase)

NBD (Nucleotide binding domain)

NHERF (Na^+/H^+ exchanger regulatory co-factor)

Nrf2 (Nuclear factor erythroid 2- related factor 2)

OATP (Organic anion transporting polypeptide)

P-gp (P-glycoprotein)

P_i (Inorganic phosphate)

PMEA (9-(2-phophonylmethoxyethyl) adenine)

PNP (Purine nucleoside phosphorylase)

RNS (Reactive nitrogen species)

ROS (Reactive oxygen species)

SAM (S-adenosylmethionine)

SCHH (Sandwich cultured human hepatocytes)

SCRH (Sandwich cultured rat hepatocytes)

shRNA (Short hairpin RNA)

siRNA (Small interfering RNA)

SLC (Solute carrier)

SNP (Single nucleotide polymorphism)

VP-16 (Etoposide)

WHO (World Health Organization)

XRE (Xenobiotic responsive element)

Chapter 1

Introduction

1.1 Arsenic

1.1.1 Natural occurrence of arsenic

Arsenic (As) is the 54th most abundant trace element found naturally in the Earth's crust [1]. It can be found in rocks (igneous and sedimentary), soil, water, and air [2]. The main source of human exposure to unacceptable levels of As, defined as > 10 ppb by the World Health Organization (WHO), is oral ingestion through naturally contaminated drinking water [3]. In an effort to avoid microbial contaminated water, tube wells are dug. This process disturbs As containing geological formations and results in the release of high levels of As into water [4]. In the 1970s tube wells were dug in Bangladesh in order to find "clean" drinking water and alternatively found drinking water with high levels of As [4]. The levels of As found naturally in the environment can depend on many factors including local geology and its associated biochemical state, proximity to geothermal fluids, and other processes such as volcanic activity [2].

1.1.2 Anthropogenic sources of arsenic

Arsenic also enters the environment through anthropogenic sources and often at high levels. Such sources of As include pharmaceuticals, pesticides, and preservatives [3]. Occupational sources of As include but are not limited to mining, smelting, coal burning, and glass manufacturing which can result in As contamination of the soil, air, and water [3].

1.1.3 Worldwide arsenic exposure

The WHO estimated that more than 150 million people are exposed to levels of As exceeding 10 ppb [3,5]. Many regions of the world are of concern regarding As exposure such as Asia including China, India, Taiwan, and Vietnam; regions of South America including Brazil, Chile and Argentina; and all regions of North America including the United States of America, Canada, and Mexico [5-7]. There are so called As "hot spots" with Bangladesh being the most famous example. The contamination of groundwater in Bangladesh has been described as the "largest mass poisoning" in history with ground water levels higher than 50 ppb in 35% of the wells tested and over 8% with levels higher than 300 ppb [4].

1.2 Arsenic is a health hazard

1.2.1 Toxicity

Arsenic has no taste or smell rendering it impossible for detection and evasion [7]. The valency state of As will determine the level of toxicity as the pentavalent species, arsenate (As^{V}), monomethylarsonic acid (MMA^{V}), and dimethylarsinic acid (DMA^{V}), are roughly 1000-fold less toxic than the trivalent species, arsenite (As^{III}), monomethylarsonous acid (MMA^{III}), and dimethylarsinous acid (DMA^{III}) [8,9]. Methylation also plays a role in the level of toxicity as the mono- and dimethylated trivalent species are more toxic than the inorganic trivalent species [10]. The chemical reactivity of trivalent As species and mimicry of phosphate by As^{V} allow it to interfere with many biochemical reactions and this is the

basis for As toxicity, cancer, and all the other detrimental health effects associated with exposure [11].

Acute As toxicity presents itself as various gastrointestinal symptoms, shock, coma, and sometimes death. The lethal limit of ingestion for humans ranges from 1-3 mg/kg [12]. Chronic As toxicity has the ability to affect almost all organ systems with the first signs being trademark skin lesions [13]. One of the first well documented diseases associated with chronic As exposure was Blackfoot disease. This severe peripheral vasculature disease results in peripheral gangrene and was observed in specific populations in Taiwan [14]. Blackfoot disease was found to be associated with the dose and duration of exposure to As in well water [14]. To date, there are multiple diseases, both noncancerous and cancerous, affecting many organ systems in the human body that are associated with As exposure. Non-cancerous ones include diseases affecting the skin, vascular, respiratory, neurological, reproductive, and endocrine systems. The mechanisms by which As acts as a carcinogen will be discussed further in Sections 1.2.2 below.

1.2.2 Mechanisms of toxicity

As^{V} and As^{III} have somewhat different mechanisms of toxicity although the majority of As^{V} taken up by cells is rapidly reduced to As^{III} [15]. Phosphate mimicry is the means by which As^{V} causes toxicity. As^{V} competes with phosphate transport for cellular uptake, inhibits phosphorylation reactions, and uncouples ATP production [11,16]. As^{III} is highly reactive with proteins containing thiol groups (preferably dithiols) or vicinal thiol groups allowing it to inhibit many biochemical processes, thus, leading to toxicity [1,11,17]. The trivalent forms of As can also inhibit ATP production and alter the redox status of cells by

reacting with antioxidant proteins important for cellular redox balance such as GSH reductase and thioredoxin [18]. Arsenic metabolism has been shown to generate both reactive oxygen species (ROS) and reactive nitrogen species (RNS) in various cell lines [16]. One of the most vulnerable and well characterized targets of As induced ROS is the vascular system, specifically endothelial cells. Low doses of As can result in NADPH oxidase (Nox2) activation and ROS formation within endothelial cells and this mechanism is thought to be responsible for cardiovascular diseases [19]. The role of RNS does not seem to be as well understood due to the variability of results between studies [16,20]. RNS generation is thought to occur by As induced generation of $NO^{\bullet}$, which is reactive, and can interact with reduced thiol groups, metals, and molecular oxygen (O_2), thus, has the ability to interfere with many biochemical processes [20]. Lastly, $NO^{\bullet}$ can react with superoxide ($O_2^{\bullet-}$) to form the toxic and reactive peroxynitrite anion [20,21]. Studies report increased, decreased, or no change in $NO^{\bullet}$ production after As exposure so the general consensus seems to be that the effects of As on RNS generation are cell-type and dose-dependent [16,20,22].

Generally, As exposure and subsequent generation of various ROS leads to oxidative stress and the promotion of DNA, lipid (including cell membrane), and protein damage [21]. Furthermore, the As induced ROS generation activates signaling pathways that result in various diseases and lead to carcinogenesis [23]. Arsenic as a carcinogen and modifier of cell signaling will be described in more detail below (Section 1.2.3).

1.2.3 Mechanisms of carcinogenesis

Arsenic exposure can lead to carcinogenic effects through both genotoxic and epigenetic mechanisms [24]. Genotoxicity from As exposure has presented itself as

micronuclei formation, DNA strand breaks, sister chromatid exchanges, and aneuploidy [25]. A recent review of all *in vitro*, *in vivo*, and As genotoxicity epidemiological studies has been published by Bustaffa *et al*. [24]. The mechanism by which As causes genotoxicity is not completely clear, but current data suggests that possible mechanisms include As-induced generation of ROS which can then damage DNA repair enzymes [24]. It has also been shown that As can directly interfere with DNA repair mechanisms by competing for the phosphate in ATP and covalently bonding with DNA repair enzymes such as DNA polymerase [13,26].

Epigenetic modifications include As-induced alteration of DNA methylation, histone tail modifications, and microRNAs (miRNAs) [27]. The most studied epigenetic modification is DNA methylation and will be discussed further. Arsenic metabolism in hepatocytes involves methylation to form other metabolites, hence, consumption of S-adenosylmethionine (SAM), the methyl donor. [24]. SAM is a necessary cofactor for DNA methlytransferases and the lack thereof, due to As methylation, provides a means of altered DNA methylation patterns [28]. The altered methylation patterns in turn result in aberrant gene expression and potential up-regulation of oncogenes and/or down-regulation of tumor suppressor genes [24,28].

The ability of As to generate ROS and bind sulfhydryl groups also allows As to alter signal transduction pathways which again result in aberrant gene expression and pathways that induce inflammation [13,29]. For example, studies show that As can interfere with activity of the tumor suppressor protein p53. Studies in human mammary epithelial cells (MCF-10A) treated for 12 h with 10 μM As^{III} resulted in induction of mouse double minute

2 (Mdm2), also known as Hdm2 [30]. The increase in Hdm2 resulted in nuclear export of p53 and accumulation in the cytoplasm where p53 loses its ability to function [30] [29].

1.2.4 The epidemiological evidence for arsenic-induced cancer

The IARC classifies As as a Group I (proven) human carcinogen that causes cancers of the lung, bladder, and skin and is also associated with liver and kidney tumors [3]. Some of the evidence related to As exposure and incidence of lung, bladder, and skin cancer will be further discussed.

There is substantial data that supports both contaminated drinking water and occupational inhalation of As as the two most common causes of As-induced carcinogenesis [3,31,32]. Ecological, cohort, and case-control studies have confirmed the causal relationship between As and lung cancer [32]. A study of Montana smelter workers provides data linking occupational As exposure and lung cancer. It is one of the largest cohort studies done examining the dose response between As and lung cancer [33]. The data from this cohort, collected between 1938 and 1977, has been analyzed by different groups, all in agreement that a definite relationship exists between As exposure and lung cancer, with differences in the mathematical modeling of the relationship [31,34]. The most recent analysis of the data from Anaconda, Montana by Lubin *et al*., accounted for exposure "delivery" and the relative risk of lung cancer, concluding that inhalation of higher As concentrations over a shorter duration was more harmful than inhalation of lower As concentrations over a longer period of time [34]. Generally, cohort and case-control studies, consistently show an increased lung cancer risk via inhalation through occupational exposure in the As exposed participants compared to unexposed controls [3].

Ecological, case-study, and cohort studies in areas with high endemic concentrations of As in water have led to the conclusion that oral ingestion of As causes an increased risk of lung cancer [32]. Studies in Taiwan, including regions from the Blackfoot Disease area, were some of the first to provide evidence that contaminated drinking water causes lung cancer although studies in other parts of Asia including Japan and Bangladesh, as well as other regions of the world such as Belgium, Argentina, and Chile have also contributed to this conclusion [3,32]. Guo *et al*., performed an ecological study in Taiwan (using available data from the government) on As levels in water from 138 villages (including 70 from the Blackfoot Disease area) and death certificates from the corresponding villages between 1971 and 1990 [35]. The analysis by this group showed an age-adjusted and statistically significant increase of lung cancer mortality rates associated in those exposed to higher As levels (above 640 ppb in both males and females). This association was not observed in those exposed to lower levels of As [35]. Many other studies evaluating the risk of lung cancer and its association with high levels of As have been summarized by Celik *et al.* [32]. The summary provided a clear understanding of the increased risk of lung cancer at high concentrations of As in water and points out the lack of studies examining the risks at lower concentrations [32]. Lamm *et al*., recently used previously published data from 42 villages in the Blackfoot Disease area to examine the risk associated with exposure to As at concentrations below 100 ppb and found that significantly increased risks do not exist at this low level of exposure [36].

Studies have shown that the cancer risks associated with As ingestion can last long after the cessation of As exposure [37,38]. Steinmaus *et al*., conducted a case-control study in a city in Northern Chile, on a population that was once exposed to high levels of As in

drinking water (12 years) followed by exposure to much lower levels of As after the installment of a water treatment plant [38]. This study concluded that there was a 4–fold increased risk of lung cancer and 7-fold increased risk of bladder cancer even up to 40 years after cessation of arsenic exposure [38].

Many of the same regions and studies described above also evaluated the relative risk for other cancers related to As exposure. A dose-response relationship between As levels in well water and bladder cancer mortality rates was first described in Taiwan [39]. In a recent review Saint-Jacques *et al*., performed a meta-analysis of data published over the past 30 years on As and its association with bladder cancer [40]. The group findings confirmed a causal relationship between As exposure in drinking water and incidence of bladder cancer and mortality from bladder cancer. The authors found an increased risk for developing bladder cancer with increasing arsenic exposure levels [40]. Exposure to 10 ppb arsenic increased risk by more than two-fold for bladder cancer development and exposure to 50 ppb and 150 ppb increased risk by four- and six-fold, respectively [40].

The evidence for skin cancer incidence and exposure to high levels of As is strong and again, much evidence comes from ecological and cohort studies in the Blackfoot Disease area in Taiwan as well as studies in regions of Chile [3]. The studies summarized by the IARC describe skin cancer risk due to high levels of As in drinking water. For example Tseng *et al*., published data collected in Taiwan (Blackfoot Disease area) showing a very obvious trend in skin cancer incidence and increasing levels of As with an 8-fold difference between the lowest (< 300 ppb) and highest (> 600 ppb) levels of exposure [41]. Karagas *et al.,* addressed a trending question in As related cancer risk and exposure level which is whether or not skin cancer risk is associated with lower levels of As [42]. Their review of

the literature and analysis of data from populations exposed to < 100 ppb of As suggested that there is a dose-dependent trend at lower levels of As exposure [42].

The risks for As related cancers is variable between populations and individuals. There is a substantial amount of evidence that suggests methylation capacity can alter how vulnerable an individual is to As toxicity and will be discussed in the next section. However, the mechanisms underlying human susceptibility to cancer are still not completely clear [24]. Animal models are only susceptible to As induced tumor formation at very high levels [43]. Therefore, understanding the mechanisms underlying As induced carcinogenesis and means of cancer prevention is very challenging due to the lack of a rodent model.

1.3 Animal models for studying arsenic

There are remarkable differences in the pharmacokinetics of As between human and rodent species, however, the rodent models have been able to provide some information about As carcinogenesis in select studies [43,44].

1.3.1 Methylation differences between species

The species specific variation in the ratio of inorganic to methylated species in urine (methylation efficiency) is a good indicator that As metabolism is unique between organisms. Methylation differs between human and rodents and furthermore, between rodent species and other mammals [45]. Humans excrete more MMA compared to other mammals while mice and dogs methylate as efficiently as rats but with pharmacokinetic differences [45].

Interestingly marmoset monkeys, chimpanzees, and guinea pigs do not methylate As at all [45,46].

1.3.2 Pharmacokinetic differences between species

One well characterized difference between species is that the urinary excretion of As in rats is very low compared to other animals despite the fact that they efficiently methylate As [46]. Csanaky *et al.* anesthetized, bile duct cannulated, and injected rats, mice, hamsters, rabbits, and guinea pigs with As^{III} (50 μmol/kg) and found biliary excretion of As into bile at 75%, 50,%, 50%, 40%, and 92% of the initial As^{III} dose, respectively, thus, with the exception of rabbit, As was excreted predominantly into bile [47]. There are also species differences in the elimination rates of As. Studies of mice and rats administered ^{74}As-DMA^{V} orally showed that rat is slower at eliminating [48]. The slow elimination in the rat is due to the retention of DMA in rat erythrocytes [48]. Lu *et al.* treated rats with As^{V}, MMA^{V}, or DMA^{V} for several weeks and showed that over 99% was bound to hemoglobin as DMA^{III}, which is an explanation for the red blood cell retention of As in rats [49]. Further studies identified the DMA binding site in rats as a cysteine residue in the alpha chain of hemoglobin that is not present in humans which explains why this retention is observed only in rats [50]. In fact, mice and dogs are able to methylate as efficiently as rats, as mentioned above, however they rapidly excrete DMA into urine and although the monkey and chimpanzee do not methylate at all; they excrete As into urine at a similar rate as humans [45,46,51]. The bottom line is that all animal models have limitations, however, these studies demonstrate that rats are definitely not an ideal physiological animal model for studying As toxicity in

humans. Although there are mammalian species with comparable urinary excretion rates to humans, there does not seem to be one with a similar methylation efficiency as humans.

1.3.3 Carcinogenesis in animal models

In general, administering rodents inorganic As does not result in carcinogenesis and production of tumors must be forced with extremely high levels of As and co-administration of another carcinogen [52].

The CH3 mouse transplacental model provided evidence of inorganic As alone inducing cancer in an animal model [53]. The maternal mice were administered 42.5 or 85 ppm of As^{III} in drinking from day 8 of gestation through delivery [44]. Waalkes *et al.* observed induction of tumor formation in several tissues from As exposed offspring including liver and lung [44]. It should be noted that these doses are 100 to 200 times higher than doses known to cause cancer in humans [54].

Rodent models have been somewhat useful for studying the mechanism of As-induced bladder cancer [43]. In long-term bioassays it has been shown that extremely high levels of DMA^{V} administered *via* drinking water in rats resulted in an increased incidence of bladder tumors [52,55]. Cohen *et al*., went on to elucidate the mechanism of bladder tumor formation in a short-term study using similar DMA^{V} concentrations as Arnold *et al.* [55], and proposed that DMA^{III} formed from the DMA^{V} interferes with critical proteins in the epithelium of the urinary tract leading to cytotoxicity and cell regeneration with eventual uroepithelial tumor formation [43]. However, due to the unique ability of rats to sequester DMA^{III} in hemoglobin the data from these animals must be translated to human carcinogenesis with caution [50].

Recently Waalkes *et al.* published a study in mice that were exposed to doses of As more relevant to human exposure. The mice were exposed to 0, 50, 500, or 5000 ppb As^{III} *in utero* and after birth until they were killed at 104 weeks and tumor incidence was assessed [56]. The results were quite controversial in that mice exposed to the lower levels of As (50 and 500 ppb) showed 50% increases in bronchiol-alveolar tumors compared to controls (28% incidence of tumors) [56]. The mice exposed to 5000 ppb As did not show increased tumor incidence compared to controls [56]. The authors attribute this to the possibility that higher levels of As are both carcinogenic and therapeutic therefore decreasing tumor incidence. This study is contradictory to previously published studies (as described above) and was addressed by another expert in the field who stated that the "whole-life" studies were not valid. Cohen *et al*., pointed out that previously published studies by the same group showed tumor formation at levels much higher than 5000 ppb making the argument that the dose may have been paradoxically therapeutic invalid [57,58]. Furthermore, Cohen *et al.* points out that the therapeutic dose of As used for treatment of acute promyelocytic leukemia is much higher than the highest dose Waalkes *et al.* claimed could be therapeutic [57,58]. Lastly, Cohen *et al.* pointed out that the CD-1 mice used for the experiments are problematic because they are known for their ability to produce variable numbers of background lung tumors [58]. The whole-life studies by Waalkes *et al.* await to be reproduced by an independent laboratory. The previously described study is just one example of the obstacles faced when translating animal studies to human disease.

1.4 Sandwich cultured human hepatocytes are a physiological model for studying hepatobiliary transport pathways

It is clear that there are large differences in As metabolism, pharmacokinetics, and susceptibility to cancer between humans and other species. This makes it important to develop physiologically relevant human models for studying As transport pathways.

Several models have been used in this thesis to investigate the hepatobiliary transport of As and identify specific human transport proteins important in the hepatic basolateral efflux of As. The models used include heterologous expression systems to perform cytotoxicity assays and plasma membrane vesicles transport assays, as well as sandwich cultured human hepatocytes.

Isolated hepatocytes in suspension are useful for studying initial rates of xenobiotic uptake. One limitation of using hepatocytes in suspension is that after isolation the cells lose polarity. Cell polarity refers to the two distinct regions of the plasma membrane, the basolateral and apical (also referred to as canalicular in hepatocytes) membranes, each of which has its own unique physiological function [59]. Canalicular membrane transport proteins are internalized during the isolation process [60]. Bow *et al.* used rat hepatocytes to confirm that P-glycoprotein (P-gp) and Mrp2, which are both localized to the canalicular membrane of hepatocytes, were located in junctions between cells and intracellular compartments immediately after isolation [60]. Primary human hepatocytes can be cultured

on a single layer of collagen yet these cells do not become fully polarized [61]. A more physiological model for studying hepatobiliary transport are primary hepatocytes grown in sandwich configuration (between two layers of collagen). This model of hepatobiliary transport is useful for studying the polarity of drug transport in the liver. Cells cultured between two layers of collagen are superior to those cultured on a single layer of collagen because over time they maintain cell polarity and develop intact and functional canalicular networks [62]. They are also able to maintain metabolic capabilities such as CYP450 expression and induction [63]. Furthermore membrane transport proteins traffic to the appropriate membranes and allow for monitoring polarized transport of drugs across either the apical (canalicular) or basolateral (sinusoidal) membranes [64]. The canalicular networks are calcium sensitive which allows manipulation of culture conditions in order to measure what percentage of xenobiotics are transported into bile (across the apical surface) or blood (across the basolateral surface) [65]. The amount of substrate being effluxed into bile can be calculated as the biliary excretion index (BEI) based on the equation below [adapted for efflux from [66]].

$$BEI = \frac{Efflux_{sinusoidal + canalicular} - Efflux_{sinusoidal}}{Efflux_{sinusoidal + canalicular}} \times 100\%$$

There is a high correlation between the *in vivo* hepatobiliary clearance of xenobiotics in humans and rats and the corresponding *in vitro* biliary clearance in sandwich cultured hepatocytes (SCH), making this physiological model ideal for studying human hepatobiliary transport of As [67,68]. The studies contained in Chapters 3 and 5 of this thesis use sandwich cultured human hepatocytes (SCHH), a physiological model of hepatobiliary transport, to study the cellular handling of As by the liver.

1.5 Interindividual susceptibility to arsenic exposure

Human susceptibility to As likely depends on both non-genetic and genetic factors. Non-genetic factors that influence As susceptibility include gender, age, nutrition, and the level of As exposure. Genetic factors potentially include polymorphisms of genes that influence cellular uptake, metabolism, antioxidant defense, and retention, ultimately influencing elimination of As, and thus its overall body burden [69]. The most well supported polymorphisms associated with a higher risk of As toxicity and cancer will be discussed.

The majority of studies have examined the roles of arsenic (+3 oxidation-state) methyltransferase (AS3MT), glutathione *S*-transferase omega (GSTO), and purine nucleoside phosphorylase (PNP) and their associations with differences in urinary As methylation profiles between As exposed individuals. Arsenic is excreted in human urine as 10-30% inorganic (As^{III} + As^{V}), 10-20% as monomethylated (MMA^{III} + MMA^{V}), and 60-80% as dimethylated (DMA^{III} + DMA^{V}) As [70]. Many studies support altered methylation profiles in human urine, evidence for variable methylation capacity, as one mechanism for differences in susceptibility to As toxicity [51]. AS3MT, previously referred to as cyt19, is a major player in As metabolism; it is an enzyme that catalyzes the methylation of As [71]. Various models have been proposed to explain the methylation mechanism of inorganic As and will be discussed further in Section 1.6.2.2 [72-74] .

A recent study by Antonelli *et al*., screened 360 publications from PubMed and Web of Science in search of data on gene polymorphisms encoding proteins that potentially play a role in As metabolism and influence urinary levels of methylated As; and concluded that there were three AS3MT polymorphisms that showed statistically significant associations with changes in urinary MMA levels: M287T; rs11191439 (exon 9), T35587C; rs11191453 (intron 10), and C14215T; rs3740390 (intron 8) [75]. The Antonelli *et al.* analysis also concluded from GSTO and PNP studies that there was no association with any GSTO polymorphism and variable levels of methylated species of As in urine; and there was insufficient data from PNP studies to make any conclusions [75]. Because there are many studies, including the previously described study above, that support AS3MT polymorphisms and their role in inter-individual As susceptibility, AS3MT is the only gene that will be discussed further regarding variable human susceptibility to As.

Numerous studies have shown an association between the adverse health effects of As exposure and increased urinary levels of MMA in epidemiological, animal model studies, and cell culture studies and have been summarized by Antonelli *et al.* [75]. More importantly, increased urinary levels of MMA have been associated with the most problematic adverse health effects caused by As including skin lesions and cancers of the skin, lung, and bladder [76]. As mentioned above, the recent review by Antonelli *et al*., found three polymorphisms that demonstrated statistically significant associations with changes in percent urinary MMA [75]. Interestingly, the rs11191439 polymorphism results in a methionine to threonine missense mutation, and is the only polymorphism of the three, that is also associated with disease susceptibility and an increase in percent urinary MMA [75]. This is consistent with earlier reviews and analyses based on all available AS3MT data,

that conclude that the Met287Thr is also one of the polymorphic variants most likely involved in variable human As methylation capacity [69,77]. Studies in Central Europe and Northern Chile examining polymorphisms of AS3MT have shown that Met297Thr-AS3MT has been associated with an increase in MMA excretion hence, a reduced formation of DMA suggesting a reduced methylation efficiency [69,78]. The polymorphism responsible for Met287Thr-AS3MT has recently been examined in 207 copper mine workers exposed to As showing an increase in micronuclei found in peripheral blood lymphocytes [79]. *In vitro* studies are consistent with the epidemiological studies in providing evidence that the polymorphism resulting in the Met287Thr substitution is a genetic factor influencing methylation capacity. In cultures of primary human hepatocytes Drobna *et al*., observed variation in methylation rates between individual hepatocyte preparations and concluded that it was not just the level of AS3MT mRNA that accounted for these differences, but also identified the Met287Thr polymorphic variant as a possible candidate in the inter-individual variability in As methylation between hepatocyte cultures [80]. Although Met287Thr is strongly associated with inter-individual differences in As methylation and associated diseases, other *AS3MT* polymorphisms have been identified in various populations since AS3MT has become a major focus for investigating inter-individual susceptibility to As exposure.

An interesting paper recently reported genotypes of women from an Argentinian Andean population, who have been exposed to high levels of As in their drinking water for thousands of years [81]. It was discovered that within the Andean population the *AS3MT* gene region is substantially different from that of a Peruvian population that has over time been exposed to much less As [81]. The Argentinian population also showed a remarkable

increase in their ability to efficiently metabolize As [81]. Authors of this study conclude that *AS3MT* is definitely involved in the population differences in As metabolism [81]. In addition, they suggest that the differences between the *AS3MT* genotypes between populations, in different regions exposed to different levels of As, is evidence of human adaptation to As exposure [81].

Genes located in the 10q24.32 region other than *AS3MT* may be involved in inter-individual variation in As susceptibility. Using data on five lead SNPs identified in a genome -wide association study Pierce *et al.* identified 2 novel SNPs (rs9527 and rs11191527) in this region [76]. The function of the genes that harbor the rs9527 and rs11191527 variants are not known [76], however, this implies that there are genes other than *AS3MT* potentially involved in inter-individual differences in skin lesion risk and methylation capacity.

In addition to methylation pathways understanding the transport pathways and their involvement in the disposition of As in the human body will allow a better understanding of inter-individual susceptibility to As. The role of transport proteins in this variable susceptibility to As is in its infancy, but, increasing evidence suggests they play an important role in As detoxification and elimination [82-85]. Some of these potentially important pathways involved in As uptake and efflux will be discussed in further detail below.

1.6 Absorption, distribution, metabolism and elimination of arsenic

1.6.1 Intestinal absorption of arsenic

Oral ingestion of As in humans occurs predominantly in the forms of As^{III} and As^{V} via drinking water. Very few studies have been done to identify transport proteins important for the intestinal absorption of As. Arsenic potentially crosses the apical surface of the enterocyte through aquaglyceroporins (AQPs), sodium phosphate cotransporters, glucose transporters (GLUTs) and/or organic anion transporting polypeptides (OATPs). One study using a colorectal adenocarcinoma cell line (Caco-2) showed that gene knockdown of OATP2B1 (*SLCO2B1)*, AQP10, or GLUT5 (*SLC2A5*), resulted in a decreased As^{III} accumulation while silencing of the Na/P_i cotransporter type IIb (*SLC34A2*) resulted in a decreased As^{V} accumulation suggesting a potential role for these transporters in intestinal As absorption [86].

Aquaglyceroporins are bidirectional channels that allow the passage of neutral substances including water, glycerol, and urea across cell membranes down their concentration gradients [87]. Studies have demonstrated direct transport of As by overexpression of AQP cDNA in *Xenopus laevis* oocytes. Both human AQP7 and 9 can conduct As^{III} across cell membranes [88]. It is noteworthy that AQP7 can transport MMA^{III} at a five-fold higher rate than As^{III} which could be important for uptake by cell types other than enterocytes, due to the fact that inorganic As species are the predominant forms in

drinking water [89]. AQP9 also has the ability to conduct MMA^{III} and unlike AQP7 can also conduct MMA^{V} and DMA^{V}, although not efficiently at physiological pH [89]. Neither AQP7 nor AQP9 transport As^{V} [89]. When expressed in *Xenopus laevis* oocytes AQP3 and AQP10 conduct very little or no As, respectively [88,90]. Gene knockdown of AQP10 in Caco-2 cells resulted in a decrease in As^{III} uptake suggesting a potential role in As uptake across enterocytes [86]. The reason for this difference is unknown.

Several studies investigating As uptake in invertebrate models have also been conducted. Zebrafish aquaporins aqp3, aqp3I, aqp9a, aqp9b, and aqp10, named for their similarity to human homologues, all demonstrated As^{III} and MMA^{III} uptake when expressed in *X. laevis* oocytes [91]. Three homologous variants of hAQP3 have also been identified in killifish (*Fundulus teroclitus*) intestine. Two of these variants, kfAQPb and kfAQPc, have been shown to transport As^{III} in kfAQPb- and kfAQPc-overexpressing HEK293T cells compared to vector control [92].

Studies on both invertebrate and mammalian aquaglyceroporins suggest that AQPs play a role in As transport. Thus, according to the Catalayud *et al.* studies AQP10 may play a role in the uptake of As across the apical surface of enterocytes, however, direct transport of As by AQP10 in different cell types should first be demonstrated [86]. Once As is inside the enterocyte, AQP3, which is localized to the basolateral membrane of enterocytes, could play a role in basolateral efflux of As into blood. Following As efflux across the basolateral membrane of enterocytes into the portal circulation, As is carried in the blood to the liver sinusoid. In the sinusoid, As is likely taken up by AQP9 into hepatocytes for metabolism

followed by biliary excretion or efflux back into blood for eventual urinary elimination. Uptake and efflux mechanisms in hepatocytes will be discussed further in Section 1.6.2.

The facilitative glucose transporters (GLUTs/SLC2A) are one of the two main membrane transporter families involved in glucose homeostasis in mammals [93]. The previously described study by Calatyud *et al.,* suggests that the facilitative glucose transporter GLUT5, could possibly be involved in As uptake at the apical surface of the enterocyte, however, there is very limited data on the role GLUTs might play in As transport [86]. Both human and rat GLUT1 overexpressed in *Xenopus laevis* conducted both As^{III} and MMA^{III}, demonstrating higher MMA^{III} uptake compared to As^{III} [94]. Furthermore, studies in primary human hepatocytes found a positive correlation between GLUT2 protein expression and intracellular concentrations of As [61]. GLUT2 is present constitutively at the basolateral surface of small intestine enterocytes, but, can be recruited additionally to the apical surface in response to high lumen glucose levels [93]. Thus, GLUT2 could be both a candidate protein involved in uptake of As at the apical surface of the intestine or (more likely) movement of As across the basolateral surface of the intestine for entry into the portal circulation. Direct transport studies need to be conducted to determine if As is a substrate for GLUT2 and/or GLUT5. Northern blotting of the most recently discovered facilitative glucose transporter, GLUT7, showed high expression in the small intestine and colon as well as protein expression in brush border membranes prepared from the jejunum and ileum of Sprague Dawley rats [95]. The role of GLUT7 in As absorption across the intestine may be worth investigating. Although GLUT1 is not expressed in the gut it is likely to be involved in As uptake in erythrocytes, endothelial cells, and brain; it suggests that GLUTs may play an important role in cellular As uptake and potentially toxicity in various tissues [96]. Further

experiments are needed to confirm a definite role and identify the specific isoforms that transport As in appropriate physiological models.

Organic anion transporting polypeptides (OATP/ *SLCO*) are membrane solute carriers that transport a wide variety of substrates in a sodium- and ATP-independent manner [97]. Because OATPs generally transport large, amphipathic, organic anions it is likely that they are not involved in the uptake of As from the intestinal lumen unless in the form of As-GSH conjugates. A study in HEK293 cells overexpressing human OATP1B1 showed a GSH-dependent increase in the accumulation of iAs (As^{III} +As^{V}) compared to vector expressing HEK293 cells [98]. These transporters are more likely to be involved in extrusion of As-GSH conjugates from enterocytes after metabolism inside the cell rather than uptake of the inorganic forms detected in drinking water. Arsenic-GSH conjugates are not found in drinking water because they are extremely unstable in the absence of high concentrations of GSH. If OATPs are involved in the efflux of As-GSH conjugates they would be more likely to play a role in tissues where As metabolism occurs such as the liver.

The AQPs are the best characterized of the As^{III} uptake transporters, however, it has been shown that they do not transport As^{V} which is a major component of contaminated drinking water. The shared physicochemical properties between phosphate and As^{V} oxyanions led to studies of the role of phosphate transporters in As^{V} uptake. There are three type II sodium phosphate cotransporter proteins (Na^+/P_i-IIa-c/ *SLC34A1-3*) that control phosphate homeostasis in various tissues by secondary active cotransport of divalent P_i into cells using the inwardly directed Na^+ gradient generated by the Na^+/K^+-ATPase [99]. Studies examining the kinetic parameters of P_i and As^{V} transport by rat Na^+/P_i cotransporters led to the conclusion that under the average P_i concentration of 5 μM in the intestine from drinking

water, with an average exposure to As contaminated drinking water resulting in 0.3-1.5 μM As^V in the intestine, that only Na/P_i cotransporter type IIb (*SLC34A2*) was capable of transporting As^V under average physiological conditions [100]. Using brush border membrane vesicles prepared from rat tissue Villa-Bellosta and Sorribas determined that apparent K_m for P_i uptake is 0.1 mM and the K_i for As^V is only 3-times higher at 0.34 mM [100]. Depending on the P_i and As^V concentration present in the intestine different levels of As^V could theoretically be transported into the enterocyte. Even if the P_i concentration consumed is high, as soon as the initial P_i has been transported across the intestine, As^V transport would occur [100]. The same group went on to characterize the kinetic parameters of human Na^+/P_i cotransporter type IIb and were able to draw similar conclusions. The apparent K_m of human Na^+/P_i cotransporter type IIb for As^V was calculated to be 10 μM compared to the K_m of human Na/P_i cotransporter type IIb for P_i which was calculated as 29 μM [101]. The 3-fold higher affinity for As^V would thus allow for it to transport As^V under physiological concentration of P_i in the intestine after ingesting As contaminated water [101]. It is however, unlikely that Na/P_i cotransporter type IIb would be responsible for any As^V uptake in other tissues because under homeostatic conditions the extracellular concentrations of P_i are approximately 1 mM and As^V would likely exist in the nM range [100,101].

The only functional studies of As transport in the intestine have been done using CaCo-2 cells [86]. While CaCo-2 cells are considered to be a good model for studying the physiology of the human intestine, a study has shown that there are differences in mRNA levels for membrane transport proteins between CaCo-2 cells and the primary human enterocyte [102]. Noteworthy, Englund *et al.* found a 5-fold higher level of MRP2 and OATP2B1 mRNA transcripts in the CaCo-2 cells compared to the enterocyte [102].

Furthermore, variable mRNA transcript levels in CaCo-2 cells has been documented between labs [103] [102]. Studies examining the differences between membrane protein levels in CaCo-2 cells compared to the human intestine would be very useful information because mRNA levels do not reliably predict transport protein levels. The role of individual membrane transporters expressed at the apical and basolateral surfaces of the small intestine should be evaluated in other *in vitro* systems including a small intestine cell line to better understand how As is absorbed across the intestine.

1.6.2 Hepatobiliary transport and methylation of arsenic

1.6.2.1 Uptake pathways across the basolateral surface of the hepatocyte

Once As is absorbed across the basolateral surface of the intestine it enters the portal circulation and is carried to the liver sinusoids. Arsenic must then traverse the basolateral surface of the hepatocyte. Potential transmembrane pathways for this process include AQP9 and GLUT2 which are localized to the basolateral membrane of hepatocytes. Mouse hepatocytes with AQP9 knocked-down by 50 % using targeted siRNA followed by treatment with 25μM As^{III}, showed an approximate 25% reduction in As^{III} accumulation compared to the siRNA control [104]. Other candidate proteins expressed at the basolateral surface of hepatocytes include AQP7 and GLUT9. AQP7 transport of various As species has been characterized as described above, however, AQP9 is a much more efficient transporter of As and AQP7 would likely be important if AQP9 transport was compromised. Currently there is no evidence for GLUT9 involvement in the transport of As. GLUT9 is a high affinity

transporter for glucose and fructose and interestingly it is the only GLUT known to transport urate (with high affinity) [105]. The basolateral localization of both GLUT2 and GLUT9 in hepatocytes warrants further investigation regarding their potential roles in As uptake.

Several OATPs may be considered as transporters involved in As uptake across the hepatocyte basolateral membrane in the form of free As or As-GSH conjugates. However, it is unlikely that As-GSH conjugates would remain stable in blood because they have extremely short chemical half-lives in the absence of GSH [106-108]. Regardless, the OATPs expressed at the basolateral surface of hepatocytes that could potentially allow As uptake into liver from the blood include, OATP1B1 (*SLCO1B1*), OATP2B1 (*SLCO2B1*), and OATP1B3 (*SLCO1B3*).

1.6.2.2 Hepatic methylation and glutathionylation of arsenic

Once taken up by the hepatocyte, As is extensively methylated and also forms As-glutathione conjugates [61,107,109]. Arsenic methylation is catalyzed by AS3MT using S-adenosyl-L-methionine (SAM) as the methyl donor and requires a reducing agent, which is likely glutathione [71,110]. There are three proposed models for inorganic As methylation. The first proposed or classical pathway describes the enzymatic reduction of pentavalent As species followed by oxidative methylation of the previously formed trivalent species. This pathway proposes that after intracellular As^{V} is reduced to As^{III}, it is then methylated to form MMA^{V}, MMA^{III}, DMA^{V}, and DMA^{III} [73] (Fig. 1.1). The second and third proposed models for As methylation describe As-GSH conjugates and As- protein complexes as substrates for AS3MT [72,74].

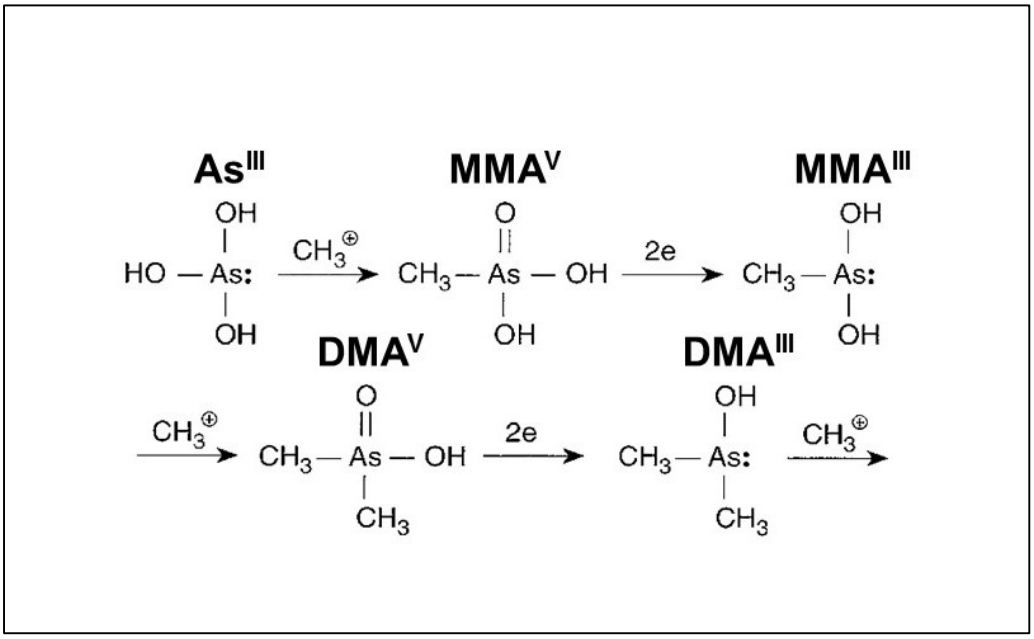

Adapted from: William R. Cullen; *Chem. Res. Toxicol.* **2014,** 27, 457-461. Copyright © 2014 American Chemical Society; http://pubs.acs.org/doi/pdf/10.1021/tx400441h. Modifications made to this figure include the addition of chemical abbreviations for structures and removal of trimethylated arsenic species from the image.

Fig. 1.1. The Challenger pathway.

In human cells intracellular As^{V} is reduced to As^{III} and then undergoes a series of oxidative methylation and reduction steps resulting in the formation of the predominant species MMA^{V}, MMA^{III}, DMA^{V}, and DMA^{III}.

The second model proposed by Hakyakawa *et al*., is based on the fact that in their *in vitro* studies, they observed more DMA^{V} production from reactions with As^{III} rather than from MMA^{V} in the presence of AS3MT [74]. This contradicts the original and classical Challenger pathway because their data suggests that MMA^{V} is not the intermediate species that results in DMA^{V} production [74]. However, the Cullen paper argues that the Hayakawa pathway is not chemically feasible because it requires the unfavorable release of a negatively charged methyl group (CH_3^-) from a positively charged SAM [111].

The third model proposed by Naranmandura *et al*., proposes that both oxidative methylation and reduction occur at the same time, rather than two separate reactions (as proposed in the Challenger pathway) [72]. In this model the As bound to protein can be released by conjugation with GSH or the As^{III} bound to protein is reductively methylated to produce a monomethylated As protein species [72]. The formation and release of DMA occurs by release from the methylated As protein species after nucleophilic attack on the monomethylated As bound to protein [72]. Again, this is not chemically plausible because there would be "reduced nucleophilicity of the lone pair of electrons" on the protein bound As and inhibit the entire reaction [111]. Regardless of the specific mechanism involved in the generation of various As species, several chemical species must be effluxed from inside the hepatocyte for elimination in either urine or bile.

Given that glutathione is the most abundant cellular low molecular weight thiol (0.5 - 10 mM) and the trivalent As species are highly reactive with thiols it is likely that a major proportion of As is effluxed from the hepatocyte as As-GSH conjugates [109].

1.6.2.3 Hepatic arsenic efflux pathways

There are a number of membrane transporter families that could play a role in the hepatic efflux of As. Understanding efflux pathways across the basolateral surface of the hepatocyte is critical for understanding how As ultimately undergoes urinary elimination, which accounts for 60-80% of As elimination. Efflux of As across the apical surface of the hepatocyte into bile will also be discussed as data generated using the sandwich cultured human hepatocyte model, described in this thesis (Chapter 3) suggests inter-individual variation in this pathway. Many of the transport proteins involved in hepatocyte As uptake

(AQP7, AQP9, GLUT2, GLUT5, and GLUT9) are also candidate proteins for involvement in hepatic basolateral As efflux because they are bidirectional transporters/channels. Under physiological conditions where the intracellular As concentration exceeds that outside the cell, these transporters could efflux certain species of As across the basolateral surface of hepatocytes into blood.

The multidrug resistance proteins (MRPs) are ATP-binding cassette transporters that are particularly important to examine as hepatobiliary As transporters. Prior to describing their role in As transport I will provide background on the ATP-binding cassette superfamily of which they are members.

1.7 ATP-binding cassette transporter subfamilies

The ATP binding cassette (ABC) transporter family is the largest family of membrane transporter proteins, and are expressed in both eukaryotic and prokaryotic cells [112]. In humans there are 49 genes and 48 functional protein members of the ATP binding cassette (ABC) transporter family that are further divided into 7 subfamilies (A-G) based on sequence homology and nucleotide binding domain (NBD) structure [113]. ABC transporters harness energy from ATP to efflux a variety of substrates, both endogenous and xenobiotic, across cellular membranes [114].

The typical structure of the mammalian ABC transport protein consists of two polytopic membrane spanning domains (MSDs) usually with 6 membrane spanning α-helices

[115]. The ATP- binding cassette consists of two nucleotide binding domains (NBDs) [115]. The NBDs have characteristic Walker A and Walker B motifs inherent in all ATP-binding proteins [116]. The ABC family of proteins also have a signature C- loop located upstream of the Walker B sequence [117]. In a mammalian ABC transporter the Walker A and Walker B motifs of one NBD interact with the signature C-motif of the second NBD to form an "ATP- sandwich" which is vital for ATPase activity [118,119]. The "half transporters" which have only have one MSD and NBD are an exception to the typical mammalian ABC protein structure, however they form homo or hetero dimers to become a functional full transporter unit [120].

1.8 ABC drug transporters

There are several ABC drug transporters known for their ability to confer multidrug resistance which include but are not limited to P-glycoprotein (P-gp/ABCB1), breast cancer resistance protein (BCRP/ABCG2), and the multidrug resistance proteins (MRPs/ABCCs) [121,122]. P-gp and BCRP are localized to the apical membranes of epithelial cells whereas the MRPs are localized to either the apical or basolateral membrane depending on the subfamily member [114,121,123]. All of these ABC transporters play a role in protecting cells from xenobiotic exposure however, the multidrug resistance proteins are the focus of this thesis and will be discussed in more detail below (Section 1.9).

1.9 ABCC transporters: multidrug resistance proteins

The MRPs are members of subfamily C of ABC transporter proteins. There are two forms of MRPs, "long" and "short". The 'long' forms are MRPs 1,-2,-3,-6, and -7 and they have an additional MSD composed of 5 membrane spanning α-helices at the NH_2-terminus and are thus configured as MSD0-MSD1-NBD1-MSD2-NBD2 (Fig. 1.2A). The "short" forms are MRP4, -5, -8, and -9 and are the more typical mammalian ABC protein configuration MSD1-NBD1-MSD2-NBD2 [113] (Fig. 1.2B). The extra MSD of MRP2 is necessary for apical membrane localization [124]. Interestingly, the extra MSD of MRP1 initially appeared to have no function. However, it appears that there are redundant trafficking signals within the protein [125]. The MSD0 of MRP1 becomes necessary for proper basolateral trafficking when the COOH terminus is mutated or missing and likewise for the COOH terminus [125,126]. The first multidrug resistance protein (MRP1) was discovered due to its ability to confer drug resistance in a human lung cancer cell line [127]. Since that discovery it has been well established that MRP1 and other members of the ABCC subfamily can efflux a diverse array of xenobiotic and physiological substrates from cells and will be discussed in more detail below (Section 1.9.1-1.9.7)

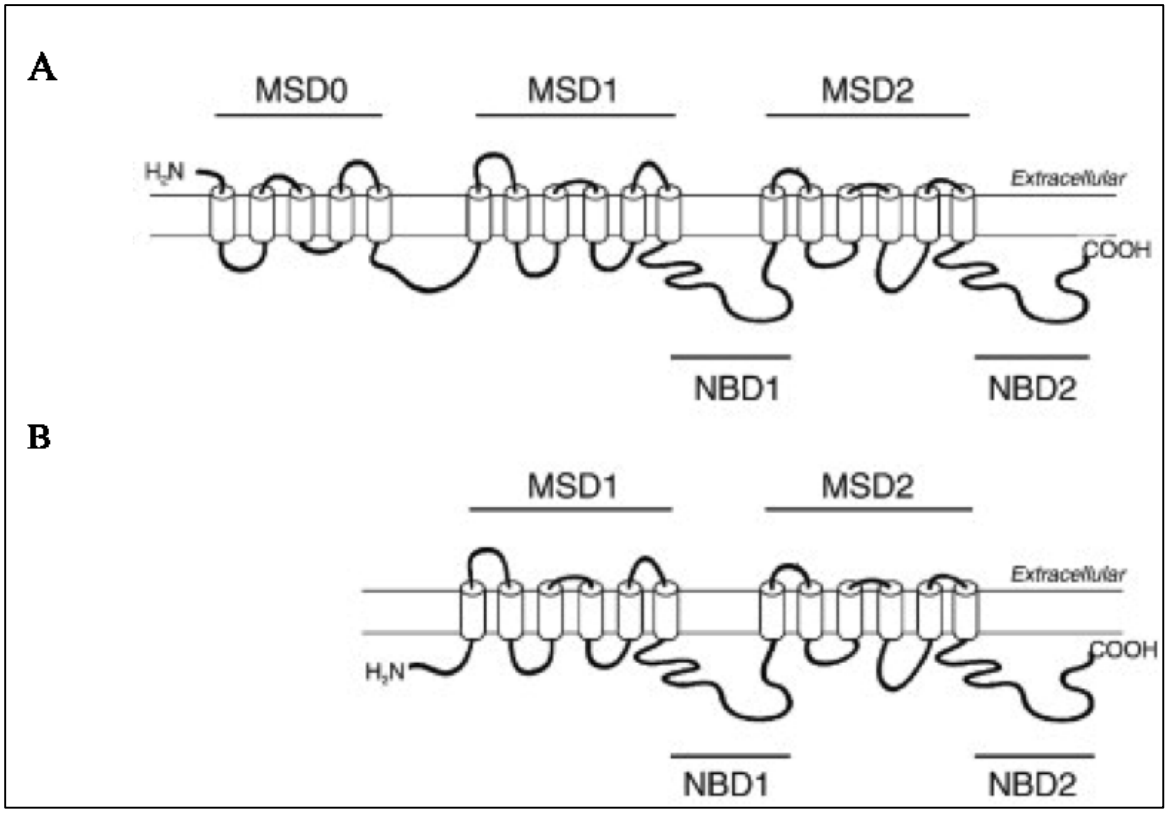

From: Elaine M. Leslie, Arsenic-glutathione conjugate transport by the human multidrug reistance proteins (MRPs/ABCCs) Journal of Inorganic Biochemistry, Volume 108, 2012, 141-49 http://dx.doi.org/10.1016/j.jinorgbio.2011.11.009. Modifications have not been made to this figure.

Fig. 1.2. The long and short forms of the MRPs.

Predicted secondary structure for the MRPs that (A) have the extra NH2-terminal membrane spanning domain (MSD0) (MRP1, MRP2, MRP3, MRP6, and MRP7) and (B) the smaller MRPs (MRP4, MRP5, MRP8, and MRP9) with the more typical ABC four domain structure.

1.9.1 MRP1

MRP1 is expressed in many physiological barriers such as the blood brain barrier, choroid plexus, placenta, and testis thus, providing support for its role in tissue protection [121]. It is expressed at moderate to high levels in the lung, testis (Leydig and Sertoli cells), kidney (distal tubules), skeletal and cardiac muscle, peripheral blood mononuclear (mast cells, helper T cells) and polymorphonuclear cells (eosinophils, erythrocytes), placenta, gut (Paneth cells), skin, brain (capillaries), and ocular tissues [114,127]. In polarized epithelium, MRP1 traffics to the basolateral membrane pumping its substrates towards the blood [114]. This is also the case in brain capillary endothelial cells where MRP1 is localized at the luminal surface [114]. MRP1 is not found at the protein level in healthy human hepatocytes, however, protein levels can be induced during liver regeneration and under cholestatic conditions [128,129].

MRP1 has a very diverse substrate specificity including many glutathione, glucuronide, and sulfate conjugated organic anions, a characteristic it shares with several other ABC subfamily C (MRP) members [130,131]. Xenobiotics transported include chemotherapeutic drugs, antiviral drugs, antibiotics, and various toxicants [130].

MRP1 also mediates transport of physiological substrates such as leukotrienes (LTC_4), prostaglandins, folic acid, vitamin B-12, bilirubin conjugates, and estrogen conjugates including the well characterized MRP1 substrate estradiol-17β-glucuronide ($E_2$17βG) [132].

1.9.2 MRP1 transport of glutathione and glutathione conjugates

In addition to the transport of GSH conjugates MRP1 transports free reduced and oxidized glutathione (GSH and GSSG, respectively) [133]. Glutathione plays an important role in the transport of many MRP substrates through several different mechanisms [133]. The presence of GSH without GSH conjugate formation is a requisite for efflux of some substrates. For example, GSH is required for the transport of the anti-cancer drug vincristine and it has been shown that vincristine stimulates GSH transport suggesting a "cotransport" pathway [134]. GSH also stimulates the transport of substrates, including GSH and glucuronide conjugates, without GSH transport occurring [133]. Lastly, there are substrates such as apigenin and verapamil that can stimulate GSH transport without being substrates themselves [135]. The role of GSH in the transport mechanisms described above also applies to other MRPs.

1.9.3 MRP2

MRP2 is expressed in the liver, kidney (proximal tubules), small intestine (villi in proximal jejunum), placenta, gallbladder, colon, lung, and brain (capillaries) [114,136,137]. MRP2 localizes only to the apical membrane in polarized epithelium [132]. The apical localization of rat Mrp2 is regulated by the scaffolding protein Na^+/H^+ exchanger regulatory factor 1 (NHERF-1) [138]. Despite the low (50%) amino acid sequence identity between MRP1 and MRP2 they have many common substrates [132]. Similar to MRP1, MRP2 transports conjugated organic anions including glucuronide and GSH conjugates. MRP2 also transports leukotrienes and glucuronide conjugates of estrogen, steroids, and bile salts [139].

However, MRP2 transports LTC_4 and $E_2$17βG with lower affinity than MRP1 but, transports bilirubin glucuronide conjugates with higher affinity than MRP1 [132]. Like MRP1, MRP2 also transports GSH and GSSG [140]. Although there is substantial overlap between MRP1 and MRP2 substrates, unlike MRP1, MRP2 has the unique ability to confer resistance to cisplatin [141]. The apical localization of MRP2 in the liver and kidney provide support for its role in detoxification by the elimination of compounds into bile and urine.

1.9.4 MRP3

MRP3 is the most closely related of the ABC subfamily C members to MRP1 from an evolutionary perspective with 58% amino acid homology [142]. The protein is found in the adrenal cortex, pancreas, gut (enterocytes in ileum and colon), gall bladder (cholangiocytes), and placenta [114,132,143]. Low levels of protein are found in the liver (levels can vary up to 80-fold), kidney and prostate [114,132,142]. The drug substrate profile of MRP3 is more restricted than that of MRP1 and MRP2. MRP3 confers resistance to drugs used in clinical settings poorly compared to MRP1 and MRP2 [142]. The other distinguishing feature of MRP3 is that it prefers transport of glucuronide conjugates such as $E_2$17βG and bile salt glucuronide conjugates over other conjugates, especially GSH conjugates [144]. Unlike MRP1 and MRP2, MRP3 does not transport GSH or GSSG at all [143]. MRP3 is upregulated under cholestatic conditions [137,145]. A well characterized example of this is the upregulation of MRP3 in patients with Dubin-Johnson syndrome who lack functional MRP2 [137,146]. This is a compensatory mechanism to protect the liver from bilirubin and bile salt accumulation and/or injury from other toxic compounds [137].

1.9.5 MRP4

MRP4 is expressed either apically or basolaterally in polarized epithelium depending on the tissue type [132]. It is expressed at the basolateral membrane in hepatocytes and in pancreatic duct, prostate, and choroid epithelium, but expressed apically in kidney proximal tubule cells [114,132]. The cellular trafficking of MRP4 is regulated by NHERF-1 [147]. HeLa cells transfected with NHERF-1 targeted siRNA displayed an increased expression of MRP4 at the plasma membrane and increased drug efflux [147]. The role of NHERF-1 in MRP4 trafficking was shown using two polarized cells lines: MDCK and LLC-PK1. LLC-PK1 cells express high levels of endogenous NHERF-1 and MRP4 traffics to the apical membrane in this cell line [148]. The MDCK cell line does not express endogenous NHERF-1 and MRP4 traffics to the basolateral membrane of this cell type unless NHERF-1 is ectopically expressed which results in apical localization [148]. Other cell types that express MRP4 include dendritic cells, astrocytes, platelets and red blood cells [114,132]. MRP4 is unique compared to MRP1, MRP2, and MRP3 in its ability to confer resistance to the anticancer nucleobase analogs 6-mercatopurine (6-MP) and 6-thioguanine (6-TG) [149]. MRP4 also transports many physiological substrates including cyclic adenosine monophosphate (cAMP), cyclic guanosine monophosphate (cGMP), bile salts, folic acid, leukotrienes, prostaglandins, urate, and adenosine diphosphate (ADP) [142,150].

1.9.6 MRP5

MRP5 is expressed basolaterally in brain (astrocytes, pyramidal neurons), fetal placenta, heart endothelial cells, smooth muscle cells, urethra, and is found at the luminal

surface of the blood-brain barrier capillaries [142]. MRP5 levels in human liver are low but increased during disease including primary biliary cirrhosis [151]. MRP5 is unique amongst the other MRPs in its ability to transport methotrexate-glutamate conjugates [152]. However, the ability of MRP5 to play a role in clinical drug resistance is questionable because studies have shown conflicting results regarding its ability to confer resistance to several chemotherapeutic drugs including doxorubicin, etoposide, and cisplatin [142]. Like MRP4, MRP5 also shares the ability to transport the cyclic nucelotides cAMP and cGMP [153].

1.9.7 MRP6

MRP6 expression is restricted compared to the other MRPs in that it is only found at the protein level in the basolateral membrane of hepatocytes and the kidney proximal tubule [154]. Some transport of GSH conjugates has been reported including N-ethylmaleamide-glutathione (NEM-GSH) and LTC_4 [155]. Studies have also shown that MRP6 confers low drug resistance to some anti-cancer drugs [156]. Mutations in the *ABCC6* gene result in the heritable connective tissue disorder pseudoxanthoma which affects the elasticity of the skin, eyes, and heart [157].

1.10 The role of MRPs in arsenic efflux

The high levels of GSH in liver and the established reactivity of arsenicals with thiols makes it likely that As is transported from the hepatocyte by MRPs as As-GSH conjugates. Indeed, MRP1, MRP2 and MRP4 have been established to transport As-GSH conjugates.

MRP2 is expressed at the canalicular surface of hepatocytes and transport of arsenic tri-glutathione [$As(GS)_3$] and the seleno- bis (*S*-glutathionyl) arsinium ion [$(GS)_2AsSe]^-$ have been characterized in MRP2-enriched plasma membrane vesicles [84]. *In vivo* studies have also shown a physiological role for rat Mrp2 in biliary excretion of arsenic. Thus, intravenous administration of As^{III} to Wistar rats deficient in Mrp2 (TR^- rats) resulted in less than 1% of As in bile compared to the wild -type Wistar rats [107]. Wildtype Wistar rats pretreated with buthionine sulfoxamine (BSO), an inhibitor of GSH synthesis, also resulted in less than 1% of As in bile compared to the GSH depleted wild-type control [107]. The same study also showed that 80-90% of As detected in the bile of Wistar rats after administration of either oral or intravenous As (5 mg/kg) was in the form of $As(GS)_3$ and $MMA(GS)_2$, however, when administered lower doses of As (0.5 mg/kg) only $MMA(GS)_2$ was detected [107]. This dose dependent difference in As metabolites in bile is likely due to saturation of As methylation pathways. These data showed that rat Mrp2 is responsible for the biliary excretion of GSH conjugates and that As-GSH conjugates account for 99% of As excreted in bile [107].

Although biliary transport of $As(GS)_3$ and $MMA(GS)_2$ by rat Mrp2 is excretion it does not necessarily represent elimination. The alkaline pH of bile causes these conjugates to fall apart, resulting in the opportunity for free As^{III} and MMA^{III} to continue its toxic insult to the body through enterohepatic circulation [158]. On the other hand, MRP2 transport of $[(GS)_2AsSe]^-$ is thought to play a more protective role because this conjugate is more stable at alkaline pH and could remain intact for fecal elimination [84,109,159,160]. Recently, MRP4 which is localized to the basolateral surface of hepatocytes has been shown to be a high affinity transporter of DMA^V ($K_{0.5}$, 0.22 μM) and $MMA(GS)_2$ ($K_{0.5,}$ 0.70 μM) [82].

The transport of DMA^V, the main urinary metabolite of As found in human urine, by MRP4 suggests this protein could play a pivotal role in the elimination of methylated As species. MRP6 is also expressed at the basolateral membrane of hepatocytes and its role in As transport is unknown.

MRP1 transport of both $As(GS)_3$ and $MMA(GS)_2$ has been characterized using MRP1-enriched plasma membrane vesicles [161,162]. Healthy human hepatocytes do not express MRP1, however, MRP1 is expressed at the basolateral surface of many tissue types with higher levels in the lungs, testes, and kidneys where it may play a role in extrahepatic transport of As into the systemic circulation and concomitant cellular and tissue protection against As [121]. This is likely an important means for prevention of tumor formation in As susceptible tissues such as the skin, lung, and bladder. Extrahepatic transport of As into the systemic circulation from the basolateral surface of gut epithelia is also potentially important because biliary excretion of As can result in enterohepatic recirculation of As.

The focus of my thesis project was hepatobiliary transport of As, and specifically the role that the MRPs play in As transport in hepatocytes, therefore, I will elaborate further on the MRPs. The candidate MRP proteins that could play a role in hepatic As efflux include MRP1, MRP2, MRP3, MRP4, MRP5, and MRP6. Although MRP1 and MRP5 are not expressed in healthy human hepatocytes I considered any MRP that could have been upregulated during As exposure and those with documented hepatocyte expression.

1.11 The role of Nrf2 in arsenic detoxification

The transcription factor nuclear factor erythroid 2- related factor 2 (Nrf2) and its regulation of antioxidant response elements (AREs) plays an important role in As detoxification. [29]. Studies have shown that As regulates Nrf2 through molecular interactions that result in decreased Nrf2 degradation [163]. Furthermore there are many examples in the literature of Nrf2 regulation of the MRPs which will be discussed in the next few paragraphs.

Using mouse embryo fibroblasts from wild type and Nrf2 (-/-) mice Hayashi *et al.* first demonstrated the role of Nrf2 in the regulation of both constitutive and inducible Mrp1 mRNA and protein [164]. Constitutive expression of Mrp1 mRNA was reduced by 38% in Nrf2 (-/-) mouse fibroblasts compared to the wild type fibroblasts [164]. The pro-oxidant diethyl maleate (DEM) induced Mrp1 expression 2-4 fold in the wild type but not the Nrf2 (-/-) fibroblasts [164]. Western blotting showed that constitutive Mrp1 protein was reduced by 32% in Nrf2 (-/-) fibroblasts and there was no induction of Mrp1 protein by DEM whereas the wild type showed a 1.6-fold induction [164]. Studies in H69AR cells (a human small cell lung cancer cell line) also confirmed a role for Nrf2 in MRP1 regulation. H69AR cells transfected with Nrf2 targeted siRNA showed a 50% decrease in Nrf2 protein expression with a similar decrease in MRP1 expression [165]. Cytotoxicity assays also showed that

siRNA treated cells were more sensitive to several chemotherapeutic compared to the control H69AR cells [165].

To investigate the role of Nrf2 on MRP2 regulation, Vollrath *et al*. treated mice with butylated hydroxyanisole (BHA), a classical activator of the Nrf2 pathway and examined the MRP2 mRNA and protein levels in the livers of treated mice. [166]. The studies showed that the BHA treated mouse livers had much higher levels of Mrp2 mRNA and a 3-fold increase in Mrp2 protein levels compared to the controls [166]. Studies in mice treated with acetaminophen, which has been shown to modulate expression of several MRPs, also provides evidence of Nrf2 regulation of Mrp2. Mrp2 mRNA and protein expression in the acetaminophen treated mouse brain was significantly increased in the control, but not the Nrf2 knockout mice [167].

MRP4 expression levels have been shown to be upregulated by Nrf2 during cellular oxidative stress. For example, As^{III} and MMA^{III} induce Nrf2 levels by reducing the cellular ubiquitination and degradation of Nrf2 [163]. This is accomplished through As mediated enhancement of the E3 ubiquitin ligase Keap1/Cul3 complex [163]. Xu, S. *et al*., identified Nrf2 and aryl hydrocarbon receptor (AhR) response elements ARE and XRE (xenobiotic response element) in the MRP4 sequence, respectively. These studies also showed increased levels of MRP4 protein in HepG2 cells after treatment with the Nrf2 activator, oltipraz [168]. Similar results were found by immunofluorescence staining in primary human hepatocytes [168].

1.12 Objectives and Rationale

Arsenic is metabolized extensively in the liver but the majority of As is excreted in urine. The transport pathways for efflux of As across the basolateral surface of hepatocytes into blood for urinary elimination are not well understood. Several animal models have been used to study As transport, however, rodents are not susceptible to the carcinogenic effects of As and have different pharmacokinetics, thus, the detoxification mechanisms and transport pathways are likely different.

The overall goal of this thesis was to characterize hepatobiliary transport of As. The main hypothesis was that one or more multidrug resistance protein(s) play a role in As transport across the hepatocyte basolateral membrane. To address this hypothesis the specific objectives were as follows:

Objective 1: Characterize arsenic transport using sandwich cultured human hepatocytes.

The study presented in Chapter 3 used SCHH to determine the extent of biliary and basolateral excretion of As. SCHH from fourteen different preparations were treated with As and experiments were designed in order to characterize apical and basolateral transport of As in hepatocytes with a focus on the role of the MRPs.

Objective 2: Determine if MRP3 or MRP5 provide cellular protection against As^{III}, As^{V}, MMA^{III}, MMA^{V}, DMA^{III}, or DMA^{V}.

The study which is presented in Chapter 4 extended our observations in the SCHH model that an MRP was likely responsible for at least a portion of the hepatic basolateral transport of As. In order to identify the MRP(s) responsible for this basolateral efflux, stable cell lines were generated for MRP3 and MRP5 and cytotoxicity testing was done. Candidate MRPs at the basolateral surface of the hepatocyte in addition to MRP3 and MRP5 include MRP4 and MRP6. The role of MRP4 in basolateral As was characterized in a separate study completed in parallel [82] and the role of MRP6 is currently under investigation.

Objective 3: Optimize conditions for knockdown of MRP4 using shRNA lentiviral particles and determine the contribution MRP4 makes to As efflux from sandwich cultured human hepatocytes.

Studies published in our lab revealed that MRP4 is a high affinity transporter of DMA^{V} and $MMA(GS)_2$, therefore, the role of MRP4 in As basolateral efflux in SCHH was investigated. MRP4-targeted shRNA containing lentiviral particles were used to optimize conditions for knock down and eventually decrease endogenous levels of MRP4 in SCHH. Speciation analysis of As in efflux media was performed in the SCHH incubated with MRP4 targeted shRNA and compared to controls in order to determine the contribution of MRP4 to As efflux from the hepatocyte.

Chapter 2

Materials and Methods

2.1 Materials

Table 2.1 Common Reagents

Name	Source
5 (and 6)- carboxy 2',7'dichlorofluoresecin-diacetate (CDFDA)	Sigma-Aldrich (Oakville, ON, Canada)
6-mercaptopurine (6-MP)	Sigma-Aldrich (Oakville, ON, Canada)
Adenosine monophosphate (AMP)	Sigma-Aldrich (Oakville, ON, Canada)
Adenosine triphosphate (ATP)	Sigma-Aldrich (Oakville, ON, Canada)
Arsenic oxide (As^{III})	Sigma-Aldrich (Oakville, ON, Canada)
Bicinchoninic acid assay (BCA) kit	Pierce Chemicals (Rockford, IL)
Bradford protein assay solution	Bio-Rad Laboratories, Inc. (Hercules, CA)
Buthionine sulfoximine (BSO)	Sigma-Aldrich (Oakville, ON, Canada)
Calcium chloride ($CaCl_2$)	Thermo Fisher Scientific (Waltham, MA)
Creatine kinase (CK)	Roche Applied Science (Torrance, CA)
Creatine phosphate (CP)	Roche Applied Science (Torrance, CA)
Deoxynucleotides (dNTPs)	Thermo Fisher Scientific (Waltham, MA)
Diiodomethylarsine (MMA^{III})	Gift from Dr. X.Chris Le
Dimethylarsinic acid (DMA^{V})	Sigma-Aldrich (Oakville, ON, Canada)
Iododimethylarsine (DMA^{III})	Gift from Dr. William Cullen
Dimethyl sulfoxide (DMSO)	Thermo Fisher Scientific (Waltham, MA)
DNA polymerase (Pfu turbo)	Agilent Technologies (Santa Clara, CA)
DNA ladder (GeneRuler 1kb Plus)	Thermo Fisher Scientific (Waltham, MA)
Ethylenediamine tetraacetic acid (EDTA)	EMD Chemicals (Gibbstown, NJ)
Etoposide (VP-16)	Sigma-Aldrich (Oakville, ON, Canada)
GenElute ™ Plasmid Mini (Midi/Maxi) Prep Kit	Sigma-Aldrich (Oakville, ON, Canada)
Glass fiber filters (type A/E)	Pall Life Sciences (East Hills, NY)
Glucose ($C_6H_{12}O_6$)	Thermo Fisher Scientific (Waltham, MA)
Glutathione (GSH)	Sigma-Aldrich (Oakville, ON, Canada)
GSH reductase	Roche Applied Science (Torrance, CA)
Hexadimethrine bromide (polybrene)	Sigma-Aldrich (Oakville, ON, Canada)
HIV p24 ELISA assay	ZeptoMetrix Corporation (Buffalo, NY)
Iododimethylarsine (DMA^{III})	Gift from Dr. William Cullen
Lactate dehydrogenase (LDH) Cytotoxicity Detection Kit	Roche, Applied Sciences (Indianapolis, IN)
Magnesium sulfate ($MgSO_4$)	Thermo Fisher Scientific (Waltham, MA)
Mini PROTEAN ® TGX ™ gels	Bio-Rad (Hercules, CA)
Methotrexate	Sigma-Aldrich (Oakville, ON, Canada)
MISSION ® shRNA plasmid DNA glycerol stocks	Sigma-Aldrich (Oakville, ON, Canada)

MISSION ® shRNA plasmid packaging mix	Sigma-Aldrich (Oakville, ON, Canada)
Diiodomethylarsine (MMA^{III})	Gift from Dr. X. Chris Le
Monomethylarsonic acid (MMA^{V})	Sigma-Aldrich (Oakville, ON, Canada)
Nicotinamide adenine dinucleotide phosphate (NADPH)	Roche Applied Science (Torrance, CA)
Nitric acid	Thermo Fisher Scientific (Waltham, MA)
Potassium phosphate monobasic (K_2HPO_4)	Sigma-Aldrich (Oakville, ON, Canada)
Protease inhibitor cocktail tablets (Complete ™ mini EDTA-free)	Roche, Applied Sciences (Indianapolis, IN)
Protein ladder (Precision Plus Protein-Dual color standard (4-20%))	Bio-Rad (Hercules, CA)
Sodium arsenate dibasic heptahydrate (As^{V})	Sigma-Aldrich (Oakville, ON, Canada)
Sodium bicarbonate ($NaHCO_3$)	EMD Chemicals (Gibbstown, NJ)
Sodium choride (NaCl)	Thermo Fisher Scientific (Waltham, MA)
Sodium taurocholate	Sigma-Aldrich (Oakville, ON, Canada)
Sucrose ($C_{12}H_{22}O_{11}$)	Thermo Fisher Scientific (Waltham, MA)
SuperSignal ™ West Pico Chemiluminescent Substrate	Pierce Chemicals (Rockford, IL)
T4 DNA ligase	Promega Corporation (Madison, WI)
Tris base	Sigma-Aldrich (Oakville, ON, Canada)

Table 2.2 Hepatocyte isolation and cell culture reagents and buffers

Name	Source
Adhesive Prism 401 Tube	VWR (Radnor, PA)
Ascorbic acid	Sigma-Aldrich (Oakville, ON, Canada)
Biocoat culture plates	BD Biosciences (Franklin Lakes, NJ)
Bovine serum albumin (BSA)	Sigma-Aldrich (Oakville, ON, Canada)
Collagenase (type IV)	Sigma-Aldrich (Oakville, ON, Canada)
Cryopreserved rat hepatocytes	Xenotech (Lenexa, KS)
Dexamethasone (DEX)	Sigma-Aldrich (Oakville, ON, Canada)
Dulbecco's modified Eagle's medium (DMEM)	Life Technologies (Carlsbad, CA)
Fetal bovine serum (FBS)	Sigma-Aldrich (Oakville, ON, Canada)
Human recombinant insulin	Life Technologies (Carlsbad, CA)
ITS^+ (insulin, transferrin, and selenium)	BD Biosciences (Franklin Lakes, NJ)
L-glutamine	Life Technologies (Carlsbad, CA)
Liberase HI solution	Roche, Applied Sciences (Indianapolis, IN)
Matrigel ™	BD Biosciences (Franklin Lakes, NJ)
Modified essential media nonessential amino acids	Life Technologies (Carlsbad, CA)
Percoll ™	Sigma-Aldrich (Oakville, ON, Canada)
Phenol red-free DMEM	Life Technologies (Carlsbad, CA)
Perfusion Buffer 1 (P1)	118 mM NaCl, 4.7 mM KCl, 1.2 mM KPO_4 -pH 7.4 (prepared from 1 M K_2HPO_4 and 1M KH_2PO_4 (5:3:1 ratio)), 2.5 mM $NaHCO_3$, 0.5 mM EDTA, 5.5 mM glucose, 0.5% BSA, pH to 7.2
Perfusion Buffer 2 (P2)	118 mM NaCl, 4.7 mM KCl, 1.2 mM KPO_4 - pH 7.4, 25 mM $NaHCO_3$, 5.5 mM glucose, 2.0 mM $CaCl_2$, 1.2 mM $MgSO_4$, 0.3% BSA, pH to 7.2
Media One (seeding media)	phenol red-free DMEM supplemented with 5% FBS, 0.1 mM modified essential medium nonessential amino acids, 2 mM L-glutamine, 100 U/ml penicillin, 100 μg/ml streptomycin, 4 μg/ml human recombinant insulin, 1 μM dexamethasone
Media Two	phenol red-free DMEM supplemented as above in Media One except with 0.1 μM dexamethasone, ITS^+ (6.25 μg/ml insulin, 6.25 μg/ml transferrin, 6.25 ng/ml selenium) and no FBS

Table 2.3 Buffers

Name	Composition
Hanks' balanced salt solution (HBSS) +Ca	1.26 mM $CaCl_2$, 0.49 mM $MgCl_2$-$6H_2O$, 0.40 mM $MgSO_4$-$7H_2O$, 5.3 mM KCl, 0.44 mM KH_2PO_4, 4.2 mM $NaHCO_3$, 137.9 mM NaCl, 0.34 mM Na_2HPO_4, and 5.5 mM D-Glucose -supplemented with 0.35 g/L $NaHCO_3$ [Sigma-Aldrich (Oakville, ON, Canada)]
Hanks' balanced salt solution (HBSS) –Ca	5.3 mM KCl, 0.44 mM KH_2PO_4, 4.2 mM $NaHCO_3$, 137.9 mM NaCl, 0.34 mM Na_2HPO_4, and 5.5 mM D-Glucose -supplemented with 0.35 g/L $NaHCO_3$ and 0.38 g/L EGTA [Sigma-Aldrich (Oakville, ON, Canada)]
Homogenization Buffer	Tris-Sucrose Buffer- pH 7.4, 0.25 mM $CaCl_2$, protease inhibitor tablet /10ml
Laemmli Buffer (6X)	4ml of 1M Tris-pH 6.8, 3.2 ml glycerol, 3.2 g SDS, pinch bromophenol blue, 5.47 ml H_2O, dispense into 1 ml aliquots (Add 236 µl mercaptoethanol per ml prior to use)
Low Sucrose Buffer	50 mM Tris- pH 7.4, 50 mM sucrose
PBS (10X)	1.4 M NaCl, 30 mM KCl, 10 mM Na_2HPO_4-$7H_2O$, 14 mM KH_2PO_4
RIPA Buffer	0.1% SDS, 1% sodium deoxycholate, 1% Triton X-100, 10 mM Tris pH 8.0, 140 mM NaCl
Tank Buffer (10X)	250 mM Tris- pH 7.41, 92 M glycine, 1% SDS
TBS-Tween (10X)	100 mM Tris- HCl, 150 mM NaCl, 0.3% Tween® 20
Transfer Buffer (10X)	25 mM Tris, 192 mM glycine, 10% methanol
Tris-Sucrose Buffer (TSB)	50 mM Tris- pH 7.4, 250 mM sucrose

Table 2.4 Antibodies

Name	Source	Application
AQP9 [C-18] (polyclonal)	Santa Cruz Biotechnology	Western Blotting (WB)
MRP1 [MRPr1] (monoclonal)	Novus Biologicals (Originally from [169])	WB
MRP2 [M_2I-4] (monoclonal)	Thermo Fisher Scientific (Originally from [169])	WB
MRP2 [M_2III-6] (monoclonal)	Abcam Inc (Originally from [169])	WB
MRP3 [M_3II-9] (monoclonal)	Abcam Inc (Originally from [169])	WB, Immunocytochemistry (ICC)
MRP4 [M_4I-10] (monoclonal)	Abcam Inc (Originally from [169])	WB
MRP5 [M_5I-1] (monoclonal)	Abcam Inc (Originally from [169])	WB, ICC
MRP6 [M_6II-7] (monoclonal)	Novus Biologicals (Originally from [169])	WB
Na^+/K^+ ATPase [H-300] (polyclonal)	Santa Cruz Biotechnology	WB
OATP1B1 (polyclonal)	Dr. Richard Kim, Western University	WB

Table 2.5 Antibiotics

Name	Source
Ampicillin	Life Techonologies (Carlsbad, CA)
Geneticin (G418)	Life Technologies (Carlsbad, CA)
Penicillin/Streptomycin	Life Technologies (Carlsbad, CA)

Table 2.6 Radiochemicals

Name	Source
$^{73}As^V$ (5.45 mCi/mL)	Los Alamos Meson Production Facility (Los Alamos, NM).
[6,7-^{3}H]17β-estradiol 17-(β-D-glucuronide) ($E_2$17βG) (47 Ci/mmol)	PerkinElmer Life and Analytical Sciences (Woodbridge, ON, Canada).
[3',5',7-^{3}H (N)]- Methotrexate	Moravek Biochemicals Inc. (Brea, CA)
[^{3}H(G)]–Taurocholic acid (5.0 Ci/mmol)	PerkinElmer Life and Analytical Sciences (Woodbridge, ON, Canada).

Table 2.7 Cell line descriptions

Cell line	Description	Source
H69AR	Derived from H69 small cell lung cancer cell line through selection in doxorubicin	Susan P. C. Cole
HEK- 293	Human embryonic kidney cells (www.atcc.org)	ATCC
HEK- 293T	Human embryonic kidney cells transformed with simian virus 40 (SV40) large T antigen (www.atcc.org)	ATCC
HEK-V4	HEK-293 cells stably expressing pcDNA 3.1(+)	Leslie lab
HEK-MRP3-18	HEK-293 cells stably expressing MRP3	This work
HEK-MRP4-1E16	HEK-293 cells stably expressing MRP4	Leslie lab
HEK-MRP5-2-6	HEK-293 cells stably expressing MRP5	This work

Table 2.8 Expression plasmids

Plasmid	Source
pcDNA 3.1 (+)	Invitrogen
pLKO.1- puro	Sigma

Table 2.9 *ABCC4*-targeted shRNA sequences

Clone	Region	Sequence
NT **	N/A	CCGGCAACAAGATGAAGAGCACCAACTCGAGTTGGTGC TCTTCATCTTGTTGTTTTT
9930**	3'UTR	CCGGCCACCAGTTAAATGCCGTCTACTCGAGTAGACGGC ATTTAACTGGTGGTTTTTG
9928**	CDS	CCGGGCTCCGGTATTATTCTTTGATCTCGAGATCAAAGA ATAATACCGGAGCTTTTTG
5264*	3'UTR	CCGGCCACCAGTTAAATGCCGTCTACTCGAGTAGACGGC ATTTAACTGGTGGTTTTT
7334**	CDS	CCGGGCCTTCTTTAACAAGAGCAATCTCGAGATTGCTCT TGTTAAAGAAGGCTTTTTG
5267*	CDS	CCGGGCTCCGGTATTATTCTTTGATCTCGAGATCAAAGA ATAATACCGGAGCTTTTT

*shRNA sequences were contained in TRC1.5 pLKO.1-puro vector

**shRNA sequences were contained in TRC2 pLKO.1-puro vector

N/A (Not Applicable)

Table 2.10 Mrp2 primers

Name	Sequence
Mrp2_750_F	5'GGGACTTTCCAAAATGTCGT3'
Mrp2_1287_F	5'CACATGGCTCCTGGTTTTG3'
Mrp2_1778_F	5'CACGGACTGAACAAGAAGCA3'
Mrp2_2266_F	5'GCAGTTGGTGTGGTCAAGTG3'
Mrp2_2766_F	5'AGGCCAGTGTTTCTGTGGAC3'
Mrp2_3266_F	5'GCCAGAGCTGCCTATCAAGA3'
Mrp2_3780_F	5'GGAAAAAGAAGTGGAAGGACAA3'
Mrp2_4277_F	5'ATCGCTGGCACTCTTGTCAT3'
Mrp2_4750_F	5'TGTGGCAGTTGAGCGAATAA3'

2.1 Methods

2.2.1 Molecular biology

The pcDNA 3.1(+) MRP3 vector encoding the full length human MRP3 cDNA was a gift from Drs. Susan Cole and Roger Deeley (Queen's University) and its construction has been described previously [170]. The full length human MRP4 cDNA was a gift from Dr. Dietrich Keppler (German Cancer Research Center, Heidelberg, Germany) [171] and was subcloned into pcDNA3.1 (+) neomycin to generate pcDNA3.1 (+) MRP4 as previously described [82]. The pGEM5-MRP5 vector containing the full length MRP5 cDNA was a gift from Dr. Piet Borst (The Netherlands Cancer Institute) [172]. The MRP5 cDNA was excised from pGEM5-MRP5 using the restriction enzymes *EcoRI* and *HindIII* and ligated into the pcDNA 3.1 (-) vector to generate pcDNA 3.1(-) MRP5 (Invitrogen, Burlington, ON, Canada). The rat Mrp2 (rMrp2) construct (Genbank accession # X96393) was a kind a gift from Dr. Dietrich Keppler (University of Heidelberg, Heidelberg, Germany) [173]. The pcDNA 3.1 (+) rMrp2 construct was generated by PCR amplification of the rMrp2 construct using a 5' primer complimentary to the rMrp2 ORF 5'GAAAAAGCTAGCATGGACAAGTTCTGCAAC3' with an engineered NheI site before the start codon and a 3' primer complimentary to Mrp2 ORF 3'-TTTTTGGTACCCTAGACTCTGTGTATTC - 5' with an engineered KpnI site at the 3' end. The PCR product and the pcDNA 3.1 (+) vector were then digested with *NheI* and *KpnI* and

ligated together. All cloning sites and cDNA sequences were confirmed by sequencing (Macrogen USA, Rockville, MD).

2.2.2 Cell culture

2.2.2.1 HEK 293/293T cell line maintenance

The human embryonic kidney (HEK 293/293T) cell lines, including HEK-V4, HEK-MRP3-18, HEK-MRP4-E161, and HEK-MRP2-6 were maintained in DMEM supplemented with 4 mM L-glutamine, 7.5% FBS, and 600 μg/ml G418 in a humidified incubator with 95% air/5% CO_2. The HEK293 and HEK293T cells were maintained as described above except without G418. Cell line descriptions can be found above in Table 2.7.

2.2.2.2 HEK293T cell transient transfection with MRP4

HEK293T cells were transfected using the calcium phosphate method as previously described [84]. Cells were seeded in 150 mm plates and 24 h post transfection media was replaced with fresh media. After 72 h media was removed, cells were washed with 10 ml of TSB, scraped into 10 ml of fresh TSB, and collected by centrifugation at 400*g* for 10 min. Cell pellets were washed twice with TSB, overlaid with 10 ml TSB with a protease inhibitor tablet, and frozen at -80°C.

2.2.2.3 HEK-MRP4 transfection with ABCC4-targeted shRNA

HEK293-MRP4 stable cells were transfected with a non-target plasmid or shRNA clones plasmids 9930, 9928, 5264, 7334, or 5267 using the calcium phosphate method as previously described [84]. Cells were seeded in 6-well plates and 24 h post transfection media was replaced with fresh. After 72 h media was removed, cells were washed with 2 ml PBS, cells were scraped into a microcentrifuge tube, and centrifuged at 16,000*g* for 10 min. The supernatant was removed and pellets were stored at -20°C.

2.2.2.4 Generation of HEK-MRP3 and HEK- MRP5 stable cell lines

To generate stable cell lines expressing MRP3 and MRP5, 2.5×10^5 HEK293 cells were seeded in each well of a six-well plate, and 24 hours later DNA (1 μg) was transfected with 3 μl FuGENE 6 transfection reagent (Roche Diagnostics Co., Mannheim, Germany), according to the manufacturer's instructions. Forty-eight hours later, cells were subcultured (1:24) onto 4 six-well plates and medium was replaced with DMEM containing 1000 μg/ml G418 (Invitrogen) and 10% FBS. Cells were grown for ~2 weeks with regular media replacement; once cell colonies were visible, they were individually removed by scraping and aspirating with a pipette tip as described previously [174]. Levels of MRP3 and MRP5 in G418-resistant cell populations were then determined by immunoblot analysis with the anti-MRP3 MAb M_3II-9 (1:5000) and anti-MRP5 MAb M_5I-1 (1:2000). The positive clones (MRP3-18 and MRP5-2-6) were tested for the proportion of cells expressing the MRP of interest by flow cytometry (BD FACSCalibur; Cross Cancer Institute Flow Cytometry Facility, Edmonton, AB, Canada) or confocal microscopy (Zeiss, 510 NLO; Cell Biology

Imaging Facility, University of Alberta) as described previously [175]. Populations were further cloned by limiting dilution to obtain populations of >80%.

2.2.2.5 Human hepatocyte isolation

Human liver tissue was obtained from adult (>18 years) patients undergoing hepatic resection at the University of Alberta Hospital (Edmonton, AB) by qualified medical staff with the approval of the University of Alberta human ethics review board. Patients were free of infectious disease (Hepatitis B/C and HIV) and significant liver disease. Hepatocytes from livers were isolated using a modified two-step collagenase perfusion method [[176] for livers 1-19] and [[177] for livers 21 – 26]. For livers 1-19 a cannula attached to a 50 ml syringe filled with ice cold P1 buffer was used to flush the tissue of blood and identify the vessel that will perfuse the tissue most effectively. The vessel of choice was then cannulated with a 16G Teflon cannula and to secure the cannula a glue collar was created around the periphery where the cannula and tissue join. All other vessels and openings were closed with glue. The cut surfaces of the tissue were covered with a layer of glue followed by a piece of gauze and a second layer of glue to complete reconstruction of the liver capsule. The liver was then perfused with 37°C P1 buffer starting at 5 ml/min to check for any leaks and slowly increased to a maximum flow rate of 35 ml/min. Following perfusion with P1 buffer, tissue was perfused with P2 buffer containing collagenase until tissue was soft to touch but not overdigested. Forceps and scissors were then used to tease out the cells and undigested tissue into a 50 ml beaker containing Media One. The cells and digested tissue were filtered through a 100 μm mesh filter, divided equally into two 50 ml tubes, and spun at 50*g* for 2 min. The supernatants were removed, pellets resuspended in 10 ml Media One (by gently rocking tube back and forth), and combined. The 50 ml tube containing the combined pellets

was filled to 30 ml with 90% isotonic Percoll (3 parts Media One: 1 part Percoll), and spun at 100*g* for 6 min. The pellets were resuspended in 30 ml Media One and spun at 50*g* for 2 min. The pellets were combined, resuspended in 30 ml Media One, and cultured as described in Section 2.2.2.6.

2.2.2.6 Hepatocyte culture

Human hepatocytes were cultured according to previously described methods [67], with alterations. Cryopreserved rat hepatocytes were thawed according to the manufacturer's instructions and cultured in the same manner as the primary human hepatocytes as described above. Viabilities of the isolated primary human hepatocytes and cryopreserved rat hepatocytes were estimated by trypan blue exclusion. Cells were seeded on six- or twelve-well Biocoat culture plates at 1.5×10^6 or 6.25×10^5 cells/well, respectively, in seeding media and maintained at 37°C in a humidified incubator with 95% air/5% CO_2. After cell attachment to plates (2-4 h post seeding) media was replaced with Media Two. Media Two was used for the rest of the time in culture. Cells were overlaid 12 to 16 h post-seeding with 0.25 mg/ml Matrigel in 1.5 ml of ice-cold medium. Cultures were maintained with daily media changes for 6 days prior to use in experiments.

2.2.2.7 Lentiviral particle production

Lentivirus particles were produced according to the MISSION ® shRNA protocol provided by Sigma and concentrated as previously described [178] with modifications. HEK293T cells were seeded at 1.8×10^6 cells in a T75 flask in DMEM supplemented with

10% FBS and incubated for 24 h. Once they reached 50-70% confluency cells were transfected with 34 µl of MISSION shRNA plasmid packaging mix and 3.4µl shRNA transfer vector using 21 µL XtremeGene9 transfection reagent. Twenty four hours after transfection media was replaced with fresh DMEM containing 10% FBS. Supernatants from T75 flasks were collected 48 (Day 4) and 72 h (Day 5) post- transfection and stored at 4°C. On Day 5, the pooled Day 4 and Day 5 supernatants were filtered through a 0.45µm filter into conical ultracentrifuge tubes, and concentrated by ultracentrifugation. Conical tubes were filled with supernatant, placed in a SW 32Ti rotor (Beckman) and centrifuged at 23,875 r.p.m. (98,000*g*) for 2 h at 20°C. Following ultracentrifugation, the supernatant was removed, and either the tubes were filled to capacity with virus-containing tissue culture supernatant and recentrifuged for 2 h at 98,000*g*, or the virus pellet was resuspended in 50 µl phenol red free DMEM, and transferred to a microcentrifuge tube. The conical tube was washed with 50 µl of phenol red free DMEM and added to microcentrifuge tube for a total volume of 100 µl. The virus suspension was aliquoted and frozen at -80°C. The virus physical particle number was determined using the ZeptoMetrix HIV p24 ELISA assay according to the manufacturer's instructions.

2.2.2.8 Human hepatocyte lentivirus transduction

Freshly isolated hepatocytes were suspended in sterile filtered (0.45 µm filter) Media One supplemented with 8 µg/µl polybrene and the appropriate volume of lentivirus (to obtain the specified MOI) prior to seeding. Cell culture media was replaced with sterile filtered (0.45 µm filter) fresh Media Two supplemented as described above, 1-2 h post-seeding and

cells were maintained as described in Section 2.2.2.6. All efflux studies and immunoblotting were performed as described below in Sections 2.2.6 and 2.2.8.

2.2.3 Cytotoxicity testing

2.2.3.1 MTS assay using HEK-MRP3, HEK-MRP4, and HEK-MRP5 stably expressing cell lines

The cytotoxicity of six As species was measured using HEK-vector, HEK-MRP3-18, and HEK-MRP5-2-6 stable cell lines, as previously described [162]. Briefly, cells were seeded in 96-well plates at 1 x 10^4 cells/well, grown for 24 h and treated in quadruplicate with As^{III} (0.1-100 μM), As^{V} (0.001-10 mM), MMA^{III} (0.1-100 μM), MMA^{V} (0.3-100 mM), DMA^{III} (0.1-100 μM), or DMA^{V} (0.01-100 mM) for 72 h. In parallel with As species, the positive controls etoposide (0.1-100 μM) (for HEK-MRP3) and 6-mercaptopurine (0.1-100 μM) (for MRP5) were run [142].

Cell viability was determined using the CellTiter96® AQueous Non-Radioactive Cell Proliferation [3-(4,5-dimethylthiazol-2yl)-5-(3-carboxymethoxyphenyl)-24-sulfophenyl)-2H-tetrazolium, inner salt] (MTS) Assay (Promega) according to the manufacturer's instructions. Data were analyzed and EC_{50} values determined using the sigmoidal dose response equation in Graphpad Prism (GraphPad Software, San Diego, CA, USA). Relative resistance values were calculated as the ratio of the EC_{50} values of HEK-MRP to HEK-vector.

2.2.3.2 LDH assay using sandwich cultured human hepatocytes

For all SCHH experimental conditions, cytotoxicity was monitored by measuring the release of lactate dehydrogenase (LDH) using the Cytotoxicity Detection Kit (Roche, Mississuaga, ON), as described previously [179]. The degree of LDH release was calculated as a percentage of the maximum cellular LDH release, which was measured by adding 2% Triton X-100 to SCHH based on equation 1 below. When LDH was detected, >5% cytotoxicity was considered unacceptable and data was not used.

Equation 1:

$$\text{Cytotoxicity (\% of control)} = \frac{(LDH_{sample} - LDH_{blank})}{(LDH_{Triton\ X\text{-}100} - LDH_{blank})} \times 100$$

2.2.4 Plasma membrane-enriched vesicle preparation

Plasma membrane vesicles were prepared as previously described by [180]. Cells were homogenized in TSB supplemented with protease inhibitor tablets. Nitrogen cavitation was used to disrupt the cells with a 5 min equilibration at 200 p.s.i. followed by release into a 50 ml tube containing EDTA (1 mM) and PMSF (1 mM) at atmospheric pressure. The cell suspension was centrifuged at 800*g* at 4°C for 10 min and the supernatant was layered onto 12 ml of a 35% (w/w) sucrose, 50 mM Tris, pH 7.4 cushion. The layered cell suspension was then centrifuged at 100,000g at 4°C for 1 h, the interface was removed and placed in a fresh tube that was then filled with low sucrose buffer and centrifuged at 100,000*g* at 4°C for 30 min. The supernatant was removed and the pellet was resuspended in TSB by syringing through a 27-gauge needle approximately 20-times. Protein concentrations were determined using a Bradford assay and membrane protein aliquots were stored at -80°C.

2.2.5 Plasma membrane-enriched vesicle transport assays

2.2.5.1 Radioactive transport assays

2.2.5.1.1 $^{73}As(GS)_3$ and transport assays

$^{73}As^{III}$ was prepared from $^{73}As^{V}$ with a metabisulfite-thiosulfate solution as previously described [181]. Briefly, an equal volume of reducing solution (0.1 mM $NaAsO_2$, 66 mM $Na_2S_2O_5$, 27 mM $Na_2S_2O_3$, and 82 mM H_2SO_4) was added to an equal volume of carrier-free $^{73}As^{V}$ and incubated overnight at room temperature. $^{73}As(GS)_3$ was prepared as described previously by Delnomdedieu *et al.* with modifications [17]. $^{73}As^{III}$ (final concentration 0.1-1 μM) and GSH (final concentration 75 mM) were mixed under a nitrogen atmosphere in TSB.

^{73}As transport assays were carried out by a rapid filtration method as previously described [161]. Membrane vesicles (20 μg of protein/point) were incubated at 37°C in a final volume of 60 μl (single time point) in TSB containing either AMP or ATP (4 mM), $MgCl_2$ (10 mM), creatine phosphate (10 mM), creatine kinase (100 μg/ml), GSH reductase (5 μg/ml), NADPH (0.35 mM), GSH (3 mM), and $^{73}As(GS)_3$ (30 nCi, 0.1 μM) or (100 nCi, 1 μM). At the indicated time points, 60 μl of transport reaction mix was removed and placed in 800 μl of TSB, filtered through glass fiber filters (type A/E; Pall Life Sciences, East Hills, NY), washed twice, and radioactivity was quantitated by liquid scintillation counting. Transport in the presence of AMP was subtracted from transport in the presence of ATP and reported as ATP-dependent $^{73}As(GS)_3$ transport.

2.2.5.1.2 [^{3}H]-$E_2$17βG and [^{3}H]-methotrexate transport assays

Plasma membrane enriched vesicles were prepared from MRP3, MRP4, MRP5, and empty pcDNA 3.1 (+) transfected HEK293 cells. Briefly, 10 µg or 20 µg of MRP4-enriched membrane vesicles were incubated with either [^{3}H]-$E_2$17βG (1 µM, 40 nCi/pt) or [^{3}H]-methotrexate (1 µM 100 nCi/pt), respectively, AMP or ATP (4 mM), $MgCl_2$ (10 mM), creatine phosphate (10 mM), creatine kinase (100 µg/uL), Tris (50 mM, pH 7.4), sucrose (250 mM) at 37°C for 3 min. [^{3}H]-$E_2$17βG (1µM, 80 nCi/pt) transport inhibition was completed as previously described in the absence or presence of phloretin (50 to 500 µM) [162]. Transport was stopped by diluting with 800 µl ice cold TSB, filtering over glass fiber filters, washing twice with 3.5 ml TSB, and radioactivity was quantified by liquid scintillation counting using a Microbeta^2 counter (PerkinElmer Life and Analytical Sciences). Transport in the presence of AMP was subtracted from transport in the presence of ATP and reported as ATP-dependent transport for both substrates. IC_{50} values for inhibition experiments were determined using Graphpad Prism 6.05 Software (non-linear regression log (inhibitor) vs normalized response analysis).

2.2.5.2 Non-radioactive transport assays.

2.2.5.2.1 $MMA(GS)_2$ transport assays

$MMA(GS)_2$ was synthesized from MMA^{III} and GSH as described previously [107,162]. Briefly, MMA^{III} (final concentration of 50 µM) was combined with GSH (final concentration of 75 mM) in degassed Tris-sucrose buffer and incubated under a nitrogen atmosphere for >30 min at 4°C. Membrane vesicles (20 µg) were incubated at 37°C in Tris-sucrose buffer, with $MMA(GS)_2$ (1-250 µM for MRP2 studies) or (0.07-6.7 µM) for MRP4 studies), AMP or ATP (4 mM), $MgCl_2$ (10 mM), creatine kinase (100 µg/ml), creatine

phosphate (10 mM), GSH reductase (5 µg/ml), and NADPH (0.35 mM), and GSH (3 mM) for 3 min. At the indicated time point(s), transport was stopped by diluting the transport reaction in 800 µl ice-cold TSB and pelleting vesicles by centrifugation at 100,000*g* for 20 minutes at 4°C. Pelleted membrane vesicles were washed twice with 1 ml ice-cold TSB, then digested in 250 µl concentrated nitric acid for 24 hours, diluted 1:1 with deionized distilled water, and filtered with 0.45-µm syringe filters (Whatman). The total concentration of As in each sample was determined by ICP-MS using the standard addition method as described previously [162,182]. ATP-dependent transport was determined as described in Section 2.2.5.1.1.

2.2.5.2.2 DMA^V transport assays

DMA^V transport assays were performed as described above (Section 2.2.5.2.1) for $MMA(GS)_2$ except membrane vesicles (20 µg) were incubated at 37°C in Tris-sucrose buffer, with DMA^V (1 or 100 µM), AMP or ATP (4 mM), $MgCl_2$ (10 mM), creatine kinase (100 µg/ml), and creatine phosphate (10 mM), Tris (50 mM, pH 7.4), and sucrose (250 mM) at 37°C for 5 min.

2.2.6 SCHH accumulation and efflux studies

SCHH were cultured for six days to allow for maximum development of canalicular networks and limit variability due to donor health, life-style and xenobiotic exposure [61,67]. On day five, SCHH were incubated with $^{73}As^{III}$ (0.1-1 µM, 100 nCi/well) in media 2 for 24 h to allow accumulation and metabolism of As. $^{73}As^{III}$ was prepared from $^{73}As^V$ using metabisulfite-thiosulfate reducing agent as previously described [181]. To measure As

accumulation $^{73}As^{III}$ (1 μM, 100 nCi/well) containing media was removed and cells were washed three times with 4ºC standard Hank's balanced salt solution (HBSS). Cells were then lysed with 0.5% Triton X-100, and 500 μl was analyzed by liquid scintillation counting. Arsenic efflux experiments were performed as previously described [183]. Cells were washed twice with 4ºC standard HBSS and efflux of As across the hepatocyte basolateral surface was initiated by the addition of 1 ml of 37°C fresh standard HBSS. In parallel, efflux from both basolateral and canalicular surfaces was measured after the addition of 1 ml of 37°C Ca^{2+}/Mg^{2+}-free HBSS (with 1 mM EGTA) [using B-CLEAR® technology (Qualyst Transporter Solutions)], removal of Ca^{2+} from the HBSS results in the disruption of canalicular networks (Fig. 2.1) [65]. Plates were incubated at 37ºC and HBSS (100 μl) was sampled at the indicated time points. Samples were placed in scintillation vials and quantified by liquid scintillation counting. Accumulation and efflux activity was normalized for total hepatocyte protein determined using a BCA assay.

Temperature sensitivity of $^{73}As^{III}$ efflux was assessed as described above except cells were incubated on ice and transport was initiated with 1 ml of ice cold HBSS. To determine the influence of GSH on $^{73}As^{III}$ efflux, hepatocytes were treated with BSO (0.5 mM), an inhibitor of glutamate cysteine ligase, the rate limiting step of GSH synthesis, for 24 h prior to $^{73}As^{III}$ (1 μM) treatment (day 4 of culture) and for the duration of ^{73}As exposure or 48 h total. The influence of MK-571 and phloretin were tested by incubating $^{73}As^{III}$ (1 μM) treated cells with MK-571 (100 μM) or phloretin (500 μM) 30 min prior to the initiation of efflux and for the duration of the efflux time course studies. The effect of oltipraz (50 μM), an activator of Nrf2, on ^{73}As efflux was determined by treating cultures for 48 h prior to efflux experiments. To ensure canalicular networks were properly developed and hepatocytes were functional, each SCHH preparation was tested for ^{3}H-taurocholate efflux as

described above for $^{73}As^{III}$ except preincubation with ^{3}H-taurocholate (1 µM, 100 nCi/ well) was done for 15 min instead of 24 h.

The biliary excretion index (BEI) for As and taurocholate efflux was calculated based on equation 2 below [adapted for efflux from [66]].

Equation 2:

$$BEI = \frac{Efflux_{sinusoidal + canalicular} - Efflux_{sinusoidal}}{Efflux_{sinusoidal + canalicular}} \times 100\%$$

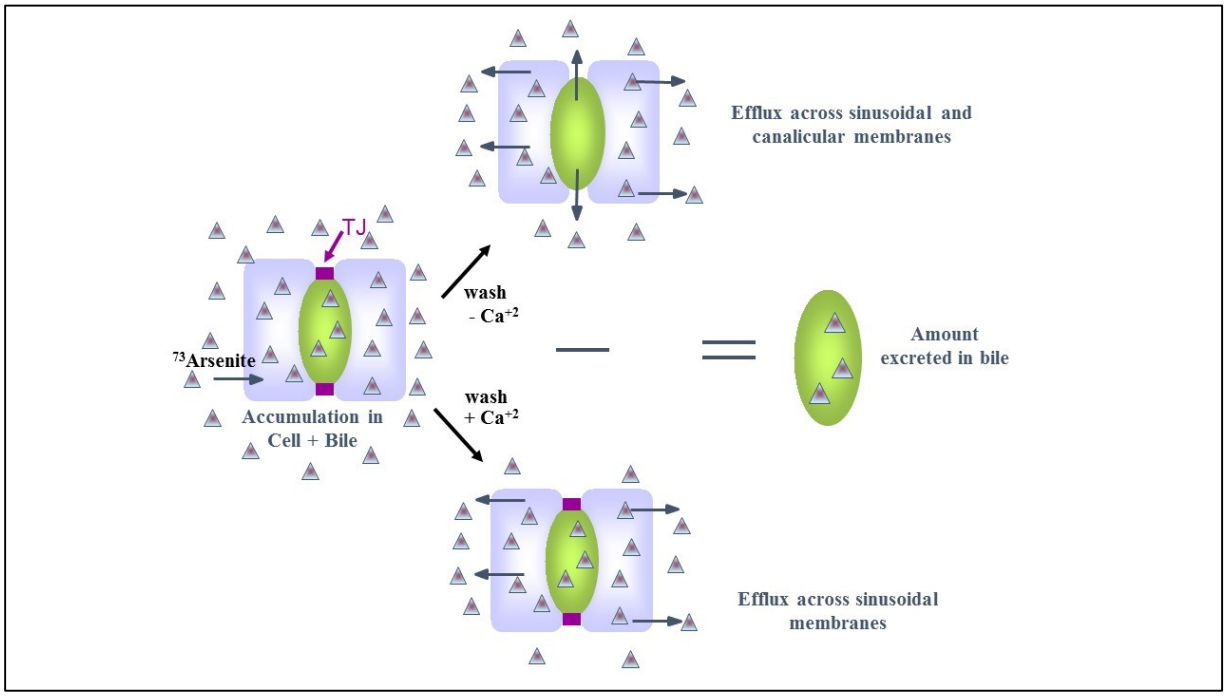

Fig. 2.1. Schematic illustrating As efflux across the sinusoidal and sinusoidal plus canalicular membranes of SCHH.

Cells were washed twice with 4ºC standard HBSS and efflux of As across the hepatocyte basolateral surface was initiated by the addition of 1 ml of 37°C fresh standard HBSS. In parallel, efflux from both basolateral and canalicular surfaces was measured after the addition of 1 ml of 37°C Ca^{2+}/Mg^{2+}-free HBSS (with 1 mM EGTA) [using B-CLEAR® technology (Qualyst Transporter Solutions)], removal of Ca^{2+} from the HBSS results in the disruption of canalicular networks.

2.2.7 Visualization of CDF accumulation in canalicular networks of SCHH using fluorescence microscopy

SCHH were seeded onto 12- well Biocoat plates and cultured as described above. Cells were treated with As^{III} under conditions identical to SCHH transport assays (described in Section 2.2.6). On day 6 of culture, cells were washed 3-times with 1 ml HBSS (37ºC), incubated with 5 (and 6)- carboxy 2',7'dichlorofluoresecin-diacetate (CDFDA) (2 μM) for 10 min at 37ºC, and washed again 3-times with 1 ml standard HBSS (37ºC) followed by the addition of 1 ml standard HBSS [66]. Cells were then viewed under a fluorescent microscope (Olympus, IX81, Olympus Canada, Richmond Hill, ON).

2.2.8 Cell lysate preparation and immunoblotting of SCHH

As described for transport assays SCHH were incubated with As^{III} (0.1-1 μM), oltipraz (50 μM), BSO (500 μM) or remained untreated. Cells were washed twice with 1 ml PBS, then scraped into 1 ml PBS, and spun at 16,000*g* for 5 min. Pellets were thawed on ice and then lysed with RIPA buffer with Complete™ protease inhibitors for 30 min at 4°C. Nuclei and cell debris were pelleted by centrifugation for 10 min, at 16,000*g* at 4ºC. Proteins (30 μg) were resolved by SDS-PAGE and transferred to a PVDF membrane. PVDF membranes were blocked at room temperature with 4% nonfat milk in Tris-buffered saline with 0.3% Tween-20 pH 7.4, incubated with either the MRP1-specific monoclonal antibody MRPr1 (1:10,000), the MRP2-specific monoclonal antibody M_2I-4 (1:2000), the MRP4-specific monoclonal antibody M_4I-10 (1:500), the MRP6-specific monoclonal antibody M_6II-7 (1:500), the AQP9-specific polyclonal antibody [C-18] (1:500), or the OATP1B1

polyclonal antibody (1:500) as previously described [184]. Blots were then stripped and incubated with the Na^+/K^+-ATPase-specific antibody [H-300] (1:10,000) as a loading control. Densitometry analysis was done using Image J software.

2.2.9 High performance liquid chromatograph-inductively coupled plasma mass spectrometry analysis of arsenic species in SCHH media

SCHH were treated with non-radioactive As^{III} (0.5 or 1 μM) for 24 h in media 2. Media was then collected and immediately stored at -80°C. Hepatocytes were then washed twice with ice cold As-free media and then As-free 37°C media 2 was added and cells incubated for 1 h at 37ºC. Media was again collected and stored immediately at -80°C.

An Agilent 1100 series high performance liquid chromatography (HPLC) system consisting of a pump, degasser, autosampler, column temperature control, and reverse-phase C_{18} column (ODS-3, 150 mm × 4.6 mm, 3-μm particle size; Phenomenex, Torrance, CA, USA) was used for the separation of arsenicals. The mobile phase consisted of 5 mM tetrabutylammonium, 5% methanol, and 3 mM malonic acid (pH 5.85). The column was equilibrated with the mobile phase for at least 0.5 h before sample injection. Separation of samples was performed at a flow rate of 1.2 ml/min; 50 μl of sample was injected; the column temperature was maintained at 50°C. The effluent from the HPLC was introduced directly into the nebulizer of a 7500ce ICP-MS instrument (Agilent Technologies, Japan) using PEEK tubing. The collision cell of the ICP-MS instrument was operated in helium mode. Helium (3.5 ml/min) was used in the octopole reaction cell to reduce isobaric and

polyatomic interferences. The ICP operated at a radio-frequency power of 1,550 W, and the flow rate of carrier gas was 0.9–1.0 L/min. Arsenic was monitored at *m*/*z* 75. Chromatograms from HPLC separation were recorded by ICP-MS ChemStation (Agilent Technologies, Santa Clara, CA, USA). Certified reference material No.18 "Human Urine" was used for quality control. There was good agreement between the certified and analyzed values.

Chapter 3

Characterization of Arsenic Hepatobiliary Transport Using Sandwich Cultured Human Hepatocytes

This thesis chapter was published as: *Roggenbeck, B.A., Carew, M.W., Charrois, G.J., Douglas, D.N., Kneteman, N.M., Lu, X., Le, X.C., and Leslie*, *E.M.*, Characterization of arsenic hepatobiliary transport using sandwich cultured human hepatocytes, Toxicol Sci. 2015 Jun;145(2):307-20. doi: 10.1093/toxsci/kfv051. Epub 2015 Mar 9. Barbara A. Roggenbeck completed all experiments with SCHH preparations 5-26. Elaine M. Leslie and Gregory J. Charrois completed experiments with SCHH preparations 1-4. Michael W. Carew assisted with hepatocyte isolations and experiments for SCHH preparations 5-19. Norman M. Kneteman and Donna N. Douglas provided hepatocytes for preparations 21-26. X. Chris Le and Xiufen Lu completed the arsenic speciation analysis on SCHH efflux samples in Fig. 3.9.

3.1 Introduction

The As contamination of groundwater in Bangladesh has been referred to as "the largest mass poisoning of a population in history" [4]. Arsenic is found at levels that exceed the WHO limit of 10 ppb in many other parts of the world and is a Group I (proven) human carcinogen [3,5]. Exposure to As is also associated with a broad range of other adverse health effects including peripheral vascular disease, neurological disorders, and diabetes mellitus [5]. Despite the known deleterious health effects caused by As and the prevalence of human exposure, key steps of As toxicokinetics and elimination are not fully understood.

The vast majority of As in contaminated drinking water is inorganic and thus a combination of arsenate (As^{V}) and arsenite (As^{III}). Cellular uptake of As^{V} can be mediated by phosphate transporters such as the Na^{+}/phosphate cotransporter type IIb (*SLC34A2*) [101], while As^{III} uptake pathways include aquaglyceroporins (AQPs) and glucose transporters (GLUTs) [90]. Evidence from AQP9 knock-out mice suggests that AQP9 can function in both the cellular uptake and efflux of neutral As species [90].

Once inside human cells, the methylation of As is catalyzed by the enzyme arsenic (+3 oxidation state) methyltransferase (AS3MT), resulting in four major products: monomethylarsonic acid (MMA^{V}), monomethylarsinous acid (MMA^{III}), dimethylarsinous acid (DMA^{V}), and dimethylarsinic acid (DMA^{III}) [111]. Arsenic is methylated predominantly in the liver, however, the majority of As is excreted in human urine. The transport pathways responsible for the basolateral efflux of As from the

human hepatocyte into blood for renal elimination have not been characterized in a physiologically relevant human model.

The multidrug resistance proteins MRP1, MRP2, and MRP4 (*ABCC1*, *ABCC2*, and *ABCC4,* respectively) are ATP-binding cassette transporter proteins with established roles as As efflux transporters [82,109]. *In vivo* rat studies have shown that Mrp2 is responsible for the biliary excretion of As as $As(GS)_3$ and $MMA(GS)_2$ [107]. MRP3, MRP4, MRP5, and MRP6 are localized to the basolateral surface of hepatocytes and can transport substrates from the liver to blood. Recent studies have shown that DMA^V and $MMA(GS)_2$ are high affinity substrates for MRP4, while MRP3 and MRP5 do not protect cells from inorganic or methylated As species (Chapter 2). The ability of MRP6 to transport or protect cells from As has not been investigated.

Primary human hepatocytes cultured in a sandwich configuration (between two layers of collagen) have correct polarization and develop extensive functional canalicular networks. Furthermore, sandwich cultured hepatocytes (SCH) retain their metabolic capacity and express transport proteins at levels comparable to hepatocytes *in vivo* [66,67]. The *in vivo* hepatobiliary clearance of xenobiotics in humans and rats and the corresponding *in vitro* biliary clearance in SCH are highly correlated, making this physiological model ideal for studying human hepatobiliary transport of As [67,68]. Thus, in the current study, As hepatobiliary transport was characterized using sandwich cultured primary human hepatocytes (SCHH). The basolateral efflux of As was detected in all fourteen SCHH preparations characterized, and five of these preparations also effluxed As across the canalicular membrane. Speciation of basolateral efflux media revealed that SCHH methylate As and the inorganic, monomethylated, and dimethylated

forms are transported. The results presented suggest basolateral efflux of As is mediated at least in part by one or more MRPs, and one likely candidate is MRP4. Furthermore, results suggest that basolateral efflux of As prevails over its biliary excretion.

3.2 Results

3.2.1 Arsenic is transported across only the basolateral membrane in certain SCHH preparations

Large differences exist among animal species in the toxicokinetic pathways and carcinogenic effects of As making it essential to study As transport using relevant human model systems [54]. Thus, SCHH were used to characterize As hepatobiliary efflux pathways. In the presence of calcium, the tight junctions remain fully formed and the canalicular networks intact, allowing for measurement of efflux across the basolateral membrane of the hepatocyte. Removal of calcium from the buffer disrupts the tight junctions and allows measurement of efflux across both the apical and basolateral membranes [65]. A difference in efflux between the plus and minus calcium conditions indicates that there is apical transport of a substrate. The bile acid, taurocholate, undergoes extensive biliary excretion and was used as a positive control for each hepatocyte preparation (to confirm canalicular networks were formed and functional). As expected, there was a significant increase in taurocholate efflux in the absence of calcium when compared to transport in the presence of calcium (Fig. 3.1A; Table 3.1). The BEI

for taurocholate ranged from 31% to 70% at 10 min (mean 50 ± 9%) (Table 3.1), and were similar to previously published values [67,183,185,186].

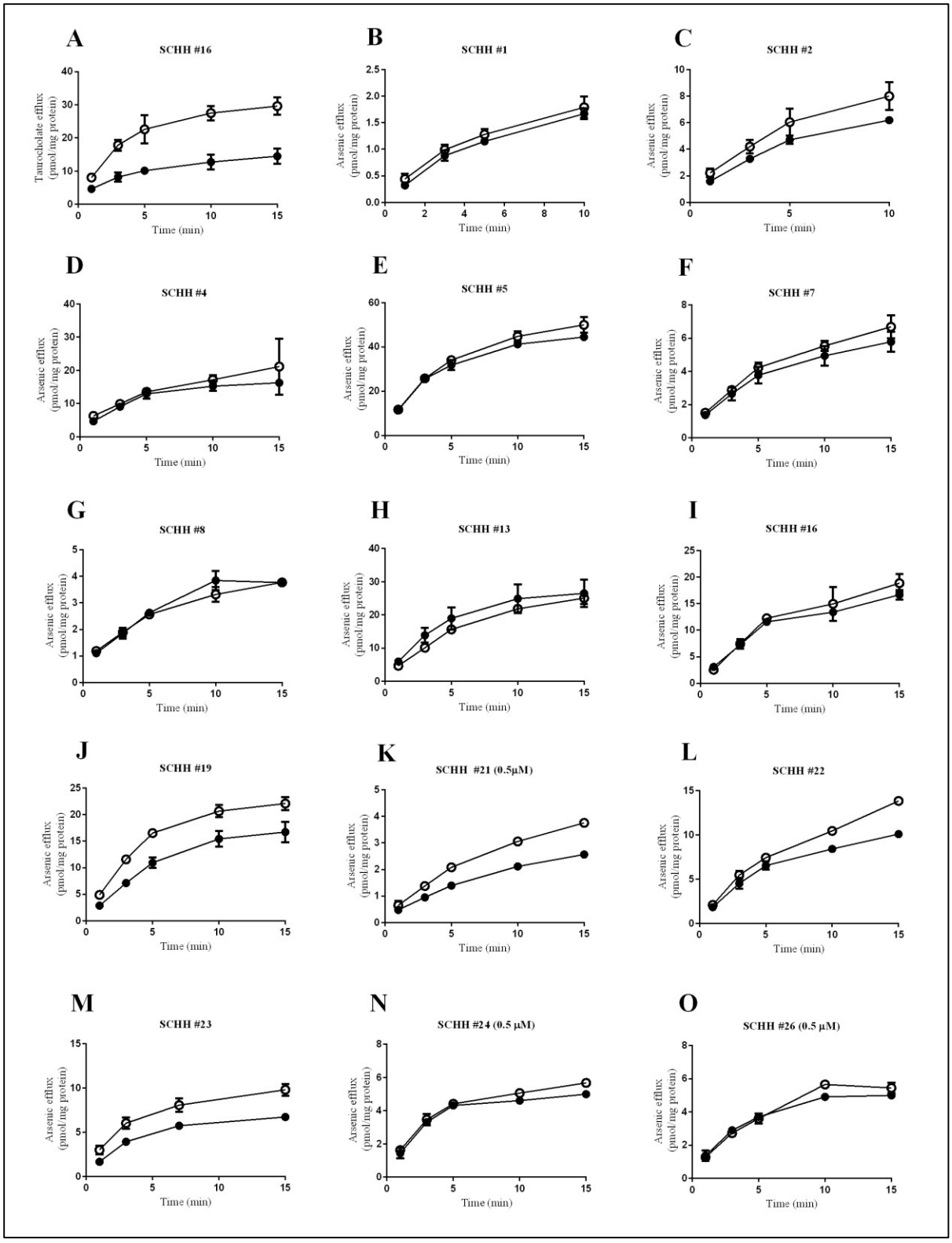

Fig. 3.1. Taurocholate and arsenic efflux from fourteen different SCHH preparations.

SCHH were incubated at 37°C with (A) [^{3}H]taurocholate (1 µM; 100 nCi) for 15 min or (B-O) $^{73}As^{III}$ (1µM unless indicated 0.5 µM; 100 nCi) for 24 h; then incubation media was replaced with

Ca^{2+}-containing (basolateral efflux, ●) or Ca^{2+}-free (basolateral + canalicular efflux, ○) HBSS. Efflux was then measured as described in methods. The difference between the closed and open circles represents substrate efflux into canalicular space. Points represent means ± SD for triplicate determinations in a single experiment.

To investigate the hepatobiliary transport of As, SCHH were treated with As^{III} (0.5 or 1μM, as indicated) for 24 h and then efflux measured as described above for taurocholate. The 24 h time point was selected because accumulation of As had reached a plateau by this time (Fig. 3.2). Accumulation in SCHH preparations #2, #4, #5, and #26 at 24 h ranged from 274 to 560 pmol mg^{-1} protein 24 h^{-1} (Fig. 3.2), consistent with previous reports from primary human hepatocytes cultured on a single layer of collagen [187]. Basolateral (+ Ca^{2+} condition) As efflux activity for preparations treated with 1 μM As ranged from 2 to 41 pmol mg^{-1} protein 10 min^{-1} (mean of 12.9 ± 10.1 pmol mg^{-1} protein 10 min^{-1}). Arsenic transport by SCHH was very similar in the presence and absence of Ca^{2+} for nine out of fourteen preparations (Fig. 3.1B, D, E, F, G, H, I, N, and O) suggesting As is effluxed only across the basolateral surface of hepatocytes in these preparations. In contrast, five out of fourteen SCHH preparations showed some degree of biliary efflux along with basolateral efflux (Fig. 3.1C, J, K, L and M). The As BEI was calculated for all preparations at 3 and 10 min time points (Table 3.1). The BEI for SCHH with moderate biliary excretion (preparations #2 and #22) ranged from 17-21%, and the more extensive biliary excretion (preparations #19, #21, and #23) ranged from 25-39% (Table 3.1). It was possible to calculate a BEI for three of the SCHH preparations that were classified as "only basolateral efflux" (preparations #5, #24, and #26) (Fig. 3.1E, N, and O), but the BEI values were low and not detectable at the 3 min time point (Table 3.1).

Table 3.1. Summary of the biliary excretion index of arsenic and taurocholate in sandwich cultured human hepatocytes and viability of freshly isolated hepatocytes

	BEI (%)			
SCHH prep #	Arsenic		Taurocholate	% viability[a]
	3 min	10 min	10 min	
1	NS	NS	31	94
2	21*	19*	45	88
4	NS	NS	40	94
5	NS	8*	50	97
7	NS	NS	52	95
8	NS	NS	53	95
13	NS	NS	65	99
16	NS	NS	54	99
19	39*	25*	43	99
21	31*	31*	44	87
22	17*	20*	48	86
23	35*	29[b]*	54	89
24	NS	10*	50	76
26	NS	13*	70	89

NS (not significant).

* BEI values were only calculated when the – Ca^{2+} condition was significantly higher ($p < 0.05$, Student's t-test) than the + Ca^{2+} condition for triplicate determinations from a single experiment.

[a]Determined using trypan blue exclusion.

[b]BEI calculated at 7 min instead of 10 min

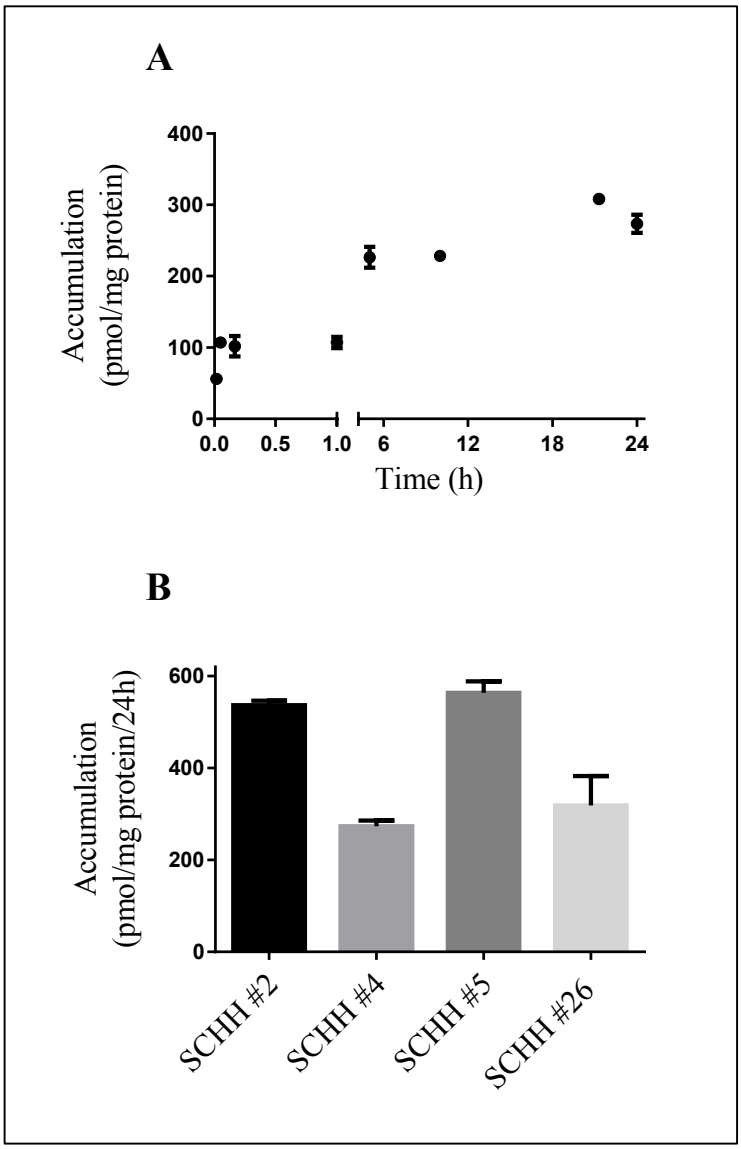

Fig. 3.2. Accumulation of arsenic in SCHH.

Arsenic (1 mM; 100 nCi) accumulation was measured after (A) incubating SCHH preparation #4 for the indicated time points or (B) incubating SCHH preparations #2, #4, #5, and #26 for 24 h. Bars and symbols represent means (± S.D.) of triplicate determinations in a single experiment.

3.2.2 MRP2 is functional in SCHH preparations lacking arsenic biliary excretion

In vivo studies using Mrp2-deficient Wistar rats have shown that Mrp2 is responsible for all As biliary excretion [107]. To determine if the lack of As biliary excretion observed with nine of the SCHH preparations was due to a lack of functional MRP2, two representative SCHH preparations that lacked As biliary excretion, #13 and #24, were tested for their ability to efflux the MRP2 substrate CDF into canalicular networks [188]. The fluorescent images clearly show accumulation of CDF in the canalicular networks, suggesting that MRP2 is expressed and functional (Fig. 3.3A and B). SCHH preparations exhibiting moderate and more extensive As biliary excretion (SCHH #22 and #23, respectively) had patterns of CDF accumulation comparable to SCHH#13 and #24 (Fig. 3.3C and D). These data suggest that MRP2 is present and functional in SCHH that exhibit no, moderate, or extensive biliary excretion of As.

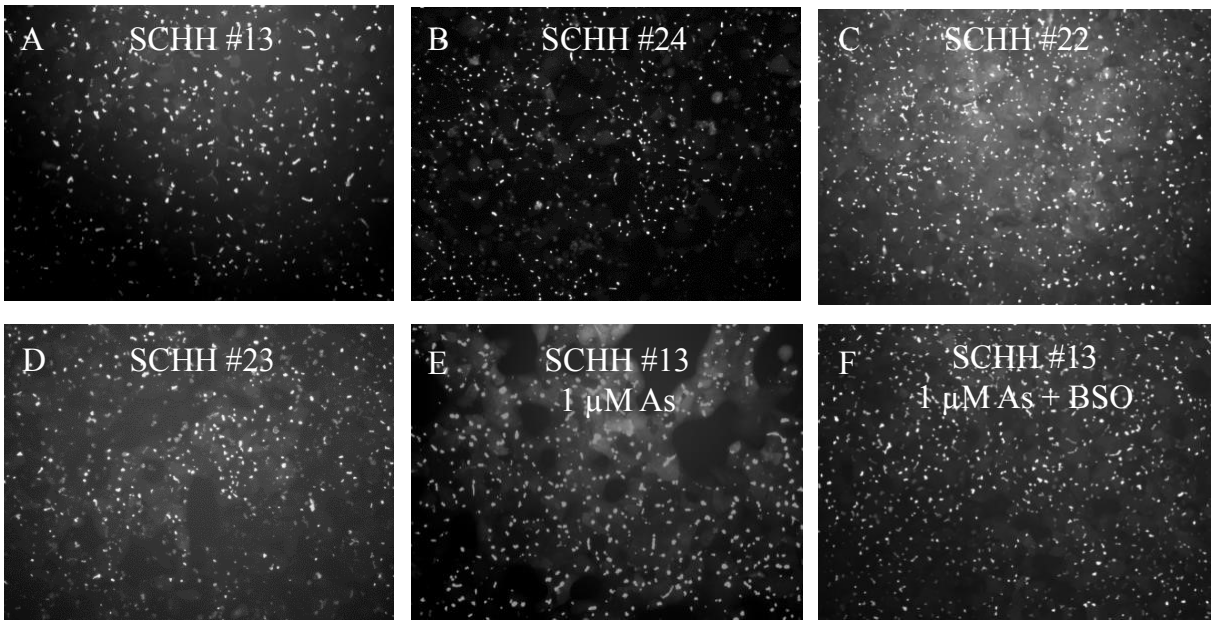

Fig. 3.3. Fluorescent images of CDF accumulation in the canalicular networks of four different SCHH preparations.

SCHH were incubated with CDF-diacetate (2 µM) in + Ca^{2+} HBSS for 10 min at 37°C and viewed with a fluorescent microscope (Olympus, IX81, Olympus Canada, Richmond Hill, ON). CDF accumulation was imaged for SCHH preparations with (A and B) undetectable, (C) moderate, or (D) more extensive As biliary excretion. The influence of (E) As^{III} (1 µM) and (F) As^{III} (1 µM) plus BSO (500 µM) treatments (under conditions identical to efflux experiments) on CDF accumulation was also tested for SCHH preparation # 13 (untreated in panel A).

3.2.3 CDF is accumulated in canalicular networks of SCHH treated with arsenic

All SCHH preparations had acceptable canalicular formation and function as assessed by measuring the taurocholate BEI (Table 3.1). However, the influence of As on the canalicular network integrity was unknown. To explore the possibility that As was disrupting canalicular networks and preventing As biliary accumulation (in cases where As biliary excretion was not detected), the accumulation and retention of CDF within the

canalicular networks of SCHH preparation #13 was imaged after treatment with As (1 μM) and As (1 μM) plus BSO (500 μM) using conditions identical to transport assays (Fig. 3.3E and F). The pattern of CDF accumulation in canalicular networks was similar between untreated (Fig. 3.3A), As^{III} treated (Fig. 3.3E) and As^{III} plus BSO (Fig. 3.3F) SCHH preparation #13. These data suggest that the integrity of the canalicular networks was not disrupted by As under the conditions used for transport assays.

3.2.4 Arsenic concentration does not change the polarized transport of arsenic

To determine if As efflux remained predominantly basolateral over a concentration range, efflux was measured after treating cells with 0.1 to 1 μM of As^{III}. Decreasing concentrations of As^{III} in SCHH preparations #4, #13, or #16 that lacked biliary excretion at 1 μM of As^{III} resulted in a dose-dependent reduction of basolateral efflux (Fig. 3.4A-C), however, no biliary excretion was detected. SCHH preparation #19 had BEI values of 25, 29, and 38% at 1, 0.5, and 0.1 μM As, respectively (Fig. 3.4D), suggesting an increased biliary excretion with decreasing As concentration.

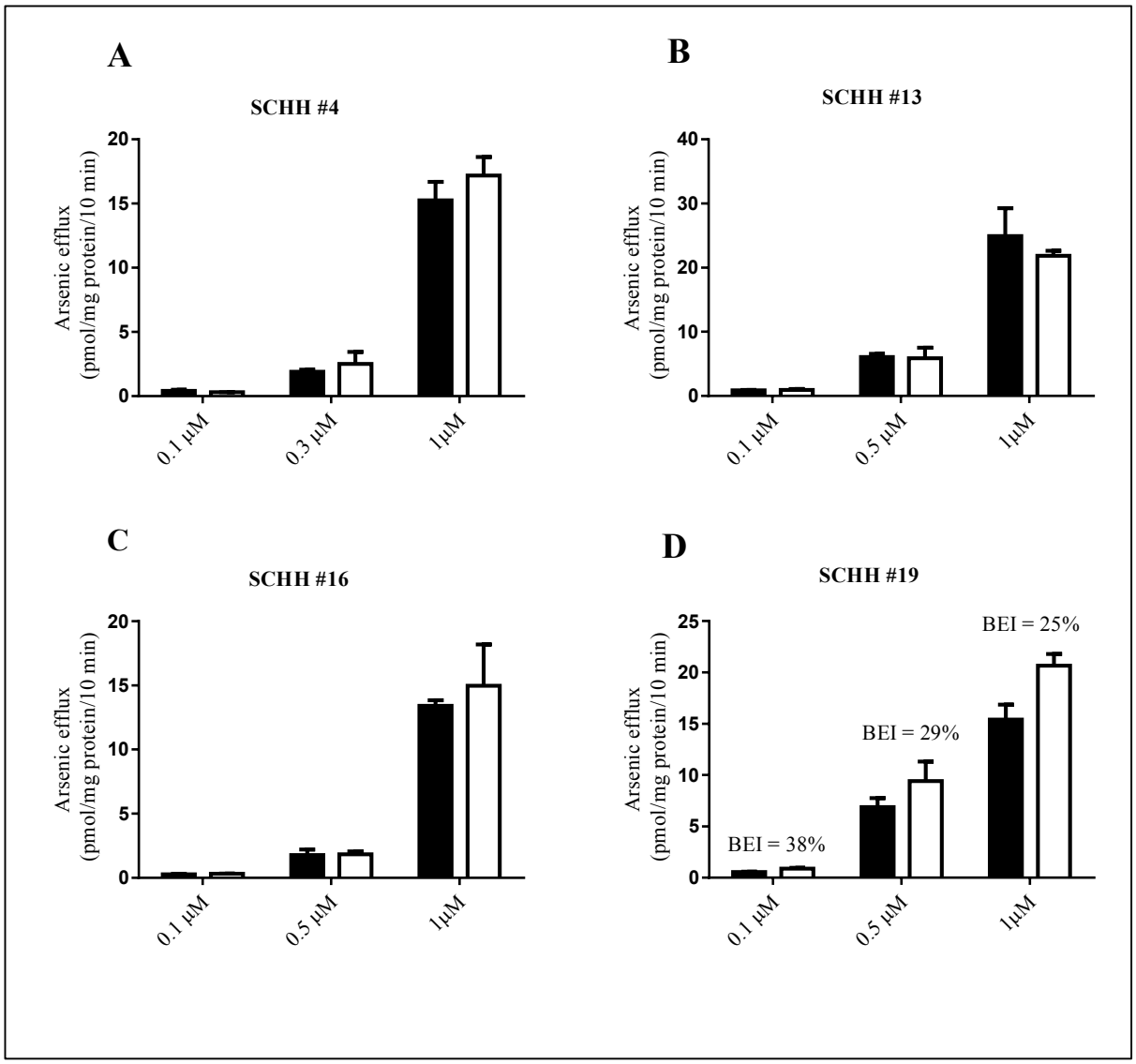

Fig. 3.4. Dose-dependent arsenic efflux from SCHH.

SCHH were incubated with $^{73}As^{III}$ (0.1 -1 µM; 100 nCi) for 24 h at 37°C; then incubation media was replaced with Ca^{2+}-containing (basolateral efflux, closed bars) or Ca^{2+}-free (basolateral + canalicular efflux, open bars) HBSS. Efflux was measured as described in methods. Bars represent means ± SD for triplicate determinations at 10 min in a single experiment for SCHH preparation (A) #4, (B) #13, (C) #16, and (D) #19. (D) BEI values were calculated [only when triplicate determinations of ± Ca^{2+} conditions were found to be statistically significant ($p < 0.05$, Student's t-test)] using equation 2 in methods.

3.2.5 Arsenic transport is temperature sensitive

Transport proteins have markedly reduced function at 4ºC and thus temperature sensitivity of substrate translocation across cell membranes indicates that a transport process is involved. To evaluate the effect of temperature on basolateral As transport, efflux was measured at 37°C and compared to efflux at 4°C for five different SCHH preparations in the presence of + Ca^{2+} HBSS (Fig. 3.5A). Efflux was decreased by 87 ± 6% (mean ± S.D., n = 5, $p < 0.001$, Student's t-test) at 4°C compared with 37°C controls (Fig. 3.5A). Similar results were obtained for the biliary efflux of As for SCHH #19 (data not shown). These data suggest a transport process is responsible for basolateral and canalicular membrane translocation of As rather than simple diffusion.

3.2.6 Arsenic transport is GSH-dependent

Previous studies have shown that As^{III} and/or MMA^{III} transport by MRP1, MRP2, and MRP4 is GSH-dependent due to the formation of As-GSH conjugates [82,109]. To determine if As basolateral efflux is dependent on GSH, SCHH were treated with BSO (500 μM) for 48 h. GSH depletion of SCHH resulted in a 48 ± 5 % (mean ± S.D. n = 5, $p < 0.001$, Student's t-test) reduction in As efflux compared with "GSH-normal" controls (10 min time point, 1 μM As treatment) (Fig. 3.5B, left panel). GSH depletion in a single SCHH preparation treated with 0.5 μM As resulted in a 70% reduction in As efflux at 10 min (Fig. 3.5B, right panel). These data show that a major portion of As basolateral efflux from SCHH is dependent on the presence of GSH. These data are consistent with MRP-dependent basolateral transport of As. SCHH preparations #19, #22, and #23

showed GSH-dependent As transport across both the basolateral and canalicular surfaces of the hepatocyte (Fig. 3.5B-E). The BEIs for #19, #22, and #23 at 10 min were decreased to 0% in the presence of BSO indicating that all canalicular As transport is dependent on the presence of GSH (Fig. 3.5C – E). These data are consistent with rat *in vivo* data that Mrp2 is solely responsible for the biliary excretion of As as $As(GS)_3$ and $MMA(GS)_2$ [107]. MRP2 is the only known GSH-dependent transport pathway at the canalicular surface of human hepatocytes and these results strongly suggest MRP2 is the human As biliary excretion pathway.

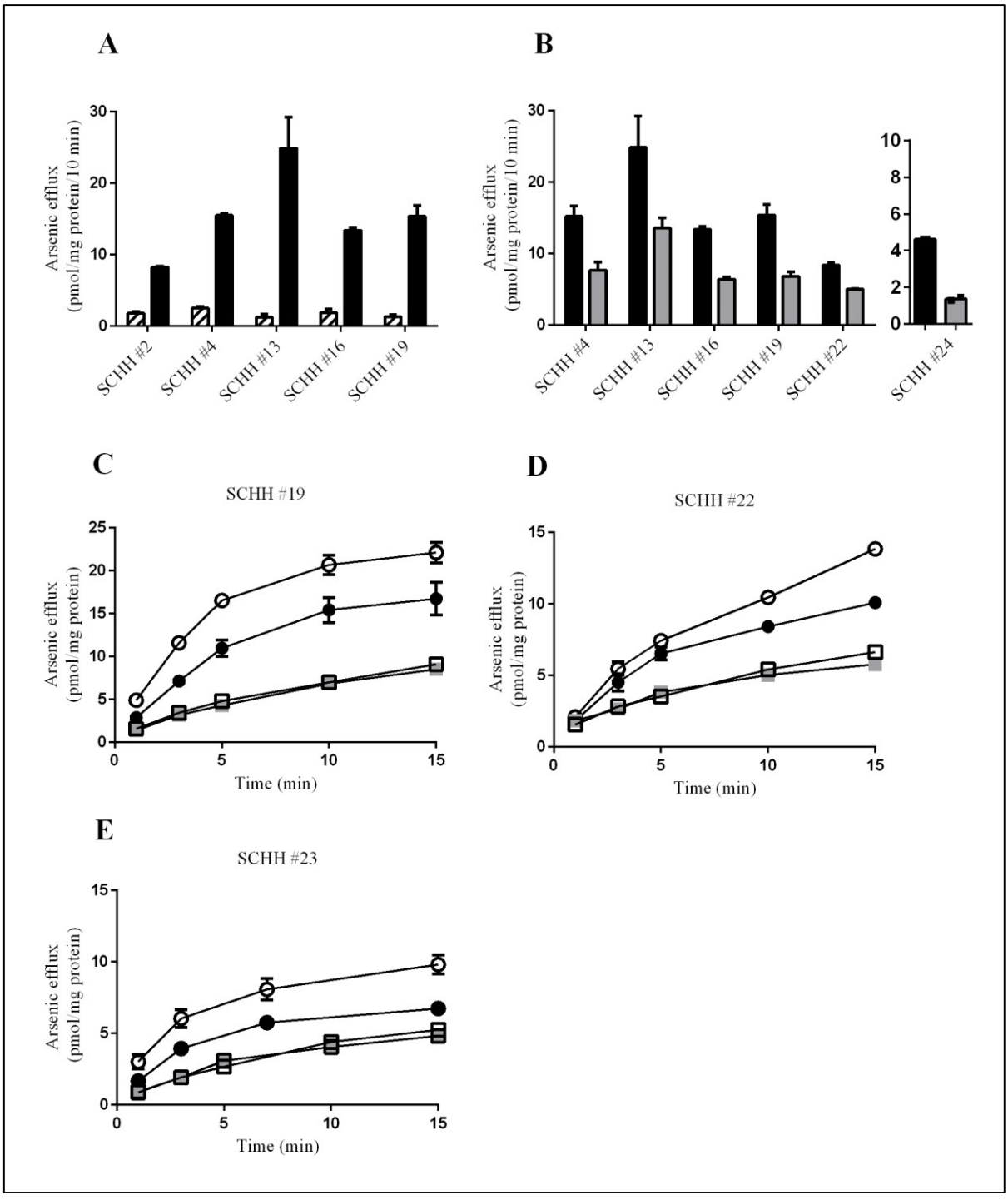

Fig. 3.5. Temperature- and GSH-dependence of arsenic efflux from SCHH.

Temperature- and GSH-dependence of arsenic efflux from SCHH. SCHH were incubated with $^{73}As^{III}$ (1 μM for all SCHH preparations except 0.5 μM for #24; 100 nCi) for 24 h at 37°C in culture media. The influence of (A) temperature and (B) GSH-depletion on basolateral arsenic efflux for multiple SCHH preparations was assessed at a 10 min time point. The influence of GSH-

depletion on the basolateral and canalicular efflux of arsenic was assessed at the indicated time points for (C) SCHH#19, (D) SCHH #22, or (E) SCHH #23. (A) Temperature sensitivity of arsenic efflux was measured in SCHH after replacement of media with either ice cold (hatched bars) or 37°C (black bars) Ca^{2+}-containing HBSS on ice or at 37°C, respectively. (B-E) GSH-dependence was assessed by measuring arsenic efflux from SCHH pre-treated with BSO (0.5 mM) for 48 h (gray bars and ■) and comparing efflux to regular conditions (black bars and ●) in Ca^{2+}-containing HBSS. For (C-E) efflux experiments were also done using Ca^{2+}-free HBSS with (□) and without (○) BSO pretreatment. Bars and data points represent means ± SD for triplicate determinations in a single experiment except (B) SCHH # 24 + BSO condition and (E) SCHH # 23 + BSO condition means of duplicate determinations are shown.

3.2.7 MRP2 levels do not correlate with BEI values for SCHH preparations #19, #21, #22 and #23

To determine if differences in MRP2 protein levels could account for the different levels of biliary excretion observed for SCHH preparations #19 (more extensive biliary excretion), #21 (moderate biliary excretion), #22 (more extensive biliary excretion) and #23 (more extensive biliary excretion), relative MRP2 protein levels in these preparations treated with As^{III} (1 μM) were analyzed by immunoblot (Fig. 3.6A top right, 3.6B left panel). SCHH preparation #19 had the lowest MRP2 level (relative level of 1) while SCHH preparations #21, #22 and #23 were 1.6-, 1.9-, and 1.6-fold higher, respectively. Thus, the total MRP2 levels in SCHH lysates did not correlate with the 3 min BEI values (Table 3.1).

To determine if MRP2 levels were increased by As^{III}, four different SCHH preparations were treated with a single concentration of As^{III} (1 μM) for 24 h and MRP2 levels were compared to untreated controls by immunoblot analysis. MRP2 levels were increased by 7.2, 1.3, 2.6 and 1.6-fold compared to untreated for SCHH preparations #19, #21, #22, and #23 respectively (Fig. 3.6A and B). The SCHH #19 untreated sample had an aberrant Na^+/K^+-ATPase banding pattern (Fig. 3.6A and D). Amido black staining of

the blot showed that the untreated and As^{III} treated #19 samples were evenly loaded, thus the As^{III} treated Na^+/K^+-ATPase band was used to normalize the loading for both samples. To determine if MRP2 levels were increased in a dose-dependent manner, SCHH preparation#23 was treated with three different concentrations of As^{III} for 24 h. Relative to its untreated control MRP2 was increased by 1, 1.9 and 2.2-fold at 0.1, 0.5 and 1 μM As^{III}, respectively (Fig. 3.6C). These results are consistent with previous reports of inorganic As inducing MRP2 mRNA and protein levels in human hepatocytes [189].

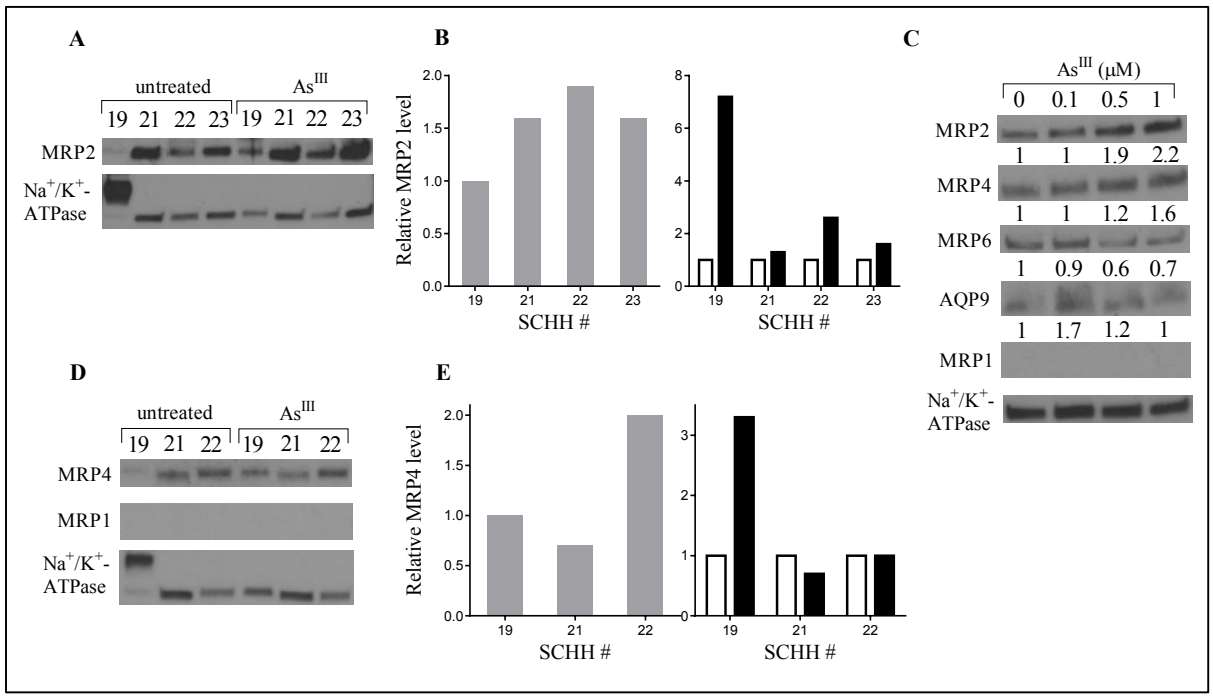

Fig. 3.6. Comparison of protein levels of MRPs and AQP9 in untreated and arsenic treated SCHH preparations.

The relative levels of MRPs and AQP9 in whole cell lysates prepared from the indicated untreated or As^{III} (1μM) treated SCHH preparations were determined after resolving protein (30 μg) by SDS-PAGE followed by immunoblotting with MRP/AQP9 specific antibodies. Blots were stripped between antibodies and the Na^+/K^+-ATPase was used as a loading control. The Na^+/K^+-ATPase loading control for untreated SCHH#19 could not be used due to an aberrant banding pattern. Amido black confirmed that total protein loading for untreated and treated SCHH#19 were equal and therefore the untreated SCHH#19 sample was normalized using the As^{III} treated Na^+/K^+-

ATPase band. Densitometry analysis of the MRP, AQP9, and Na^+/K^+-ATPase bands was performed using ImageJ software. Values shown are from single experiments. (A) MRP2 was detected using the M_2I-4 antibody. (B) Relative levels of MRP2. (Left panel) MRP2 levels in As^{III} treated hepatocytes were normalized for protein loading and plotted relative to MRP2 levels in SCHH #19. (Right panel) MRP2 levels in untreated (open bars) and As^{III} treated (closed bars) hepatocytes were normalized for protein loading and plotted relative to untreated for individual SCHH preparations. (C) The relative levels of MRP2, MRP4, MRP1, MRP6 and AQP9 in whole cell lysates prepared from SCHH #23 untreated or treated with As^{III} (0.1-1μM) were determined using specific antibodies listed in the methods section for each protein. Relative expression of each protein relative to untreated controls is indicated under each blot. (D) MRP4 was detected using the MRP4 antibody M_4I-10. (E) Relative levels of MRP4. (Left panel) MRP4 levels in As^{III} treated hepatocytes were normalized for protein loading and plotted relative to MRP4 levels in SCHH #19. (Right panel) MRP4 levels in untreated (open bars) and As^{III} treated (closed bars) hepatocytes were normalized for protein loading using the Na^+/K^+-ATPase and plotted relative to untreated for individual SCHH preparations.

3.2.8 MRP4 levels are increased by arsenic in SCHH

To determine if MRP4 was increased by As^{III} treatment three different sources of SCHH were treated with a single concentration of As^{III} (1 μM) for 24 h and MRP4 levels were compared to untreated controls by immunoblot analysis. MRP4 was detected in each of these preparations in the absence of As treatment (Fig. 3.6D) although at a relatively low level in SCHH #19. MRP4 levels were modulated by 3.3, 0.7, and 1-fold for SCHH preparations #19, #21, and #22, respectively (Fig. 3.6D and E). To determine if MRP4 levels were increased in a dose-dependent manner, SCHH preparation #23 was treated with three different concentrations of As^{III} for 24 h. Relative to its untreated control MRP4 was increased by 1, 1.2, and 1.6-fold at 0.1, 0.5, and 1 μM As^{III}, respectively.

The influence of As^{III} on protein levels of other basolateral transporters shown previously to mediate cellular efflux of As (MRP1) or that are of potential importance for efflux (MRP6 and AQP9) were also examined by immunoblot analysis. MRP1 was not detected in any of the hepatocyte preparations tested under control or As treated conditions (Fig. 3.6C and D). Relative to its untreated control MRP6 was reduced by 0.9,

0.6, and 0.7-fold at 0.1, 0.5, and 1 μM As^{III}, respectively, in SCHH preparation #23 (Fig. 3.6C). Relative to its untreated control AQP9 was modulated by 1.7, 1.2, and 1-fold at 0.1, 0.5, and 1 μM As^{III}, respectively in SCHH preparation #23 (Fig. 3.6C).

3.2.9 Pharmacological inhibition of arsenic transport in SCHH

MK-571 is a leukotriene D_4 (LTD_4) receptor antagonist that is commonly used as an MRP inhibitor. To determine if MK-571 inhibited the basolateral efflux of As, SCHH preparation #13 was treated with 100 μM MK-571. This resulted in a 25-50% reduction in As efflux over a 15 min time course (Fig. 3.7A).

Phloretin is a commonly used AQP9 inhibitor, reducing permeation of glycerol, MMA^V, DMA^V, and water through AQP9 [89]. To determine if phloretin inhibited the basolateral efflux of As, SCHH preparation #4 was treated with 500 μM phloretin. This resulted in an 80-89% reduction in As efflux across the basolateral membrane over a 15 min time course (Fig. 3.7B). Although phloretin is used as an AQP9 inhibitor it is also known to inhibit numerous other unrelated transport proteins [50,190-192]. Phloretin is a bioflavonoid and compounds from this class can be potent inhibitors of MRPs [193]. The influence of phloretin on MRP4 activity was unknown, thus the effect of increasing concentrations of phloretin on $E_2$17βG transport by membrane vesicles prepared from HEK293 cells over-expressing MRP4 was evaluated. MRP4-dependent transport of $E_2$17βG decreased with increasing concentrations of phloretin with an IC_{50} value of 53 μM (Fig. 3.7C). Therefore, the inhibition of As efflux from SCHH by phloretin could

have been mediated by inhibition of MRP4, AQP9, or any other As efflux transporter inhibited by phloretin.

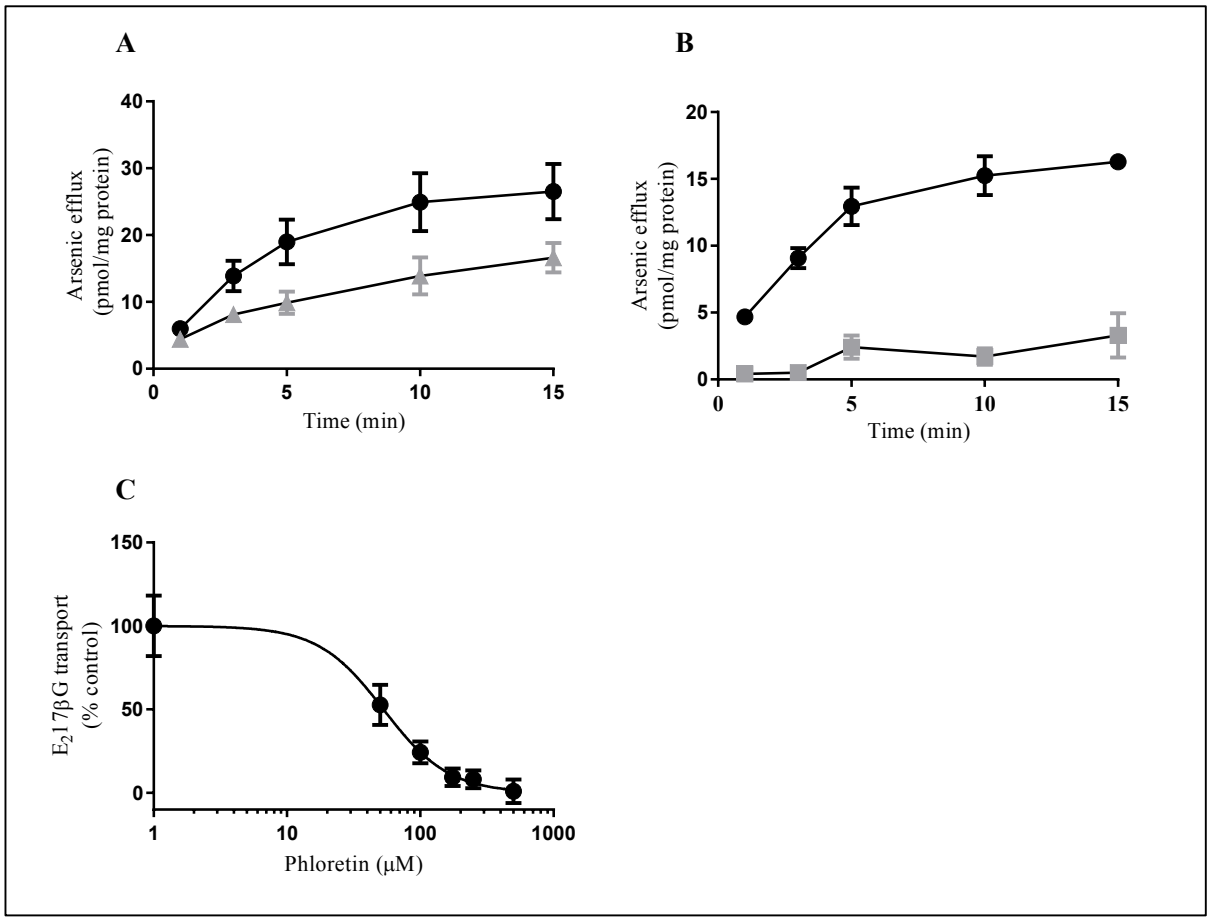

Fig. 3.7. Effect of MK-571 and/or phloretin on basolateral efflux of arsenic from SCHH and transport of $E_2$17βG by MRP4-enriched membrane vesicles.

(A, B) SCHH preparations were incubated with $^{73}As^{III}$ (1 μM; 100 nCi) for 24 h at 37°C in culture media. Thirty minutes prior to the initiation of As efflux the inhibitor was added to the culture media. Media was then replaced with Ca^{2+}-containing HBSS in the absence (●) or presence of (A) MK-571 (100 μM) (▲) or (B) phloretin (500 μM) (■) and As efflux was measured. SCHH preparations #13 and #4 were used in (A) and (B), respectively. (C) The influence of phloretin on ATP-dependent transport of $E_2$17βG by MRP4-enriched membrane vesicles was measured. Membrane vesicles were prepared from HEK293 cells transiently transfected with pcDNA3.1 (+) MRP4. Vesicles (10 μg) were incubated for 3 min at 37°C in transport buffer with $E_2$17βG (1 μM; 80 nCi/pt) in the presence and absence of phloretin (50-500 μM). Points represent means ± SD for triplicate determinations in a single experiment.

3.2.10 Basolateral and biliary arsenic efflux is increased after SCHH pretreatment with the Nrf2 activator oltipraz

Oltipraz is an Nrf2 activator and has been shown to upregulate the expression of several MRPs in human hepatocytes including MRP2, MRP3, and MRP4 (but not MRP6) [168,194]. To determine if SCHH treated with oltipraz (50 μM for 48 h) had altered As efflux, SCHH preparations #19, #22, and #23 were treated with oltipraz and As efflux across the basolateral and canalicular membranes was measured at 10 min (#19 and #22) or 15 min (#23). SCHH preparations #19, #22, and #23 treated with oltipraz showed a 21 ± 4 % (mean ± S.D., n = 3, $p < 0.0003$, Student's t-test) increase in As efflux across the basolateral membrane compared with the untreated control (compare black and gray bars in Fig. 3.8A). In contrast, the BEI was either unchanged or reduced for SCHH treated with oltipraz compared with untreated controls (Fig. 3.8A). Analysis of MRP4 and MRP2 levels in SCHH preparations #22 and #23 by immunoblot revealed a 1.2 to 3.3-fold increase in expression for both of these MRPs after oltipraz + As^{III} treatment compared to As^{III} alone (Fig. 3.8B). These data are consistent with an important role for MRP4 in the basolateral efflux of As and might suggest that if both MRP2 and MRP4 levels are increased the basolateral efflux of As prevails.

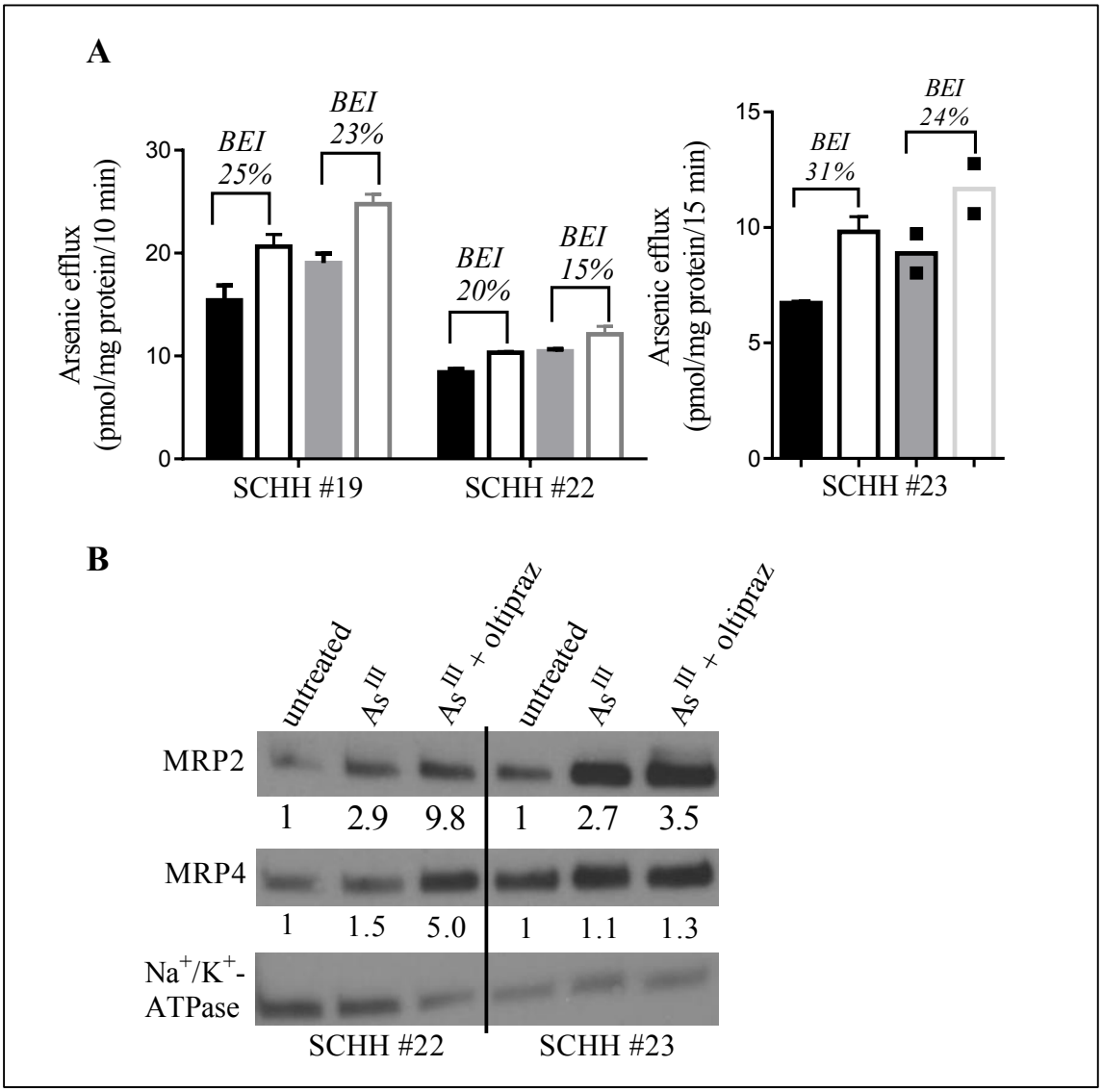

Fig. 3.8. Influence of oltipraz on basolateral and canalicular arsenic efflux from SCHH.

(A) The effects of oltipraz on As efflux from SCHH preparations #19, #22, and #23 was measured in the presence (closed bars) and absence (open bars) of Ca^{2+} and with (gray bars) or without (black bars) a 48 h pretreatment with oltipraz (50 μM). (Left panel) Bars represent means ± SD for triplicate determinations at 10 min in a single experiment for SCHH #19 and #22. (Right panel) For the no oltipraz condition (black bars) bars represent means ± SD of triplicate determinations at 15 min in a single experiment for SCHH #23 while the mean of duplicate values are plotted for the plus oltipraz (gray bars) condition. (B) Immunoblot analysis of whole cell lysates (30 μg) of SCHH preparations #22 and #23 either untreated, treated with As^{III} (1 μM for 24 h) or treated with As^{III} (1 μM for 24 h) plus oltipraz (50 μM for 48 h). MRP2, MRP4, and Na^+/K^+-ATPase were detected with the M_2I-4, M_4I-10, and H-300 antibodies, respectively. Blots were stripped between antibodies and the Na^+/K^+-ATPase was used as a loading control. Densitometry analysis of the MRP2, MRP4, and Na^+/K^+-ATPase bands was performed using ImageJ software. Levels of MRP2 and MRP4 (relative to untreated controls) are indicated with numbers below the blots and are means of duplicate blots.

3.2.11 Inorganic and methylated arsenic species are effluxed across the basolateral surface of SCHH

To determine the chemical species of As effluxed across the hepatocyte basolateral surface, culture media from four different day 6 SCHH preparations treated with 0.5 μM and/or 1 μM As^{III} for 24 h were analyzed by HPLC-ICP-MS (Fig. 3.9A). The HPLC-ICP-MS method used can differentiate between trivalent and pentavalent species of As, however, the trivalent forms are easily oxidized in culture media and during sample storage/preparation. Thus, pentavalent forms identified in culture media are referred to as inorganic As, MMA, and DMA without valency designation. DMA^{V} was the major metabolite detected in culture media accounting for 18, 11, 22, and 14% of total As for SCHH preparations #21, #22, #23 and #26, respectively, treated with 0.5 μM As^{III} (Fig. 3.9A, left panel) and 5% and 9% for SCHH preparations #22 and #23, respectively, treated with 1 μM As^{III} (Fig. 8A, right panel). MMA was detected as 4% and 3% of total As for SCHH preparations respectively, treated with 0.5 μM As^{III} (Fig. 3.9A, left panel) and 2% for SCHH preparation #23, treated with 1 μM As^{III} (Fig. 3.9A, right panel).

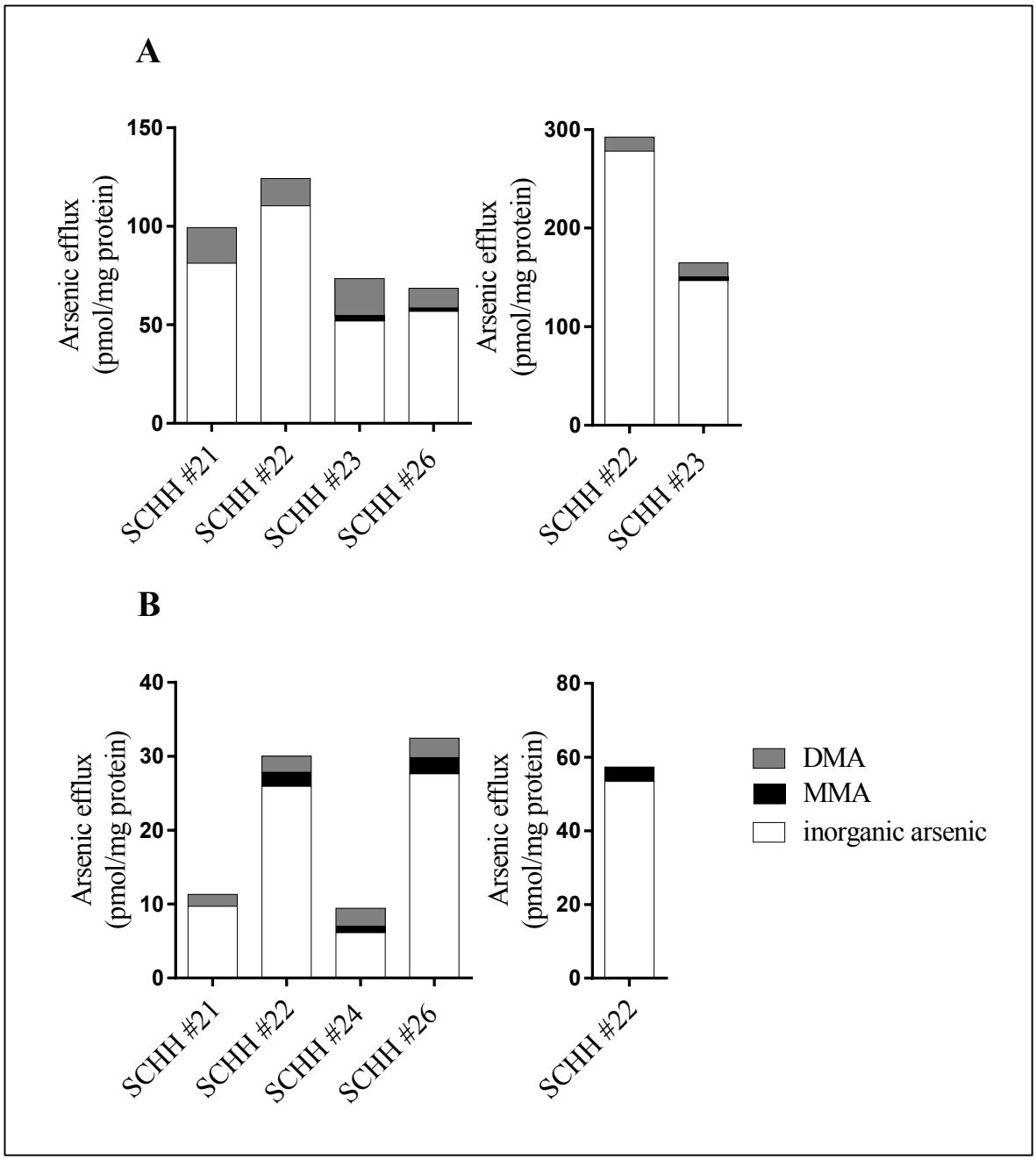

Fig. 3.9. Speciation of arsenic effluxed into culture media of SCHH.

The ability of SCHH to methylate and efflux As was determined. (A) SCHH were incubated for 24 h with (left panel) 0.5 μM As^{III} or (right panel) 1 μM As^{III}, media was then collected and analyzed by HPLC-ICP-MS as described in Materials and Methods. (B) SCHH were then washed and incubated with fresh As-free media for 1 h, media was then collected from the (left panel) 0.5 μM As^{III} or (right panel) 1 μM As^{III} treated SCHH and analyzed as above. Arsenic species are plotted as total inorganic (open bars), total monomethylated (MMA, black bars), and total dimethylated (DMA, gray bars).

Experiments were then done to determine the species of As effluxed across the basolateral surface of the hepatocyte under conditions more closely resembling the efflux assay. After treatment with 0.5 μM and/or 1 μM of As^{III} for 24 h SCHH preparations #21, #22, #24 and #26 were washed then incubated with As-free media for 1 h at 37ºC. Culture media were then collected and analyzed by HPLC-ICP-MS. DMA was again the major metabolite detected accounting for 14, 7, 26, and 9% of total As for SCHH preparations #21, #22, #24 and #26, respectively, treated with 0.5 μM As^{III} (Fig. 3.9B, left panel) and 0% for SCHH preparation #22 treated with 1 μM As^{III} (Fig. 3.9B, right panel). Under these conditions only MMA^{III} (and no MMA^{V}) was detected at 0, 6, 9, and 8% of total As for SCHH preparations #21, #22, #24 and #26, respectively, treated with 0.5 μM As^{III} (Fig. 3.9B, left panel) and 6.8% for SCHH preparation #22 treated with 1 μM of As^{III} (Fig. 3.9B right panel).

These results are consistent with previous reports of As methylation by primary human hepatocytes [61,80,195]. Variability was seen in the methylation pattern between donors and methylation was reduced with increasing concentrations of As [see Fig. 3.9A and B, left panels (0.5 μM) compared to right panels (1 μM)]. Overall these results show that SCHH methylate As and that inorganic and methylated forms are being transported across the basolateral membrane of hepatocytes.

3.3 Discussion

We present the first characterization of As hepatobiliary transport using primary human hepatocytes cultured in a sandwich configuration. In humans, approximately 80% of ingested As is eliminated in urine, predominantly as methylated metabolites (formed in liver). Consistent with this, nine out of fourteen SCHH preparations had only basolateral hepatic efflux while the remaining five had some degree of biliary excretion along with basolateral efflux. Basolateral efflux of As was temperature sensitive, partially GSH-dependent and inhibited by phloretin and MK-571. These characteristics of transport suggest a significant portion of total As basolateral efflux is likely mediated by an MRP. Based on our previous studies one likely basolateral candidate is MRP4 [82]. Consistent with this, low concentrations of As induced the level of MRP4 in SCHH in a dose-dependent manner. In addition, the Nrf2 activator oltipraz increased the basolateral efflux of As and the levels of MRP4.

Glutathione depletion reduced the basolateral efflux of As by ~50%. This partial GSH-dependence is consistent with the ability of MRP4 to transport MMA^{III} as a GSH conjugate and DMA^{V} in a GSH-independent manner [82]. Speciation analysis of culture media from cells treated under conditions most closely resembling the ^{73}As efflux assays (Fig. 3.9B) revealed that DMA and MMA^{III} were effluxed across the basolateral surface of multiple SCHH preparations, consistent with the substrate specificity of MRP4. Arsenic-GSH conjugates were not detected likely due to their chemical instability in culture media and during sample handling/storage[(reviewed in [109]], however, some of the MMA^{III} in the media could be derived from $MMA(GS)_2$. Presumably other transport

proteins and channels also contribute to the basolateral efflux of As. This is especially true for inorganic forms, which composed the majority of As species in SCHH culture media (Fig. 3.9), but are not substrates for MRP4. Basolateral efflux of $As(GS)_3$ by another MRP would fit with the GSH-dependence (Fig. 3.5B) and MK571 inhibition (Fig. 3.7A) of total As transport. We have recently shown that the basolateral MRP3 and MRP5 do not confer cellular resistance to inorganic or methylated As species (Chapter 4). MRP6 is also located at the appropriate surface of the hepatocyte for basolateral efflux of As. However, its role in As transport is unknown. MRP6 protein levels were not increased by As treatment suggesting it might not be important, but cytotoxicity and direct transport studies are needed to confirm this.

In addition to MRPs, human AQP9 is an efficient pathway for As^{III} and MMA^{III} uptake and expressed at the basolateral membrane of human hepatocytes [196]. AQPs are bidirectional channels. Thus, if the free concentration of certain As species inside the cell is higher than blood levels, As can potentially pass through AQP9 down its concentration gradient out of the hepatocyte into the blood. AQP9 is capable of transporting only neutral species of As which include As^{III} and MMA^{III}, but not GSH conjugates and the predominant forms of MMA^{V} and DMA^{V} at physiological pH [89]. GLUTs might also contribute to the GSH-independent transport of inorganic and methylated As species across the basolateral surface of the hepatocyte [90].

In contrast with the basolateral efflux of As, biliary efflux was completely lost after depleting hepatocytes of GSH. This observation was consistent with *in vivo* rat studies that show As biliary excretion results from Mrp2-dependent transport of $As(GS)_3$ and $MMA(GS)_2$ [107]. The complete lack of biliary excretion in certain SCHH

preparations was surprising given the extensive biliary excretion of As which occurs in rats prior to enterohepatic cycling [107,158,197,198]. Arsenic has been detected in bile from patients with T-tubule drainage post-gallstone removal, suggesting As can undergo biliary excretion in humans [199]. This study was somewhat limited by the small patient number (n=3) and the pathological state. A second study of healthy humans dosed orally with ^{74}As showed that 6% of the As dose was recovered in feces, however, it's not known if this was unabsorbed or from intestinal/biliary excretion [200]. Thus, very little information exists regarding the hepatobiliary handling of As in humans.

The increased efflux of As under Ca^{2+}-free compared with Ca^{2+}-containing conditions in five SCHH preparations showed that this model is suitable for the detection of both basolateral and biliary excretion of As. Experimental conditions should have promoted biliary excretion of As because SCHH were allowed to metabolize and accumulate As in canalicular networks for 24 h prior to measuring efflux. Despite this, basolateral efflux was the only efflux detected in the majority of the preparations. The reasons for variations in the extent of biliary excretion of As between the human hepatocyte preparations used in this study are not clear. One obvious possibility would be a lack of functional MRP2 in preparations lacking biliary excretion. However, accumulation of the MRP2 substrate CDF in the canalicular networks of SCHH preparations that did not transport As into bile argues against this possibility. Another possible explanation for a lack of biliary efflux could be that As reduces the integrity of the canalicular networks preventing its accumulation. However, CDF was still accumulated in canalicular networks of SCHH preparation pretreated with As^{III}, suggesting that networks were intact.

Based on the GSH-dependent nature of As biliary excretion observed with SCHH and previous studies with rats [107], human MRP2 is predicted to play a major role in the biliary excretion of As in humans. However, we found that MRP2 protein levels did not dictate the extent of biliary excretion when MRP2 levels were evaluated using whole cell lysates. However, this does not preclude the possibility that the levels of functional MRP2 residing in the plasma membrane accounts for the extent to which As undergoes biliary excretion. MRP2 (gene symbol *ABCC2*) is known to be highly polymorphic and there could be genetic variation in *ABCC2* expressed in these SCHH preparations that influences As transport activity. Factors other than MRP2 (e.g., basolateral efflux pathways and methylation), could also influence the extent of As biliary excretion. While it is known that $As(GS)_3$ is transported by human MRP2, little is known about its ability to transport methylated As metabolites.

Considerable species differences exist in the biliary excretion of MMA^{III}. Thus while rat, mouse, hamster, guinea pig, and rabbit excrete As^{III} into bile, only rats excrete MMA^{III} into bile [as $MMA(GS)_2$] [47,107]. Therefore, it is possible that $MMA(GS)_2$ is a major metabolite formed in the hepatocyte but in humans it doesn't undergo biliary excretion. The extent and pattern of As methylation is known to vary greatly between primary human hepatocyte preparations [61,80,195] and similar variability was observed with the SCHH model (Fig. 3.9). It is almost certain that the As species formed in the hepatocyte will influence the extent of biliary versus basolateral excretion, depending on the substrate specificity and affinity of the canalicular and sinusoidal transport pathways for different species of As.

In addition to methylation and efflux pathways it is important to consider the extent of As cellular accumulation and how this might influence the degree of biliary and basolateral efflux. Accumulation of As in the four SCHH preparations varied approximately 2-fold (Fig. 3.2B) and a previous study using primary human hepatocytes cultured on a single layer of collagen reported a variation of 3- to 4-fold [80]. While this difference in accumulation could have a direct effect on the extent of basolateral and biliary efflux, several data in the current manuscript suggest this is not the case. To begin with, it is known that there is a linear relationship between the concentration of As^{III} in cell culture media and accumulation by primary human hepatocytes up until at least 10 μM As^{III} [80]. Despite this, the initial concentration of As^{III} did not influence the polarized transport of total As (Fig. 3.4). Furthermore, while SCHH preparations #2 and #5 had very similar accumulation levels (Fig. 3.2B; 536 pmol mg^{-1} protein 24 h^{-1} versus 563 pmol mg^{-1} protein 24 h^{-1}, respectively) SCHH #2 had ~8-fold lower efflux activity at 10 min than SCHH #5 (Fig. 3.1C compared with 3.1E). SCHH #2 also exhibited moderate biliary excretion while SCHH #5 did not (Fig. 3.1C and 3.1E). Accumulation of As was also similar for SCHH #4 and #26, but unrelated to efflux activity (Fig. 3.2B, Fig. 3.1D and Fig. 3.1O). These data suggest accumulation does not dictate the extent or direction of efflux.

MRP4 is a high affinity transporter of $MMA(GS)_2$ and DMA^V with $K_{0.5}$ of 0.70 ± 0.16 μM and 0.22 ± 0.15 μM, respectively [82]. While it is not known if human MRP2 can transport $MMA(GS)_2$ or DMA^V it is a well characterized transporter of $As(GS)_3$ with a lower affinity (K_m of 4.2 μM) [84] compared to MRP4 transport of $MMA(GS)_2$ and DMA^V. Thus at low concentrations of As, it would be expected that MRP4 would

transport the majority of DMA^V and $MMA(GS)_2$ out of the hepatocyte, thus shunting As into blood rather than bile. This is consistent with the oltipraz induction of MRP2 and MRP4 that resulted in increased basolateral efflux of As with no change in the BEI. Thus, polymorphic variants of MRP4 or other basolateral As transporters might have more influence on the polarity of As transport than polymorphic variants of MRP2.

In summary, the physiologically relevant SCHH model has been used to characterize human hepatobiliary excretion of As. Consistent with the predominant urinary excretion of As in humans, basolateral transport was the prevailing pathway. Characteristics of the basolateral transport of As suggest it is mediated at least in part by an MRP. The current study in combination with previous work [82] suggest that MRP4 is a likely candidate. GSH-dependent hepatic basolateral transport pathways for inorganic As are yet to be identified. Previous studies have shown a strong correlation between xenobiotic *in vivo* biliary excretion and the BEI determined using human and rat SCH [67,68]. The current study strongly suggests that inter-individual differences exist in the extent of biliary excretion of As in humans. The possibility that genetic differences among human hepatocyte donors (in both efflux and methylation pathways) contribute to altered canalicular and basolateral transport pathways is worthy of further investigation.

Chapter 4

MRP3 and MRP5 Do Not Protect HEK293 Cells from Inorganic, Monomethylated, or Dimethylated Arsenic Species

Barbara A. Roggenbeck completed all experiments except Fig. 4.5, 4.6, and Table 4.3, which were completed by Michael W. Carew and Mayukh Banerjee. Table 4.1, 4.2, 4.3 and data from Fig. 4.5 and 4.6 of this chapter were published in *Banerjee, M., Carew, M.W., Roggenbeck, B.A., Whitlock, B.D., Naranmandura, H., Le, X.C., and Leslie, E.M.*, A Novel Pathway for Arsenic Elimination: Human Multidrug Resistance Protein 4 (MRP4/ABCC4) Mediates Cellular Export of Dimethylarsinic Acid (DMA^V) and the Diglutathione Conjugate of Monomethylarsonous acid (MMA^{III}), Molecular Pharmacol. 2014 Aug;86(2):168-79. doi: 10.1124/mol.113.091314. Epub 2014 May 28. Anaida Osoria Perez assisted with the confocal imaging. Diane P. Swanlund assisted with the MRP5 stable cell line cloning and performed the FACS analysis on the MRP5 stable cell line.

4.1 Introduction

Millions of people worldwide are exposed to unacceptable levels of As in their drinking water. This is considered a public health crisis because As is classified as a group I (proven) human carcinogen that upon chronic exposure can result in lung, skin, and bladder cancer [3]. Furthermore, As exposure has been associated with a myriad of other adverse health effects such as peripheral vascular disease, diabetes mellitus, and neurological disorders.

The liver is the predominant site of As metabolism where As undergoes extensive methylation in most animal species. In humans, 60-80% of As is excreted in urine as inorganic (10-30%), monomethylated (10-20%), and dimethylated (60-80%) species [70,201]. Very little is known about how As is effluxed across the basolateral membrane of human hepatocytes into the systemic circulation so that it can be eliminated at the kidneys. We and others have shown that multidrug resistance proteins transport As glutathione conjugates [107,109]. MRP1 transports $As(GS)_3$ and $MMA(GS)_2$ and is localized to the basolateral membrane of polarized cells but MRP1 protein is not detectable in healthy human hepatocytes, however, there are low levels of MRP1 mRNA [162,202]. MRP2 transports $As(GS)_3$ and $[GS_2AsSe]^-$ and is localized to the apical membrane of hepatocytes where it plays a role in biliary excretion [84]. Studies using Mrp2-deficient (TR^-) Wistar rats have shown that Mrp2 is responsible for biliary excretion of both $As(GS)_3$ and $MMA(GS)_2$ [107]. Transport of As-GSH conjugates (except $[GS_2AsSe]^-$), into bile would result in conjugate disassembly because they are

not stable at alkaline pH. Thus, free As can undergo enterohepatic recirculation, rendering this a poor means of elimination.

There are four candidate MRPs at the basolateral surface of human hepatocytes that might play a role in As efflux into the systemic circulation: MRP3, MRP4, MRP5, and MRP6. Previous studies have shown that, MRP3, MRP4, and MRP5 do not confer resistance to inorganic As, however, their ability to protect cells from methylated As species was never investigated [143,203-205]. Therefore, the ability of MRP3, MRP4, and MRP5 to confer resistance to both inorganic and methylated As species was investigated by the Leslie laboratory. The involvement of MRP3, MRP4, and MRP5 in methylated and inorganic As detoxification is presented in this chapter. The involvement of MRP4 in the detoxification of inorganic and methylated arsenicals has been previously reported, but is summarized here [82]. The role of MRP6 in As detoxification is currently under investigation.

The objectives of the study were to generate HEK293 cells stably expressing MRP3 or MRP5 and to test their ability to confer cellular protection against As^{III}, As^{V}, MMA^{III}, MMA^{V}, DMA^{III}, or DMA^{V} compared to cells expressing empty vector. MRP3 and MRP5) did not reduce the toxicity and accumulation of any As species tested. In contrast, MRP4 conferred resistance to all As species tested except for As^{III}. The species of arsenic transported by MRP4 were then identified using membrane vesicle transport assays [82]. This work combined with our observations in SCHH (Chapter 3) showed that MRP3 and MRP5 did not confer resistance to As and supported an important role for MRP4 in As transport across the basolateral surface of the hepatocyte.

4.2 Results

4.2.1 $As(GS)_3$ is not transported by MRP3 - and MRP5 - enriched membrane vesicles

To determine if $As(GS)_3$ was a substrate for MRP3 and/or MRP5, direct transport was measured using MRP3- and MRP5-enriched membrane vesicles. To determine if MRP3-enriched vesicles were functional, ATP-dependent transport of $E_2$17βG (1 μM, 40 nCi), a known substrate of MRP3, was measured. ATP-dependent transport was observed with an activity of 80 $pmol^{-1}$ mg^{-1} protein min^{-1} (Fig. 4.1A). In contrast, MRP3 transport of $As(GS)_3$ (100 nM) was not different than the HEK- vector control (Fig. 4.1B). To determine if MRP5-enriched membrane vesicles were functional, ATP-dependent transport of ^{3}H-methotrexate (1μM), a known substrate of MRP5, was measured. ATP-dependent transport was observed with an activity of 40 $pmol^{-1}$ mg^{-1} protein min^{-1} (Fig. 4.1C). MRP5 transport of 1 μM $As(GS)_3$ was not different than vector, however, MRP1 transport was observed indicating that $As(GS)_3$ is not a substrate of MRP5 (Fig. 4.1D).

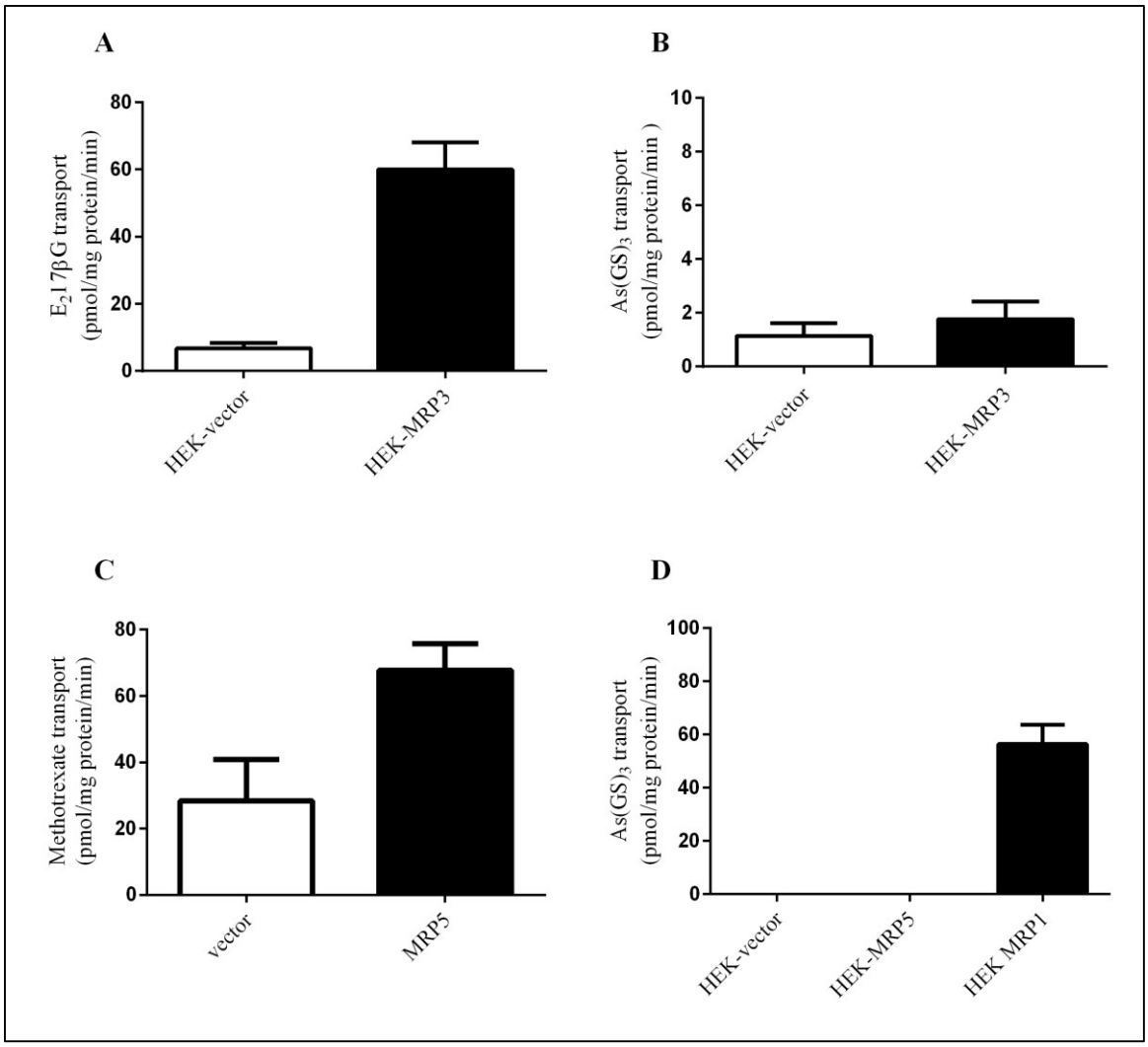

Fig. 4.1. ATP-dependent transport of ^{3}H-$E_2$17βG, $^{73}As(GS)_3$, or ^{3}H-methotrexate by MRP3- or MRP5- enriched membrane vesicles.

Transport experiments were performed with membrane vesicles (20 µg) incubated at 37°C in transport buffer prepared from HEK293 cells stably expressing HEK- V4 (open bars) or HEK293 – MRP (closed bars). (A) Vesicles were incubated for 3 min with $E_2$17βG (1 µM, 40 nCi). (B) Vesicles were incubated with $As(GS)_3$ (1 µM, 100 nCi) (C) Vesicles were incubated for 20 min with methotrexate (1 µM, 1 µCi). (D) Vesicles were incubated for 3 min at 37°C in transport buffer with $As(GS)_3$ (1 µM, 100 nCi). Bars represent triplicate points of a single experiment (± S.D.).

4.2.2 HEK293 cells stably expressing MRP3 or MRP5 did not confer protection against As^{III}, As^{V}, MMA^{III}, MMA^{V}, DMA^{III}, or DMA^{V}

To determine if MRP3 or MRP5 provided cellular protection to HEK293 cells, stable cell lines were generated expressing MRP3 or MRP5. The MRP3-18 and MRP5-2-6 stable cell lines displayed cell populations of > 80% expressing MRP3 or MRP5 by confocal microscopy. (Fig. 4.2A and B). The MRP5 clonal population was further confirmed by flow cytometry (Fig. 4.2C). A stable HEK vector cell line previously generated in the lab was used as a negative control [82].

Levels of MRP3 and MRP5 in plasma membrane enriched vesicles prepared from stable HEK-vector, HEK-MRP3, and HEK-MRP5 cell lines were also assessed by immunoblot (Fig. 4.3). Plasma membrane enriched vesicles were resolved by SDS-PAGE followed by immunoblotting with anti-MRP3 or anti-MRP5 antibody. Blots were incubated with Na^{+}/K^{+} - ATPase to visualize loading of the plasma membrane vesicles. The HEK-vector plasma membrane vesicles had undetectable levels of MRP3 and MRP5 (Fig. 4.3A and B). MRP3 was detected in HEK-MRP3 membrane vesicles using the M_3II-9 antibody (Fig. 4.3A). MRP5 was detected in HEK-MRP5 membrane vesicles using the M_5I-1 antibody (Fig. 4.3B).

The HEK - vector and HEK - MRP stable cell lines were treated with increasing concentrations of As^{III}, As^{V}, MMA^{III}, MMA^{V}, DMA^{III}, or DMA^{V}. The EC_{50} value for each As species was calculated from the ratio of HEK - MRP and HEK - vector EC_{50} values. The HEK293 cells stably expressing MRP3 or MRP5 conferred appropriate

levels of resistance to positive controls. The MRP3 stable cell line conferred a 7-fold higher level of resistance to etoposide which is consistent with previously published data [206] (Table 4.1) (Fig. 4.3A). Consistent with previously published results, the MRP5 stable cell line conferred a 2-fold higher level of resistance to 6-mercaptopurine compared to the HEK-V4 control (Table 4.2) (Fig. 4.3C) [207]. The HEK293 cells stably expressing MRP3 or MRP5 did not confer resistance to any of the As species tested compared with empty vector HEK cells (Tables 4.1 and 4.2) (Fig 4.3B and 4.3D).

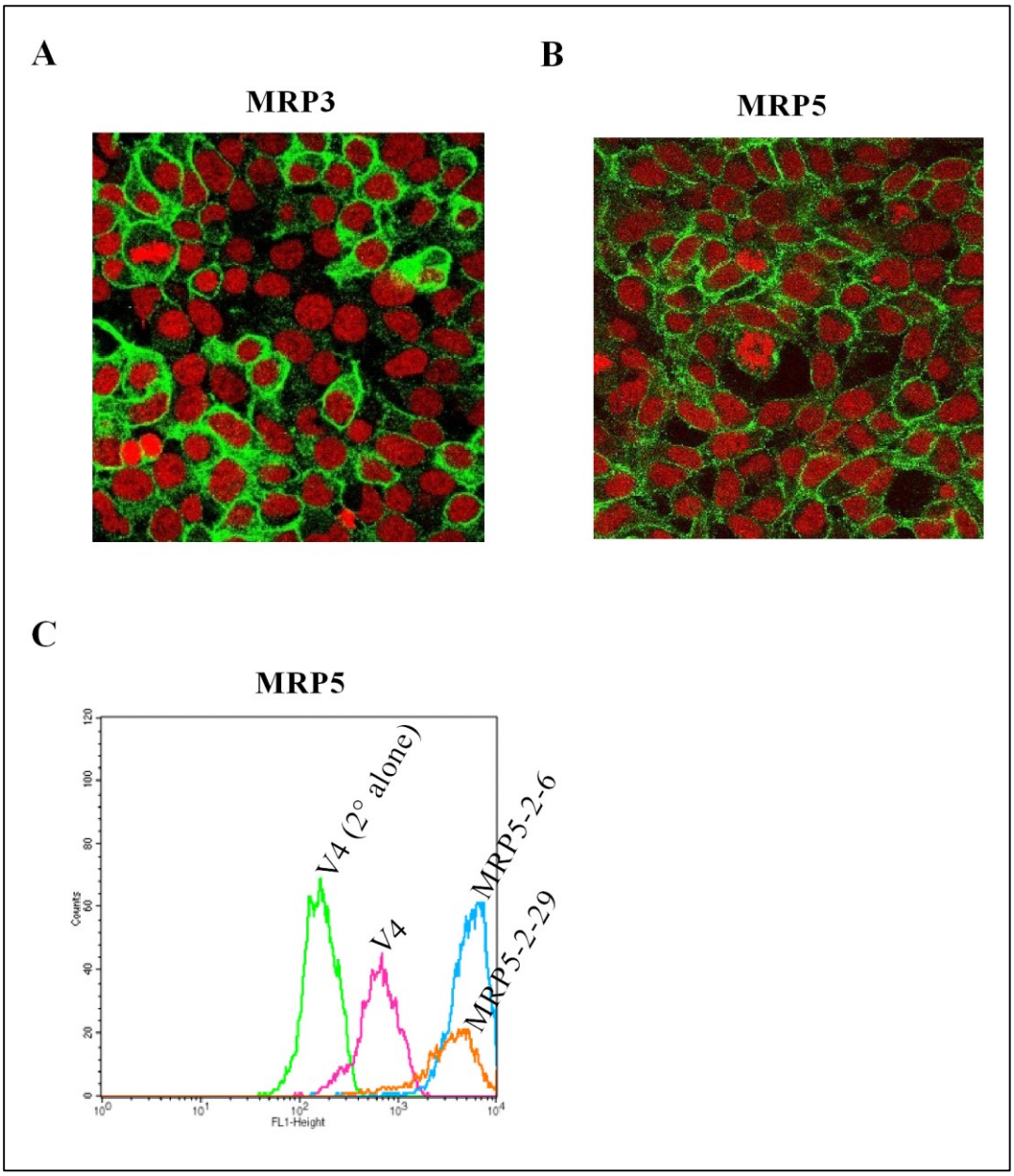

Fig. 4.2. Stable expression of MRP3 or MRP5 in HEK293 cells.

Confocal microscopy of (A) HEK-MRP3-18 and (B) HEK-MRP5-2-6 stable cell lines was done using either anti-MRP3 or anti-MRP5 and visualizing with Alexa-Fluor 488 secondary antibody (green). Nuclei were stained with propidium iodide. MRP3 and MRP5 were not detected in the HEK-V4 cells (data not shown). MRP3 and MRP5 were localized to cell membranes and the population of cells expressing the MRP was > 80%. (C) Flow cytometry was performed on HEK-V4 cells stained with secondary antibody alone (green) or anti-MRP5 antibody (pink) and compared to the HEK-MRP5 clones MRP5-2-6 (blue) and MRP5-2-29 (orange).

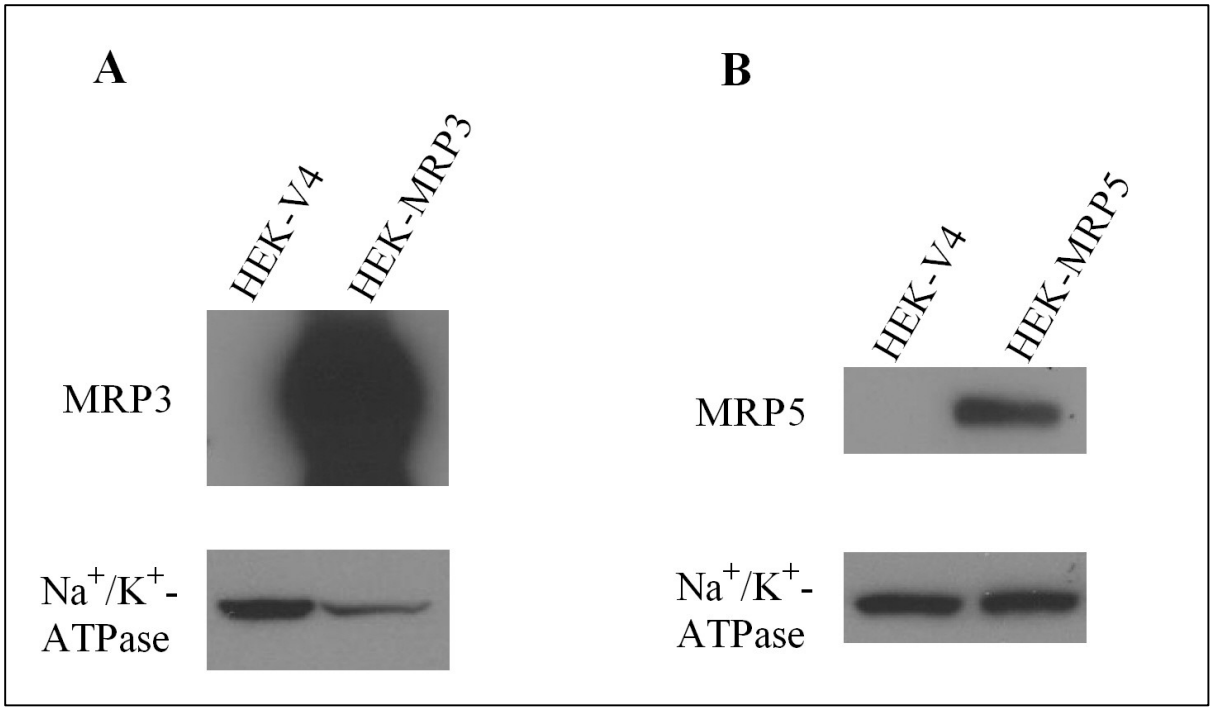

Fig. 4.3. Levels of MRP3 and MRP5 in plasma membrane enriched vesicles.

Immunoblot analysis of plasma membrane vesicles (2 µg) prepared from HEK293 cells stably expressing empty pcDNA 3.1 (+) (HEK - V4) compared to (A) pcDNA 3.1 (+) - MRP3 (MRP3-18) or (B) pcDNA 3.1 (+) - MRP5 (MRP5-2-6). Blots were probed with MRP3 (M_3II-9) or MRP5 (M_5I-1) antibodies, stripped, and probed with the Na^+/K^+- ATPase (H-300) antibody to visualize protein loading.

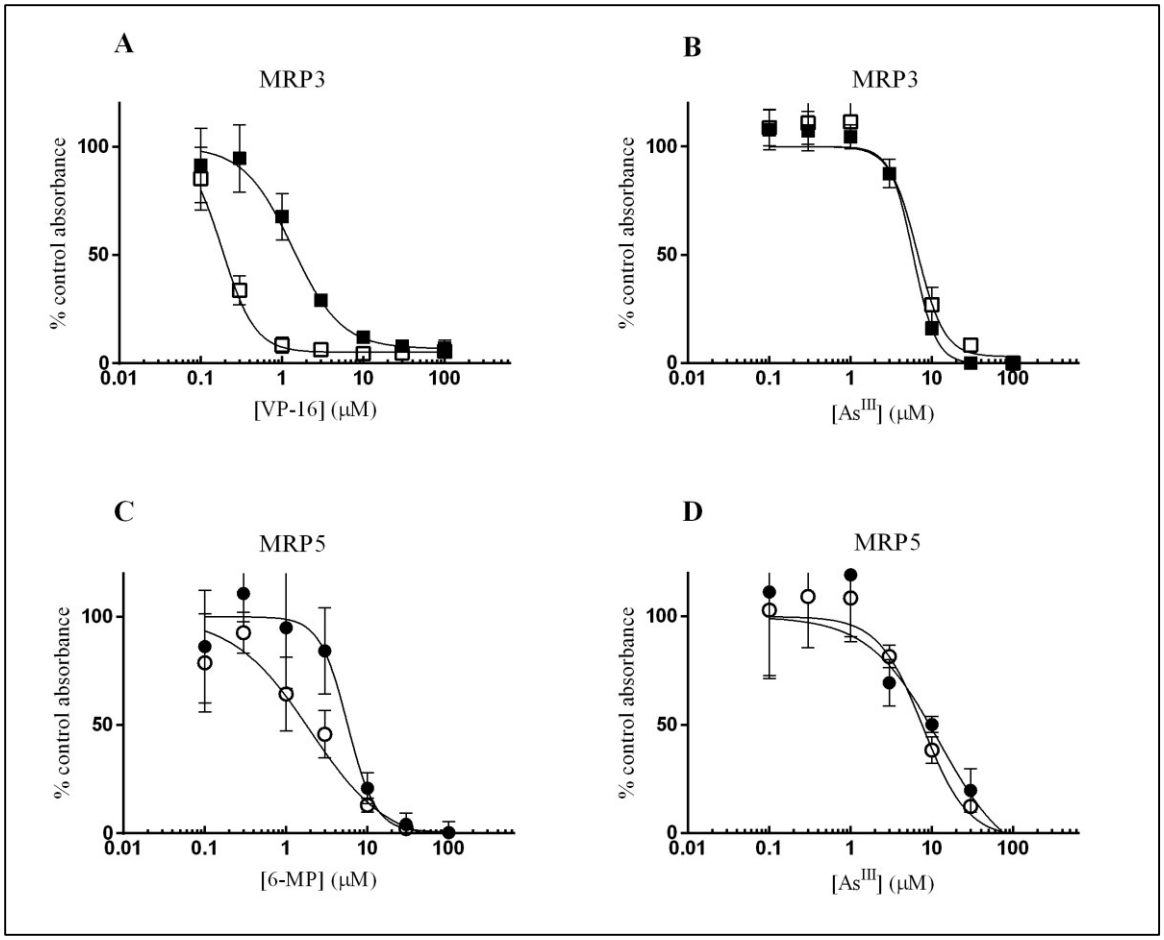

Fig. 4.4. Effect of etoposide (VP-16), As^{III}, and 6-mercaptopurine (6-MP) on the viability of MRP3 and/or MRP5 stably transfected HEK293 cells.

Cells expressing empty vector (open squares or circles), (A and B) MRP3 (closed squares), or (C and D) MRP5 (closed circles) were incubated in the presence of a positive control ((A) (VP-16) or (C) (6-MP)) or (B and D) As^{III} for 72 h. Cell viability was determined using a tetrazolium- based (MTS) cytotoxicity assay. Data points are means (± S.D.) of quadruplicate determinations in a representative experiment and similar results were obtained in at least two additional experiments for the positive control and As^{III}. Mean EC_{50} and relative resistance values are shown in Table 4.1 and 4.2.

Table 4.1 Resistance of human MRP3 transfected HEK293 cells to inorganic and methylated arsenic species

	EC_{50} (± S.D.)[a]		Relative Resistance[b]
	HEK-V4	HEK-MRP3	(± S.D.)
As^{III} *(n =3)*	5.5 ± 2.3	4.3 ± 1.6	0.8 ± 0.1
As^{V} *(n = 4)*	22 ± 7.9	34 ± 14	1.5 ± 0.2
MMA^{III} *(n = 3)*	1.5 ± 0.7	1.3 ± 0.3	0.9 ± 0.2
MMA^{V} *(n = 3)*	0.63 ± 0.1[c]	0.66 ± 0.03[c]	1.0 ± 0.2
DMA^{III} *(n = 2)*	0.5; 0.6	0.1; 0.7	0.3; 1.1
DMA^{V} *(n = 3)*	0.8 ± 0.1[c]	0.7 ± 0.1[c]	1.0 ± 0.1
Etoposide *(n=8)*	0.2 ± 0.1	1.3 ± 0.6*	6.9 ± 1.6

*EC_{50} for HEK-MRP3 is significantly different from HEK-V4, $P < 0.05$ (Student's *t* test).

[a]Values are given in μM unless otherwise indicated.

[b]Mean of the ratio of EC_{50}HEK-MRP3/ EC_{50} HEK-V4

[c]Values are given in mM

Table 4.2. Resistance of human MRP5 transfected HEK293 cells to inorganic and methylated arsenic species

	EC_{50} (± S.D.)[a]		Relative Resistance[b]
	HEK-V4	HEK-MRP5	(± S.D.)
As^{III} (*n =5)*	7.7 ± 2.8	7.4 ± 3	1.0 ± 0.4
As^{V} *(n = 3)*	33 ± 7.8	22 ± 5	0.7 ± 0.2
MMA^{III} *(n = 5)*	1.4 ± 0.5	1.7 ± 0.9	1.2 ± 0.4
MMA^{V} *(n = 3)*	0.62 ± 0.1[c]	0.55 ± 0.19[c]	0.9 ± 0.3
DMA^{III} *(n = 4)*	0.6 ± 0.2	0.8 ± 0.1	1.3 ± 0.5
DMA^{V} *(n = 6)*	1.1 ± 0.3[c]	0.9 ± 0.3[c]	0.7 ± 0.1
6-MP *(n = 8)*	3.3 ± 1.2	6.4 ± 1.5*	2.1 ± 0.8

EC_{50} for HEK-MRP5 is significantly different from HEK-V4, $P < 0.05$ (Student's *t* test).

[a]Values are given in μM unless otherwise indicated.

[b]Mean of the ratio of EC_{50}HEK-MRP5/ EC_{50} HEK-V4

[c]Values are given in mM

4.2.3 MRP4 confers resistance to monomethylated and dimethylated arsenic metabolites

While I was examining the ability of MRP3 and MRP5 to provide cellular protection against arsenicals, other laboratory members were working on the role of MRP4. To determine if MRP4 was capable of conferring resistance to inorganic and methylated species of arsenic, stable HEK-MRP and HEK-vector cell lines were generated and treated with increasing concentrations of As^{III}, As^{V}, MMA^{III}, MMA^{V}, DMA^{III}, and DMA^{V}. The EC_{50} value for each arsenical was determined and the relative resistance was calculated from the ratio of the EC_{50} values for HEK-MRP and HEK-vector (Table 4.3). HEK-MRP4-1E16 conferred low (1.5 to 3-fold), but significant levels of resistance to As^{V}, MMA^{III}, MMA^{V}, DMA^{III}, and DMA^{V}, compared to empty vector controls (Table 4.3 and Fig. 4.5) [82]. HEK-MRP4-1E16 conferred a 5-fold level of resistance to 6-MP (positive control) compared to HEK-V4 (Table 4.3 and Fig 4.5) [82].

Table 4.3. Resistance of human MRP4 transfected HEK293 cells to inorganic and methylated arsenic species

Arsenic Species	EC_{50} (± S.D.) [a]		Relative Resistance[b]
	HEK-V4	HEK-MRP4-1E16	(± S.D.)
As^{III} *(n = 6)*	3.1 ± 0.8	2.7 ± 1.5	0.7 ± 0.3
As^{V} *(n = 9)*	20 ± 8.1	49 ± 15 *	2.9 ± 1.8
MMA^{III} *(n =9)*	1.7 ± 0.4	2.9 ± 0.5 *	1.7 ± 0.4
MMA^{V} *(n = 4)*	0.54 ± 0.08[c]	0.81 ± 0.14 [c] *	1.5 ± 0.1
DMA^{III} *(n = 7)*	0.7 ± 0.1	1.2 ± 0.2 *	2.0 ± 0.6
DMA^{V} *(n = 8)*	0.8 ± 0.1 [c]	1.2 ± 0.2 [c] *	1.6 ± 0.3
6-MP *(n = 6)*	5.1 ± 1.9	26 ± 5.8*	5.4 ± 1.4

EC_{50} for HEK-MRP4-1E16 is significantly different from HEK-V4, $P < 0.05$ (Student's *t* test).

[a]Values are given in μM unless otherwise indicated.

[b]Mean of the ratio of EC_{50}HEK-MRP4/ EC_{50} HEK-vector

[c]Values are given in mM

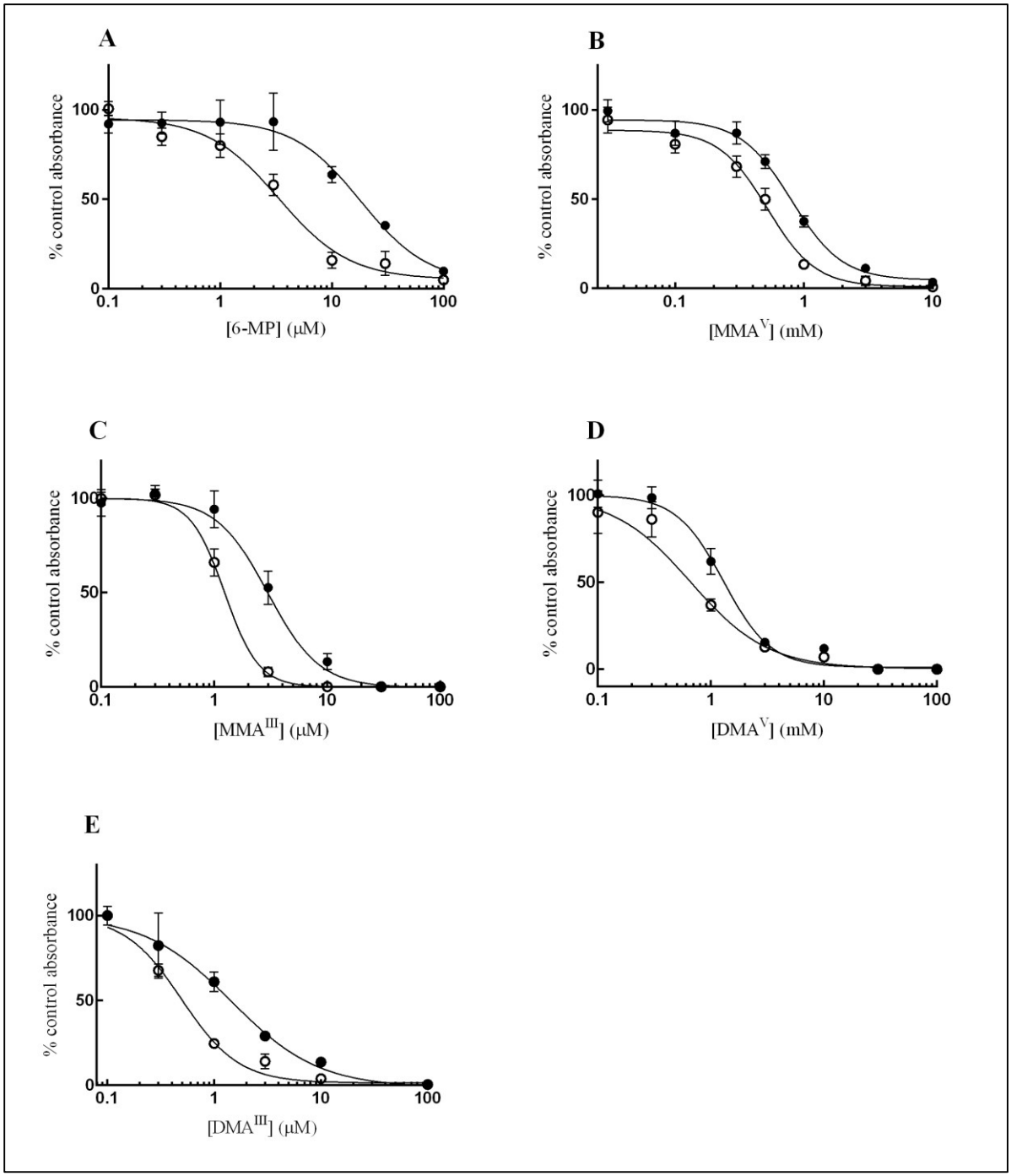

Fig. 4.5. MRP4 confers resistance to monomethylated and dimethylated arsenic species.

Empty vector (HEK-V4) (○) and MRP4 (HEK-MRP4-1E16) (●) expressing cells were incubated in the presence of A) 6-MP, B) MMA^{III} C) MMA^{V}, D) DMA^{III}, or E) DMA^{V} for 72 h. Cell viability was determined using a tetrazolium-based (MTS) cytotoxicity assay. Data points are means (± S.D.) of quadruplicate determinations in a representative experiment; similar results were obtained in at least three additional experiments.

4.2.4 MRP4 transports $MMA(GS)_2$ and DMA^V

Since MRP4 conferred resistance to various arsenicals direct transport assays were then used to identify the species of As transported. $MMA(GS)_2$ and DMA^V were identified as substrates [82]. MRP4-mediated transport of $MMA(GS)_2$ was further characterized by determining the initial rates of transport over several concentrations of $MMA(GS)_2$ (Fig. 4.6A). MRP4 showed a positive cooperative allosteric interaction with $MMA(GS)_2$. The curve fit for an allosteric interaction (allosteric sigmoidal equation, GraphPad Prism 5) was significantly better than a single binding site model (Michaelis-Menten equation, GraphPad Prism 5) (Extra sum of squares F test $P<0.0001$) with average (± S.D., *n=3*) $K_{0.5}$ of 0.70 ± 0.16 μM, V_{max} of 112 ± 6.3 pmol mg^{-1} protein min^{-1} and Hill coefficient of 1.4 ± 0.23 [82].

MRP4-mediated transport of DMA^V was characterized by determining the initial rates of transport over several concentrations of DMA^V (Fig. 4.6B). As for $MMA(GS)_2$, MRP4 showed a positive cooperative allosteric interaction with DMA^V. The curve fit for an allosteric interaction (allosteric sigmoidal equation, GraphPad Prism 5) was significantly better than a single binding site model (Michaelis-Menten equation, GraphPad Prism 5) (Extra sum of squares F test, $P<0.0001$) with average (± S.D., *n=3*) $K_{0.5}$ of 0.22 ± 0.15 μM, V_{max} of 32 ± 3 pmol mg^{-1} protein min^{-1} and Hill coefficient of 2.9 ± 1.2 [82].

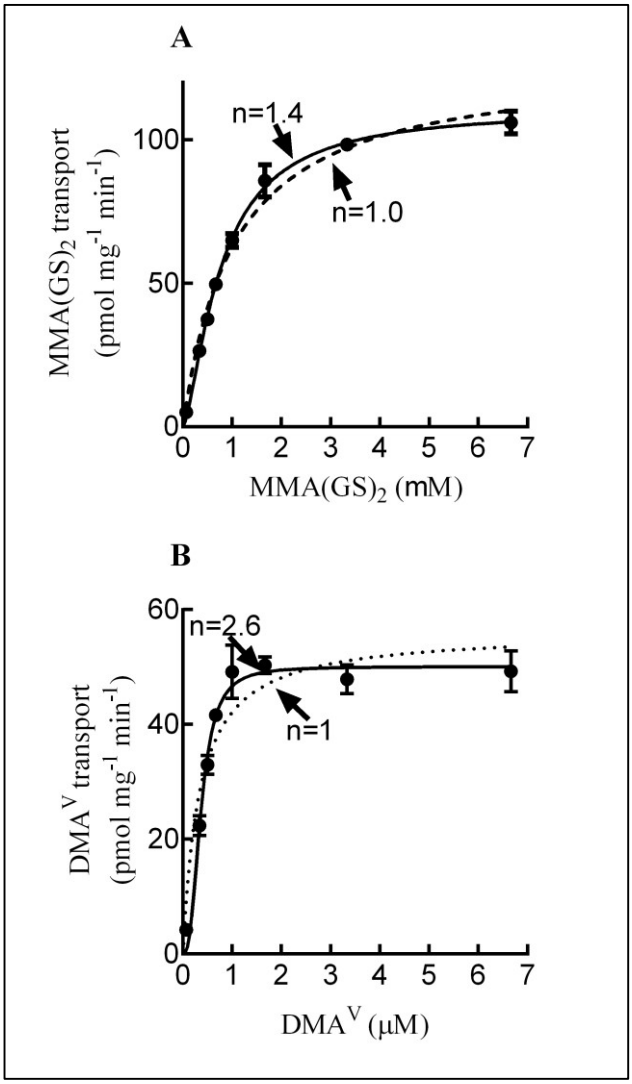

Fig. 4.6. MRP4 transports $MMA(GS)_2$ and DMA^V.

Transport experiments were done with membrane vesicles (20 µg of protein) prepared from HEK293T cells transiently transfected with pcDNA3.1(+)MRP4 (closed bars or symbols) or empty pcDNA3.1(+) (open bars or symbols). A) Membrane vesicles were incubated in transport buffer for 3 min at 37ºC with $MMA(GS)_2$ (1 µM). B) Vesicles were incubated with DMA^V (0.7 µM) for 5 min at 37ºC, in the presence or absence of GSH (3 mM). Data were fit using a one-site Michaelis-Menten kinetic model (hatched line) or the allosteric sigmoidal model (solid line) with GraphPad Prism 5. For individual experiments, transport was done in triplicate then reactions were pooled for analysis by ICP-MS. Bars and symbols represent the means of three independent experiments (±S.D.).

4.3 Discussion

This study reports the generation of HEK293 cells stably expressing MRP3, and MRP5 and their assessment in providing cellular protection to HEK293 cells from six different As species. Using these cell lines it was demonstrated that MRP3 and MRP5 do not confer resistance to As^{III}, As^{V}, MMA^{III}, MMA^{V}, DMA^{III}, or DMA^{V} relative to empty vector transfected HEK293 cells. Transport assays with MRP3- and MRP5-enriched membrane vesicles were consistent with the cytotoxicity data revealing that MRP3 and MRP5 do not transport $As(GS)_3$, but were able to transport the model substrates $E_2$17βG and methotrexate, respectively.

MRP3 is expressed at moderate levels in human hepatocytes with basolateral staining around hepatocytes surrounding the portal tracts [143]. Although MRP3 protein levels are modest in healthy human hepatocytes it has been reported to be highly upregulated in disease states such as cholestasis [143]. The substrate specificity includes a low affinity for bile salts, transport of glutathione conjugates, and preferentially glucuronide conjugates [142].

The lack of As^{III} resistance conferred by MRP3 was consistent with previously published data that MRP3 does not confer resistance to As^{III} in a human ovarian carcinoma cell line [143]. However, these studies did not confirm the role of MRP3 in cellular protection against As^{V} or methylated As species. Studies in primary human hepatocyte cultures found no statistically significant correlation between baseline MRP3 protein levels and the production or distribution of inorganic, monomethylated, and dimethylated As species after As exposure [61]. This observation suggested that MRP3

may not play a role in As transport but, it had not been confirmed using any other assay. There are likely several transport pathways in hepatocytes responsible for As efflux so change in protein expression is not a direct measurement of a protein's involvement in providing cellular protection. The cytotoxicity assays and transport assays described in this chapter do provide substantial evidence that MRP3 does not protect HEK293 cells from As.

MRP5 is expressed at very low levels in the liver but is upregulated in primary biliary cirrhosis [151] . It has a very similar substrate specificity to MRP4 including its ability to transport nucleoside monophosphate analogs [142]. Other MRP5 substrates include the glutathione conjugate 2,4- dinitrophenyl *S*-glutathione (DNP-GSH) and methotrexate-glutamate [205]. Studies in HEK293 cells overexpressing GFP-tagged MRP5 cDNA showed 3-fold resistance to antimonyl tartrate compared to GFP-tagged vector but the same study did not see any resistance conferred to arsenite or arsenate [203]. Zebrafish studies examining the role of metal-induced zebrafish *abcc5* transcript expression showed an increase in *abcc5* mRNA expression in zebrafish fibroblast-like (ZF4) cells and zebrafish embryos treated with 20 μM and 100 μM As^V, respectively [208]. However, the average death rate of zebrafish embryos overexpressing zebrafish *abcc5* was not significantly lower than zebrafish overexpressing the vector after As exposure suggesting that zebrafish *abcc5* does not provide cellular protection against As [208].

The lack of a role for MRP3 and MRP5 in conferring As resistance in HEK293 cells in combination with the SCHH studies in Chapter 3 suggest that MRP4 is important for hepatic basolateral transport of As and potentially transport of As across the apical

surface of renal proximal tubules into urine. MRP4 is expressed at low levels in healthy human hepatocytes although levels are quite variable [209], but it is upregulated after exposure to As^{III} which supports a role for MRP4 in protecting the liver against As (Chapter 3).

The localization of MRP4 to the basolateral membrane of the hepatocyte and the apical membrane of the kidney proximal tubule make MRP4 an ideal candidate for As detoxification given that the majority of As is eliminated in urine. Furthermore it was confirmed through direct transport studies that MRP4 transports DMA^{V} and $MMA(GS)_2$ with high affinity (Fig. 4.6) [82]. A portion of the As detected in urine (10-30%) is inorganic therefore, it is also likely that transport proteins other than MRP4 are important for basolateral efflux of As across the basolateral surface of hepatocytes. In addition, the majority of As transported across the basolateral surface of SCHH was inorganic (Fig. 3.8). Thus, MRP6 transport of As-GSH conjugates should be investigated. This protein is localized to the basolateral membrane of hepatocytes and studies are currently underway in our lab to address its role in As detoxification. The shRNA studies in Chapter 5 attempt to further elucidate the potential role of MRP4 in SCHH.

Chapter 5

Knockdown of MRP4 in SCHH Using shRNA

Barbara A. Roggenbeck completed all experiments in this chapter. Hepatocytes were provided by Norman M. Kneteman and Donna N. Douglas. X.Chris Le and Xiufen Lu assisted with the speciation analysis on the SCHH efflux media.

5.1 Introduction

The pathways for As elimination are not well characterized despite the fact that at least 150 million people worldwide are exposed to unacceptable levels of As (>10 ppb) in drinking water. It has been documented that the effects of As exposure vary between populations and even between humans exposed to similar levels [69]. The genetic basis of this inter-individual variation is not fully understood, however, it is likely a result of a combination of cellular processes including As uptake, metabolism, and efflux [210].

Arsenic is extensively metabolized in the liver but the majority (~80%) of As is eliminated in urine. Transport pathways for efflux of As across the basolateral membrane of hepatocytes into blood for urinary elimination are not well characterized. Some of the transport proteins that might be responsible for efflux of As across the basolateral surface of the hepatocyte into the blood include aquaglyceroporins (AQPs), glucose transporters (GLUTs/*SLC2A*), organic anion transporting polypeptides (OATPs/*SLCO*), and the multidrug resistance proteins (MRPs/*ABCC*).

Aquaglyceroporins (AQPs) are bidirectional channels that allow passage of neutral molecules down a concentration gradient, therefore, AQPs could function as efflux transporters when intracellular concentrations of substrate are higher than concentrations outside the cell. Human AQP7 and 9 have been shown to allow passage of certain As species, however, of the AQPs able to transport As, AQP9 is the only AQP localized to the basolateral membrane of hepatocytes [88,90]. Functional studies of AQP9 in *Xenopus laevis* oocytes demonstrate that As^{III}, MMA^{III}, MMA^{V}, and DMA^{V} are all AQP9 permeants [88,89]. AQP9 allows the passage of MMA^{III} more efficiently than

As^{III} at pH 7.5 and the pentavalent arsenicals do not pass through the channels as efficiently as the trivalent forms [89]. Under physiological pH conditions MMA^{V} (pKa 3.6, 8.2) and DMA^{V} (pKa 6.5) exist predominantly as negatively charged molecules and only the undissociated pentavalent forms are permeants [89].

The glucose transporters have also been shown to play a role in As transport. Human GLUT1 overexpressed in *Xenopus laevis* oocytes has been shown to directly transport As^{III} and MMA^{III}, however, GLUT1 is not localized to the basolateral membrane of hepatocytes [85,94]. Although direct transport studies have not been performed, a positive correlation between GLUT2 expression and cellular retention of iAs and MMA in human hepatocytes has been demonstrated. GLUT2, a bidirectional transporter localized to the basolateral surface of hepatocytes, could play a role in the efflux of iAs and MMA when intracellular concentrations exceed concentrations outside the cell [61].

OATP1B1 (gene symbol *SLCO1B1* previously known as OATP-C, OATP-2, or LST-1) is localized to the basolateral membrane of hepatocytes. HEK293 cells overexpressing human OATP1B1 show a glutathione-dependent increase in accumulation of iAs (As^{III} + As^{V}) but not MMA^{V} or DMA^{V} [98]. A candidate gene study on the association between human *SLC01B1* variants and urinary As metabolite patterns identified two single nucleotide polymorphisms that appear to significantly associate with altered As metabolite percentage in urine [211]. Although, OATPs are generally referred to as "uptake" transporters there is some evidence that these transporters can also function as efflux transporters. [212,213].

Finally, there are many studies that characterize direct transport of As by the MRPs. Membrane vesicle studies have confirmed that MRP1 transports both $As(GS)_3$ and $MMA(GS)_2$ [161,162]. Healthy human hepatocytes do not express MRP1 but this does not preclude MRP1 upregulation in the presence of As and consequent MRP1 efflux of $As(GS)_3$ and/or $MMA(GS)_2$. It has also been demonstrated using membrane vesicles that MRP2 directly transports $As(GS)_3$ and $[(GS)_2AsSe]^-$, but MRP2 localizes to the canalicular surface of hepatocytes from which substrates are transported into bile [84,139] [84]. Recently, MRP4 has been characterized as a high affinity transporter of DMA^V and $MMA(GS)_2$ [82]. MRP4 is localized to the basolateral membrane of hepatocytes suggesting it is potentially involved in As efflux from the hepatocyte to blood.

Although the studies described above provide very useful information about the membrane proteins that may be involved in transport of As across the basolateral surface of the hepatocyte, we wanted to elucidate this using a more physiologically relevant human hepatobiliary transport model. The pathways involved in transporting As metabolites from the liver to the blood ultimately for urinary elimination have been investigated using SCHH and candidate MRPs have been expressed and characterized in HEK293 cells (Chapters 3 and 4) [82]. These studies suggest that a multidrug resistance protein contributes substantially to As efflux across the basolateral surface of human hepatocytes. The efflux of As from SCHH was temperature sensitive and therefore not through passive diffusion. Glutathione-dependent and MK-571 sensitive transport across the basolateral membrane of hepatocytes was observed, providing strong support for an MRP-mediated process (Chapter 3). The basolateral transporters MRP3 and MRP5, do

not confer cellular protection against arsenicals when stably expressed in HEK293 cells (Chapter 4) [82]. Based on the studies completed in Chapter 4 it is unlikely that MRP3 or MRP5 play a role in As efflux.

In conjunction with previous studies showing the direct transport of As by the multidrug resistance proteins including MRP1, MRP2, and MRP4 [82,84,161,162] MRP4 was the most likely MRP candidate for As basolateral efflux from the hepatocyte. To test the hypothesis that MRP4 contributes to As efflux across the basolateral surface of hepatocytes, experiments were designed to knock-down MRP4 levels in SCHH using MRP4-targeted lentiviral shRNA followed by measurement of total As and individual As species in media of untransduced, non-target or MRP4-targeted shRNA lentiviral particles. Under the conditions tested, reduced MRP4 levels did not consistently result in reduced As (total or individual species) efflux, and viral transduction conditions resulted in several non-specific changes in transport protein expression. This led us to investigate the levels of other potential hepatic basolateral transport proteins by immunoblot analysis.

5.1 Results

5.2.1 MRP4 shRNA clone selection

To determine the most potent shRNA clones for MRP4 knockdown, five different MRP4-targeted shRNA plasmids and one non-target control plasmid were tested for their

ability to reduce endogenous MRP4 levels in HEK293T cells (Table 2.9). MRP4 levels were measured in whole cell lysates from HEK293T cells transfected with different shRNA encoding plasmids (Fig. 5.1A). After normalizing for Na^+/K^+-ATPase, MRP4 levels were plotted relative to MRP4 levels in the non-target control (Fig. 5.1B). There was a 32% increase in MRP4 levels for the non-target control transfected compared to the untreated HEK293T cells. Compared to the non-target control, MRP4 targeted clones 5267, 9928, 9930, 5264, and 7334 decreased endogenous levels of MRP4 by 29%, 43%, 53%, 58%, and 74%, respectively. The 5264 (directed at the 3'UTR) and 7334 [directed at the coding sequence (CDS)] MRP4-targeted clones had the most potent knockdown out of the five tested and were selected for use in SCHH experiments (Fig. 5.1).

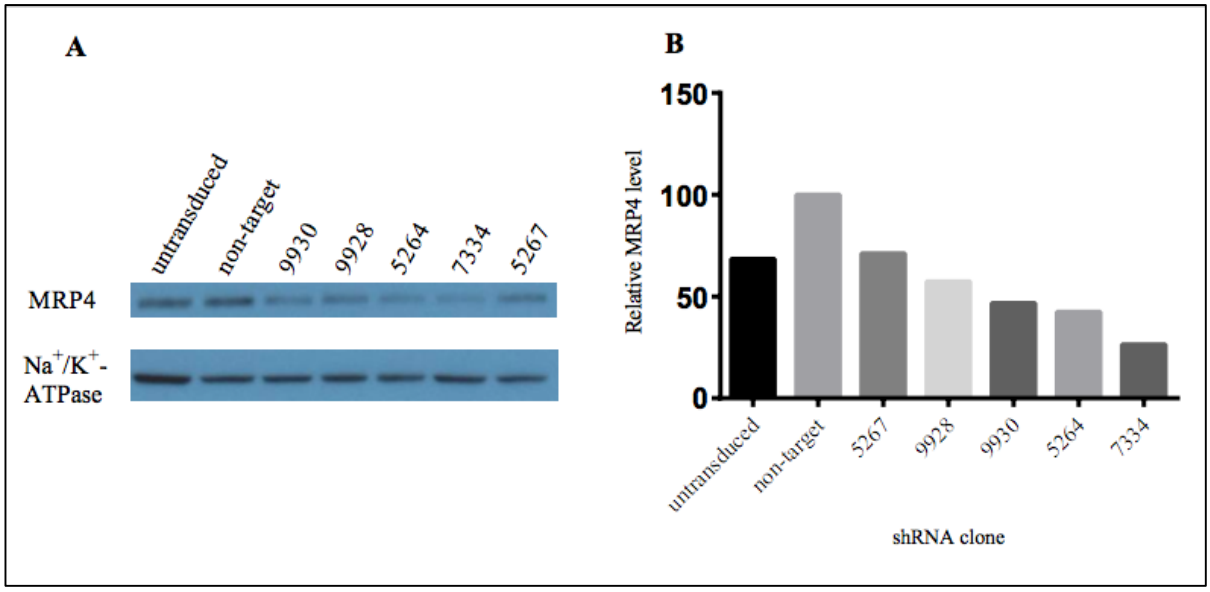

Fig. 5.1. Selection of the most potent MRP4-targeted shRNA clone through knockdown of endogenous MRP4 in HEK293T cells.

HEK293T cells were transfected with MRP4 targeted shRNA plasmids and harvested after 72 h. (A) Whole cell lysates (20 µg) from untransfected, non-target, and MRP4-targeted shRNA clones 9930, 9928, 5264, 7334, or 5267 transfected HEK293Ts were resolved by SDS-PAGE followed by immunoblotting with monoclonal anti-MRP4 [M_4I-10] antibody. Blots were then reprobed with polyclonal Na^+/K^+-ATPase [H-300] antibody. (B) MRP4 levels were normalized for protein loading using Na^+/K^+-ATPase levels and plotted as a % of the non-target transfected HEK293T cells. Bars represent a single experiment.

5.2.2 MRP4 knockdown in SCHH preparation #21

To begin optimizing conditions for MRP4 knockdown and determine its functional impact on basolateral efflux of As an MOI of 50 was used in the first shRNA experiment using SCHH preparation #21. MRP4 levels were measured in whole cell lysates from SCHH transduced with different shRNA plasmid DNA (Fig. 5.2A). After normalizing for Na^+/K^+-ATPase, MRP4 levels were plotted relative to MRP4 in the non-target control. This resulted in a 34% and 24% decrease in MRP4 levels in hepatocytes transduced with clones 5264 and 7334, respectively (Fig. 5.2A and B). This SCHH preparation formed functional canalicular networks as shown by the taurocholate BEI of 44% at 10 min (Fig. 5.2C, Table 3.1). Biliary excretion of As was observed in this preparation with a BEI of 31% at 10 min (Fig. 5.2D, Table 3.1). The BEIs of the non-target, 5264, and 7334 transduced hepatocytes were 14%, 14%, and 16%, respectively, at 10 min. Unexpectedly, there was a 35% and 20% increase in As efflux under the + Ca^{2+} and – Ca^{2+} conditions, respectively, in the non-target transduced compared to the untreated hepatocytes. There was no difference in total As efflux for the 5264 or 7334 transduced SCHH compared to the non-target control under the conditions tested (Fig. 5.2E).

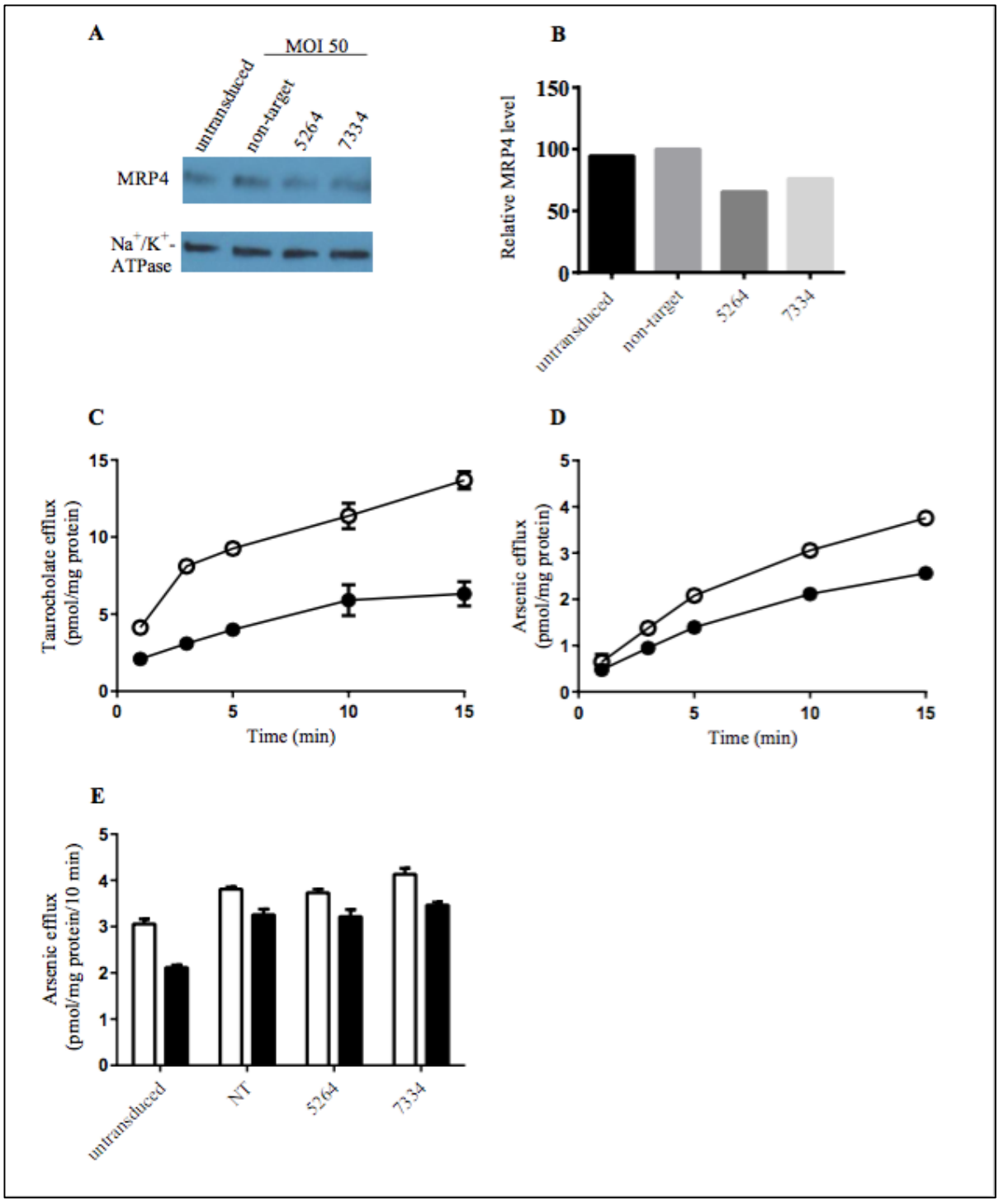

Fig. 5.2. MRP4 levels and transport function with and without lentiviral shRNA treatment of SCHH #21.

(A) Whole cell lysates (15 µg) from untransduced, non-target, and MRP4-targeted shRNA clones 5264 or 7334 transduced SCHH were resolved by SDS-PAGE followed by immunoblotting with the monoclonal anti-MRP4 [M4I-10] antibody. Blots were then reprobed with polyclonal Na^+/K^+-

ATPase antibody [H-300]. (B) MRP4 levels were normalized for protein loading using Na^+/K^+-ATPase levels and plotted as a % of non-target transduced SCHH. Untransduced SCHH were incubated at 37°C with (C) [^{3}H]-taurocholate (1µM, 100 nCi) for 15 min or (D) $^{73}As^{III}$ (0.5µM, 100 nCi) for 24 h; then incubation media was replaced with Ca^{2+}-containing (basolateral efflux, ●) or Ca^{2+} free (basolateral + canalicular efflux, ○) HBSS. Efflux was then measured as described in the Materials and Methods (Section 2.2.5). The difference between the open and closed circles represents substrate efflux into the canalicular networks. Points represent ± SD for triplicate determinations in a single experiment. (E) SCHH with and without lentiviral shRNA transduction at an MOI of 50 were incubated at 37°C with $^{73}As^{III}$ (0.5µM, 100 nCi) for 24 h; then incubation media was replaced with Ca^{2+}-containing (basolateral efflux, closed bars) or Ca^{2+}-free (basolateral + canalicular efflux, open bars) HBSS. Efflux was assessed at a 10 min time point as described in the Materials and Methods (Chapter 2 Section 2.2.6). The difference between the open and closed bars represents substrate efflux into canalicular networks. Points represent ± SD for triplicate determinations in a single experiment.

5.2.3 MRP4 knockdown in SCHH preparation #24

To determine if increasing the knockdown of MRP4 would reduce the basolateral efflux of total As, higher MOI values of 250 and 500 were tested using SCHH preparation #24. MRP4 levels were measured in whole cell lysates from SCHH transduced with different shRNA plasmid DNA. (Fig. 5.3A). After normalizing for Na^+/K^+-ATPase, MRP4 levels were plotted relative to MRP4 levels in the non-target control (Fig. 5.3B). For transduction at an MOI of 250 there was a slight increase in MRP4 protein levels in the non-target control compared to untreated SCHH. Compared to the non-target control, SCHH transduced with an MOI of 250 of clone 5264 or 7334 resulted in a 62% and 12% decrease in MRP4 protein levels, respectively (Fig. 5.3B). For transduction at an MOI of 500 there was a 40% increase in MRP4 protein levels in the non-target control compared to untransduced SCHH. Compared to the non-target control SCHH transduced with an MOI of 500 with clone 5264 or 7334 resulted in a 48% and 21% decrease in MRP4 levels, respectively (Fig. 5.3B). SCHH preparation #24 had functional canalicular network formation with a BEI for taurocholate of 50% at 10 min (Fig. 5.3C, Table 3.1). Arsenic efflux occurred only across the basolateral membrane,

therefore, an As BEI was not detected (Fig. 3.1, Table 3.1). There was no difference in total As efflux for the 5264 or 7334 transduced, at an MOI of 250 or MOI 500, compared to the non-target controls (Fig. 5.3E). Consistent with SCHH #21 (Fig. 5.2E) there was a slight stimulation of As efflux for all lentiviral shRNA transduced hepatocytes compared to the untransduced control.

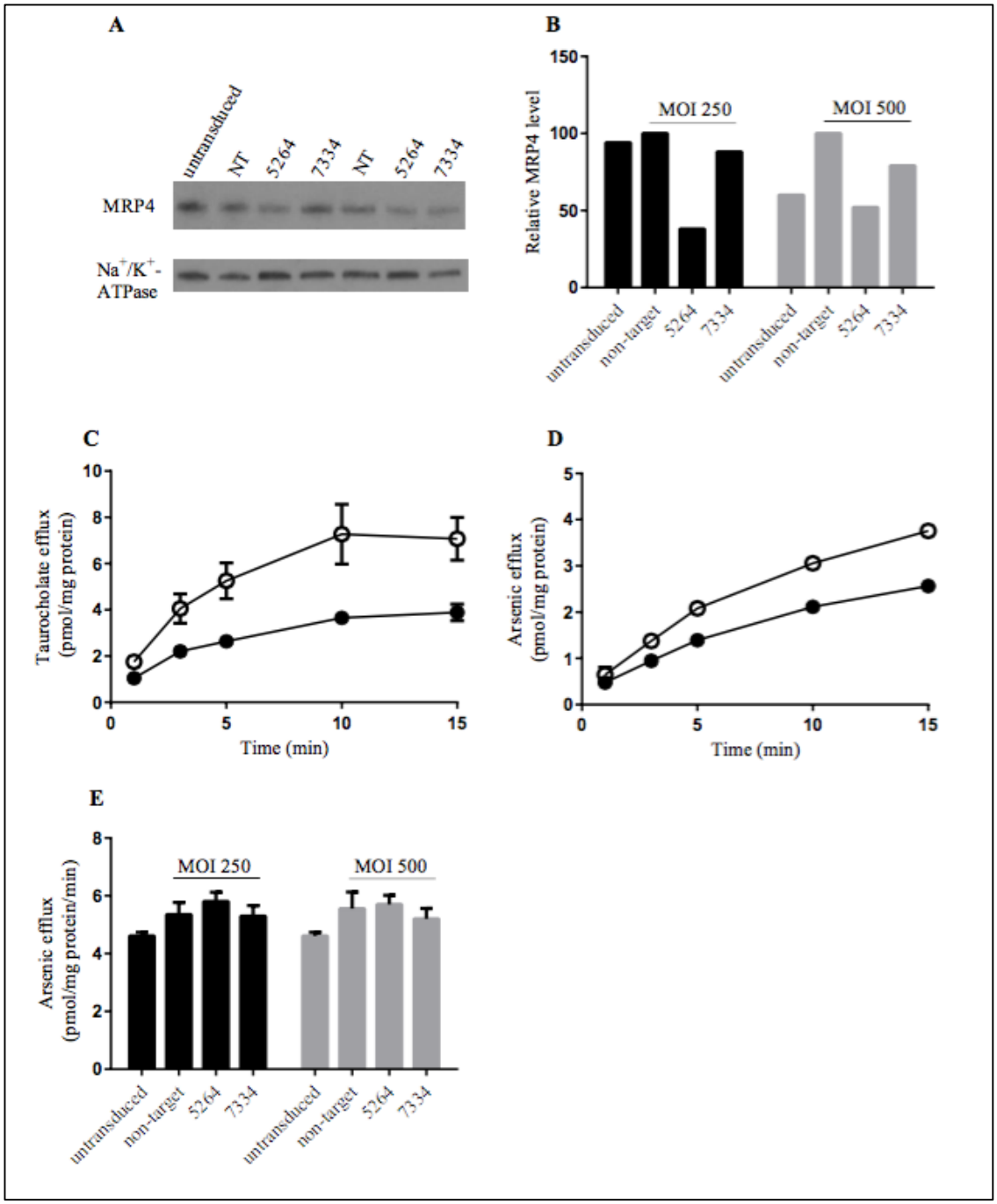

Fig. 5.3. MRP4 levels and transport function with and without lentiviral shRNA treatment of SCHH #24.

(A) Whole cell lysates (15 µg) from untransduced, non-target, and MRP4-targeted shRNA clones 5264 or 7334 transduced SCHH were resolved by SDS-PAGE followed by immunoblotting with the monoclonal anti-MRP4 [M4I-10] antibody. Blots were then reprobed with the polyclonal anti-Na^+/K^+-ATPase [H-300] antibody. (B) MRP4 levels were normalized for protein loading using Na^+/K^+-ATPase levels to determine the relative level of MRP4 in 5264 and 7334 transduced hepatocytes at an MOI of 250 (black bars) and an MOI of 500 (gray bars) compared to the non-

target transduced SCHH. SCHH were incubated at 37°C with (C) [^{3}H]-taurocholate (1μM, 100 nCi) for 15 min or (D) $^{73}As^{III}$ (0.5μM, 100 nCi) for 24 h; then incubation media was replaced with Ca^{2+}-containing (basolateral efflux, ●) or Ca^{2+}-free (basolateral + canalicular efflux, ○) HBSS. Efflux was then measured as described in the Materials and Methods (Section 2.2.4). The difference between the open and closed circles represents substrate efflux into canalicular networks. Points represent means ± SD for triplicate determinations in a single experiment. (E) SCHH transduced with and without lentiviral shRNA at an MOI of 250 (black bars) or 500 (gray bars) were incubated at 37°C with $^{73}As^{III}$ (0.5μM, 100 nCi); then incubation media was replaced with Ca^{2+} -containing (basolateral efflux, closed bars). Efflux was assessed at a 10 min time point as described in the Materials and Methods (Section 2.2.6). Bars represent means ± SD for triplicate determinations in a single experiment.

5.2.4 MRP4 knockdown in HEK-MRP4 cell lines using higher MOI values

As a first step to determine if the lack of specific effect of partial MRP4 knockdown on basolateral As efflux in SCHH preparations #21 and #24 was due to low knockdown levels, conditions were established for more complete MRP4-knockdown using HEK-MRP4 cells and higher MOI values. The HEK-MRP4 stable cells were transduced with MOI values of 500, 1000, 1500, or 1760. MRP4 levels were measured in whole cell lysates from HEK293T cells transduced with different shRNA plasmid DNA. (Fig. 5.4A). After normalizing for Na^{+}/K^{+}-ATPase, MRP4 levels were plotted relative to MRP4 levels in the non-target control (Fig. 5.4B). MRP4 levels in cells transduced with the 5264 shRNA clone were not decreased because 5264 is targeted to the 3'UTR region of MRP4 (Table 2.9) which is not contained in the MRP4 expression plasmid used to generate the stable cell line. For transduction with the shRNA clone 7334 that targets the coding sequence of MRP4, MOI values of 500, 1000, 1500, and 1760 reduced MRP4 levels by 30%, 38%, 72%, and 79%, respectively (Fig. 4B). An MOI of 1500 was selected for use with future SCHH preparations.

5.2.5 MRP4 knockdown in SCHH preparation #25

SCHH preparation #25 was transduced with an MOI of 1500 and almost complete knockdown of MRP4 was observed for both shRNA clones 5264 and 7334 (Fig. 5.5A.). After normalizing for Na^+/K^+-ATPase, MRP4 levels in the 5264 and 7334 transduced hepatocytes both showed a 95% reduction in MRP4 levels compared to the non-target control (Fig. 5.5B). The BEI for taurocholate was very low, only 19% at 10 min, suggesting only low to moderate formation of functional canalicular networks. (Fig. 5.5C). Arsenic efflux occurred only across the hepatocyte basolateral surface and therefore, a BEI was not detected (Fig. 5.5D). Transduction of hepatocytes with the MRP4 targeted shRNA clones 5264 and 7334 resulted in a 38.5 % and 0%, respectively, increase in total As efflux at 10 min (Fig. 5.5E).

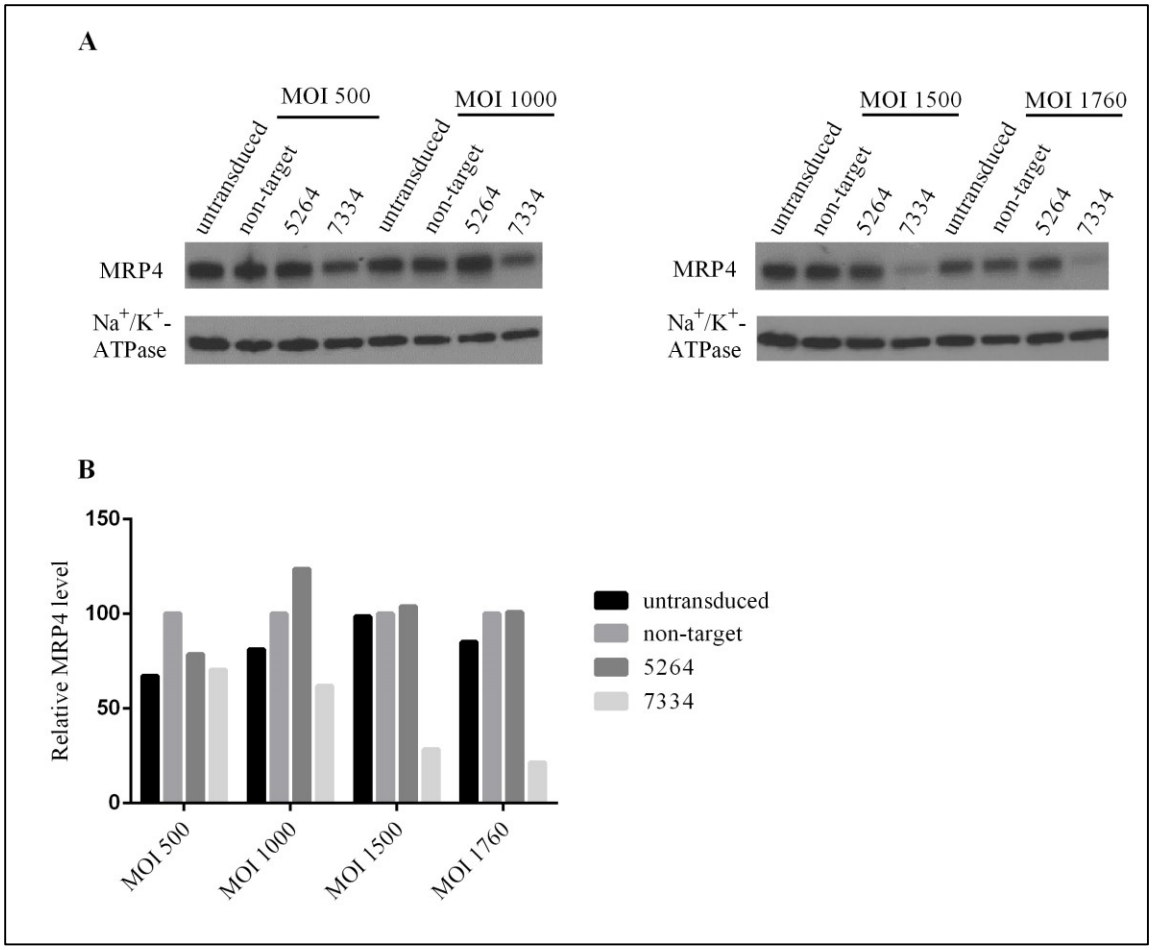

Fig. 5.4. Optimization of lentiviral shRNA MOI for maximum reduction of MRP4 levels in HEK-MRP4-1E16 stable cells.

(A) Whole cell lysates (25 µg) from HEK-MRP4-1E16 stable cells transduced with an MOI of 500, 1000, 1500, or 1760 were resolved by SDS-PAGE followed by immunoblotting with the monoclonal anti-MRP4 [M$_4$I-10] antibody. Blots were then reprobed with the polyclonal Na^+/K^+-ATPase [H-300] antibody. (B) MRP4 levels were normalized for protein loading using Na^+/K^+-ATPase levels and the relative MRP4 level in the 5264 and 7334 transduced hepatocytes was plotted as a % of the non-target transduced HEK-MRP4-E161 cells.

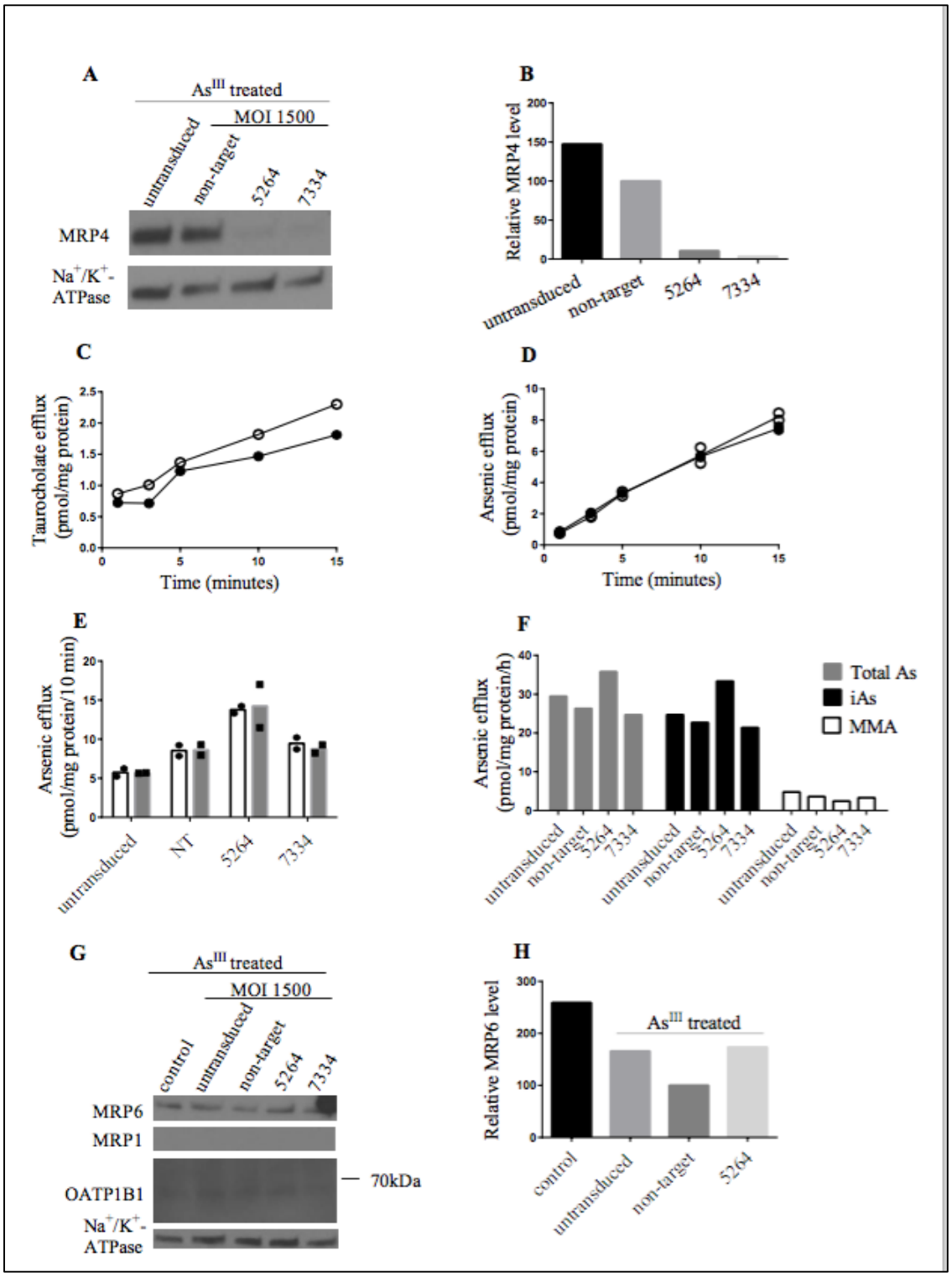

Fig. 5.5. MRP4 levels and transport function with and without lentiviral shRNA transduction of SCHH #25.

(A) Whole cell lysates (15 µg) from untransduced, non-target, and MRP4-targeted shRNA clones 5264 or 7334 transduced SCHH were resolved by SDS-PAGE followed by immunoblotting with

the monoclonal anti-MRP4 [M_4I-10] antibody. Blots were then reprobed with the polyclonal Na^+/K^+-ATPase [H-300] antibody. (B) MRP4 levels were normalized for protein loading using Na^+/K^+-ATPase levels to determine the relative MRP4 level in 5264 and 7334 transduced hepatocytes at an MOI 1500 and plotted as a % of the non-target transduced SCHH. SCHH were incubated at 37°C with (C) [^{3}H]-taurocholate (1μM, 100 nCi) for 15 min or (D) $^{73}As^{III}$ (0.5μM, 100 nCi) for 24 h; then incubation media was replaced with Ca^{2+}-containing (basolateral efflux, ●) or Ca^{2+}-free (basolateral + canalicular efflux, ○) HBSS. (E) Efflux was then measured as described in the Materials and Methods (Chapter 2, Section 2.2.6) at a 10 min time point. The difference between the open and closed bars represents substrate efflux into canalicular networks. Bars represent means of duplicate determinations with individual replicates indicated with filled points. (F) SCHH either untransduced or transduced with non-target or MRP4-targeted shRNA clones 5264 or 7334 were treated with As^{III} (0.5 μM) for 24 h, washed, and then incubated with fresh media for 1 h. The media was then collected and frozen at -80°C. Total As, inorganic As, monomethylated As, and dimethlyated As effluxed into media after 1 h were analyzed by HPLC-ICP-MS as described in the Materials and Methods (Section X). (G) The effect of lentiviral transduction on MRP6 was determined by resolving (15 μg) of whole cell lysate from untransduced, non-target, and MRP4-targeted shRNA clones 5264 and 7334 transduced SCHH by SDS-PAGE followed by immunoblotting with monoclonal anti-MRP6 [M_6II-7] antibody. Blots were then stripped and reprobed with monoclonal MRP1 [MRPr1] antibody, stripped and reprobed with polyclonal OATP1B1 antibody, and then reprobed with the polyclonal Na^+/K^+-ATPase [H-300] antibody. (H) MRP6 levels were normalized for protein loading using Na^+/K^+-ATPase levels to determine the relative level of MRP6 in 5264 transduced SCHH at an MOI 1500 and plotted as a % of the non-target transduced SCHH.

The lack of reduction of As efflux by MRP4-targeted shRNA clones compared with non-target was somewhat surprising. In order to determine if a difference existed in the efflux of a specific species of As, speciation analysis was completed using HPLC-ICP-MS. The speciation analysis showed an 11% decrease in total As in efflux media in the non-target transduced compared to the untransduced control SCHH. Consistent with the total As efflux results in Fig. 5.5E, speciation analysis revealed a 26.5% increase in total As efflux in media after 1h for hepatocytes transduced with 5264 and a 6.3% decrease in 7334 transduced compared to the non-target control. For the 5264 transduced hepatocytes there was a 32% increase in inorganic As and a 33% decrease in MMA detected in efflux media collected after 1h relative to non-target control. For the 7334 transduced hepatocytes there was a 6% decrease in inorganic As and an 8.4 % decrease in

MMA detected in efflux media collected after 1h relative to the non-target control (Fig. 5.6F).

Since decreasing endogenous MRP4 levels did not result in a decrease in the total As efflux and changes in As efflux occurred in the presence of non-target shRNA compared to untransduced controls the levels of other potential hepatic basolateral transport proteins were investigated by immunoblot analysis. Basolateral transport proteins examined were chosen based on two criteria: their potential to transport DMA^V (the main metabolite found in human urine), and/or their potential to transport glutathione conjugates, due to the GSH-dependent nature of As transport in SCHH (Chapter 3).

Therefore, MRP6, OATP1B1, and MRP1 levels were examined. Immunoblotting and densitometry analysis showed a reduction in MRP6 levels in the non-target transduced compared to the untransduced control. There was a 1.8-fold increase in MRP6 expression with the 5264 transduced cells relative to non-target (Fig 5.5G and H). The densitometry analysis could not be performed on the 7334 transduced because of the quality of the band and the experiment could not be repeated due to the lack of sample remaining. OATP1B1 levels were extremely low, essentially undetectable, and deciphering differences between the samples impossible (Fig. 5.5G). MRP1 was not detected under any condition tested (Fig. 5.5G)

5.2.6 MRP4 knockdown in SCHH preparation #26

Consistent with SCHH #25 there was almost complete knockdown of MRP4 in SCHH preparation #26 with the 5264 and 7334 transduced hepatocytes compared to the non-target control (Fig. 5.6A and B). After normalizing for Na^+/K^+-ATPase, MRP4

levels in the 5264 and 7334 transduced hepatocytes showed an 89% and 96% reduction, respectively, in MRP4 levels compared to the non-target control (Fig. 5.6B). The taurocholate positive control confirmed that canalicular networks were formed and functional with a BEI of 70% at 10 min (Fig. 5.6C). Only basolateral efflux of As occurred in this preparation, therefore, an As BEI was not detected (Fig. 5.6D).

For speciation analysis, media was collected at both 24 h and 1 h time points to determine if the MRP4 knockdown effect was time dependent and also allow higher levels of As to be analyzed for the 24 h time point. The speciation analysis showed a 20% increase in total As detected in efflux media from the non-target transduced SCHH compared to the untransduced SCHH control at the 24 h time point (Fig. 5.6E). For the 5264 transduced hepatocytes there was an 8% decrease in total As relative to the non-target transduced. When the species of As were considered there was a 12% decrease in inorganic As, a 12% decrease in MMA, and a 24% increase in DMA detected in efflux media collected after 24 h compared to the non-target transduced SCHH. For the 7334 transduced hepatocytes there was a 4% decrease in total As. When the species of As were considered there was an 8% decrease in inorganic As, a 22% decrease in MMA, and a 28% increase in DMA detected in efflux media collected after 24 h relative to the non-target control (Fig. 5.6E).

For the 1 h time point the speciation analysis revealed a 5% increase in total As detected in efflux media in the non-target transduced SCHH compared to the untransduced SCHH control (Fig. 5.6F). For the 5264 transduced hepatocytes there was a 2% increase in total As relative to the non-target. When individual As species were considered there was a 3% decrease in MMA, and a 29% increase in DMA detected in

efflux media compared to the non-target transduced SCHH. For the 7334 transduced hepatocytes there was an 11% decrease in total As. When the individual As species were considered there was a 15% decrease in inorganic As, a 3 % increase in MMA, and a 38% increase in DMA detected in efflux media collected after 1h (Fig. 5.6E).

As for SCHH preparation #25 we investigated the levels of MRP6, OATP1B1, and MRP1 by immunoblotting of SCHH #26 lysates. Similar to the results obtained for SCHH preparation #25 it appears that the 5264 transduced cells increased MRP6 expression relative to non-target control (Fig. 5.6F and G) while OATP1B1 protein expression was reduced likely due to non-specific effects of the lentivirus transduction (Fig. 5.6F and H). Non-specific lentivirus effects were also apparent on the MRP6 blot because MRP6 levels were reduced remarkably between the untransduced and non-target control (Fig. 5.6F and G). MRP1 was not detected under any conditions tested (Fig. 5.6F).

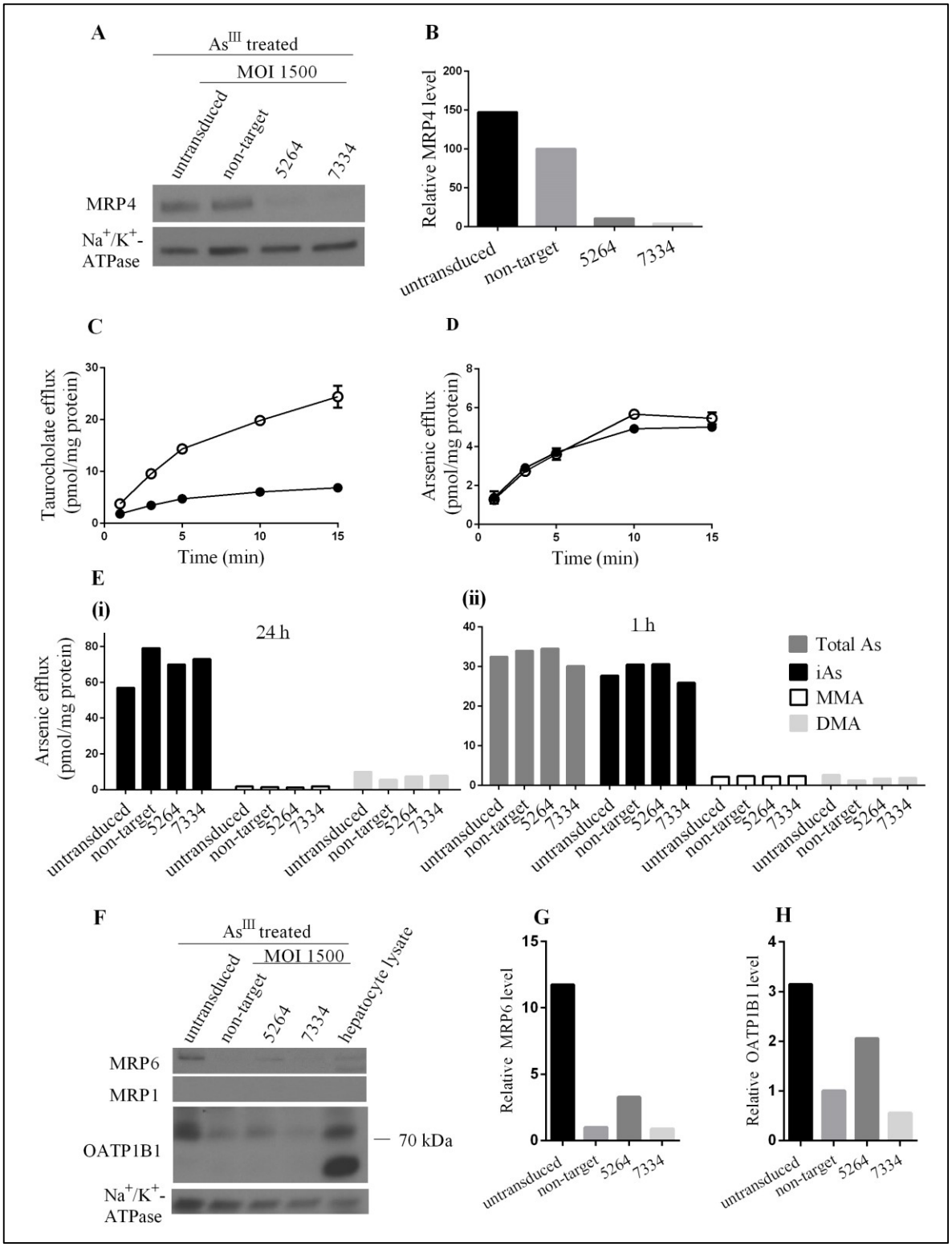

Fig. 5.6. MRP4 levels and speciation analysis with and without lentiviral shRNA transduction of SCHH #26.

(A) Whole cell lysates (15 µg) from untransduced, non-target, and MRP4-targeted shRNA clones 5264 or 7334 transduced SCHH were resolved by SDS-PAGE followed by immunoblotting with monoclonal anti-MRP4 [M_4I-10] antibody. Blots were stripped and reprobed with the monoclonal MRP1 [MRPr1] antibody, and then reprobed with the polyclonal Na^+/K^+-ATPase [H-300] antibody. (B) MRP4 levels were normalized for protein loading using Na^+/K^+-ATPase levels to determine the relative level of MRP4 in 5264 and 7334 transduced SCHH at an MOI 1500 and plotted as a % of the non-target transduced SCHH. SCHH were incubated at 37°C with (C) [^{3}H]-taurocholate (1µM, 100 nCi) for 15 min or (D) $^{73}As^{III}$ (0.5µM, 100 nCi) for 24 h; then incubation media was replaced with Ca^{2+}-containing (basolateral efflux, ●) or Ca^{2+}-free (basolateral + canalicular efflux, ○) HBSS. Efflux was then measured as described in the Materials and Methods (Section 2.2.4). The difference between the open and closed circles represents substrate efflux into canalicular networks. Points represent ± SD for triplicate determinations. (E) SCHH either untransduced or transduced with non-target or MRP4-targeted shRNA clones 5264 or 7334 were treated with As^{III} (0.5 µM) for 24 h and the media was collected and frozen at -80°C. SCHH were then washed and incubated with fresh media for 1 h. The media was collected and frozen at -80°C. Total As, inorganic As, monomethylated As, and dimethlyated As effluxed into media after 24 h and (F) 1 h were analyzed by HPLC-ICP-MS. (G) The effect of decreasing endogenous MRP4 levels on MRP6 was determined by resolving (15 µg) of whole cell lysate from untransduced, non-target, and MRP4-targeted shRNA clones 5264 or 7334 pretransduced SCHH by SDS-PAGE followed by immunoblotting with monoclonal anti-MRP6 [M_6II-7] antibody. Blots were stripped and reprobed with monoclonal MRP1 [MRPr1], stripped and reprobed for polyclonal OATP1B1, and then reprobed for polyclonal Na^+/K^+ ATPase [H-300].

5.3 Discussion

Arsenic transport pathways across the basolateral membrane of the hepatocyte to the blood for urinary elimination are not well understood. Previous studies (Chapter 3 and Chapter 4) suggested that MRP4 could play a prominent role in the movement of As from the liver into blood [82]. Using both HEK293 cell lines and SCHHs, we optimized conditions to maximize the knockdown of MRP4 in SCHH, and perform transport and speciation experiments in order to elucidate the role of MRP4 in As efflux in the physiological SCHH model.

Major reduction of MRP4 levels did not substantially decrease the total efflux of As across the basolateral surface of SCHH #25 or #26 under the conditions tested. The shRNA experiments also failed to show an MRP4-dependent difference in the species of As being effluxed by SCHH #25 or #26. This discussion will provide several possible explanations for these somewhat unexpected results.

The first concern with these experiments are the apparent non-specific effects of the shRNA plasmid transfection and the lentivirus transduction on membrane protein expression levels. In Fig. 5.1 for example, transfection of the HEK293T cells with the non-target plasmid alone (no lentivirus present) resulted in a 30% increase in MRP4 levels compared to the untransfected control HEK293T cells after normalization to Na^+/K^+ -ATPase levels. When examining results from the lentivirus transduced cells compared to the untransduced cells results are quite variable. Figures 5.2 and 5.3 show no difference between MRP4 levels in the untransduced and the non-target transduced hepatocytes at MOI values of 50 and 250 but there is an apparent increase in MRP4

levels in the non-target transduced compared to the untransduced control. The effects could be attributed to the use of higher levels of lentivirus particles, however, this does not explain why, in Fig. 5.4, there is an increase in the MRP4 levels at MOI values of 500, 1000, and 1760 but not at 1500.

The expression level of MRP6 in the MRP4-targeted shRNA transduced SCHH was reduced in preparations #25 and #26 compared to the untransduced SCHH. A similar effect in OATP1B1 levels was observed in SCHH preparation #25. The expression levels were remarkably reduced in the transduced SCHH compared to the untransduced SCHH for preparation #25 and no mature glycosylated OATP1B1 was detected in SCHH #26. These observations appear to be due to non-specific lentivirus effects. Non-specific effects on protein levels due to shRNA treatments present a major problem and complicate interpretation of results. These effects may not have occurred with lower MOI treatment. The effects appear to be different between different preparations with no consistent pattern. MRP4, MRP6, and OATP1B1 levels have been unaffected, decreased, or increased with virus treatment and currently we cannot provide any explanation for these differences. Future experiments will be performed at MOIs lower than 1500 to see if the non-specific effects of virus on expression of membrane proteins can be avoided while still achieving an optimal decrease in endogenous MRP4 levels that is suitable for studying its role in As efflux. In addition, non-viral methods of shRNA transfection should be considered.

Elimination of As is an extremely important cellular detoxification process, therefore, redundant pathways likely exist within the hepatocytes to transport As across the basolateral membrane. It is not uncommon for knockdown of a protein to result in

compensatory upregulation of another. Well characterized examples of this include the upregulation of rat and human Mrp3/MRP3 in the Mrp2-deficient TR^- rat strain and MRP2-deficient Dubin-Johnson syndrome patients [144]. In addition, Mrp4 has been shown to be upregulated at the basolateral surface of hepatocytes in Abcb11 knock-out mice. Both of these animal models are examples of a compensation mechanism to maintain bile acid homeostasis [214].

The increase in total As efflux after 5264 transduction of SCHH #25 (Fig. 5.5E and F) could be explained by a transport pathway compensating for the decrease in MRP4 protein levels that is being utilized for inorganic As efflux. SCHH #26 seems to more consistently support a compensation mechanism in place with an increased efflux of DMA^V from the hepatocytes although total efflux was only slightly decreased relative to NT control. This could also be an example of the necessity for relieving the cell of DMA^V to prevent formation of DMA^{III}.

MRPs potentially at the basolateral surface of hepatocytes that could be upregulated include MRP1, MRP3, MRP5, MRP6 and MRP8 (*ABCC11*). Although MRP1 protein is not detected in healthy human hepatocytes we investigated the possibility of MRP1 upregulation in the absence of MRP4, however, MRP1 was undetectable in SCHH preparation #25 and #26. MRP3 and MRP5 do not confer resistance to arsenicals (Chapter 4) therefore, we did not check for expression by immunoblotting. MRP6 is expressed in liver, however, it is upregulated in SCHH #25 and #26 after transduction with MRP4-targeted shRNA relative to non-target so is worthy of further investigation (check SCHH #26). However, it should also be noted that there appears to be a non-specific reduction in MRP6 after lentivirus treatment in both SCHH

#25 and #26 preparations compared to non-transduced controls. Nothing is known about the ability of MRP6 to transport As, thus direct transport and knockdown studies would be necessary to determine its role in hepatic basolateral transport of As. The *MRP8* gene codes for two major transcripts. The longer transcript is expressed predominantly in breast and testes however, a shorter splice variant is expressed in liver [215]. The MRP8 protein shares overlapping substrate specificity with other MRPs especially MRP4 and MRP5 [216].

Expression levels of AQPs and GLUTs are also worthy of further investigation. AQP9 is a well characterized transporter of iAs, MMA^{III}, and DMA^{V} but it only transports neutral molecules and is highly unlikely to transport negatively charged GSH conjugates [89]. DMA^{V} is a weak acid with a pKa of 6.3. It exists within hepatocytes predominantly (90%) as the dissociated anion [$(CH_3)_2AsO_2^-$] therefore, we would expect MRP4 to be the predominant transport protein of DMA^{V} rather than AQP9 because MRPs can transport charged molecules. DMA^{V} is not the major metabolite being effluxed across the basolateral membrane of hepatocytes under the conditions tested. MRP4 may be more important for efflux of DMA^{V} at the kidney during urinary elimination. AQP9 is most likely to be responsible for free As^{III} and MMA^{III} passage across the basolateral membrane of the hepatocyte, however, the high concentrations of glutathione in hepatocytes (0.5-10 mM) make it likely that As^{III} and MMA^{III} are GSH conjugates, and effluxed as such.

GLUT2 expression has been shown to correlate with higher retention of the inorganic and mono-methylated As species in human hepatocytes [61], however, direct transport studies have not been published that prove GLUT2 transports As in any form.

In addition to GLUT2, several GLUTs expressed in liver may be worth investigating for their potential role in As efflux including GLUT1 and GLUT9 [217].

Although an As-induced compensatory mechanism may be the reason that decreasing MRP4 protein levels resulted in no obvious role for MRP4 in As efflux, it is also possible that the experimental conditions were not optimal for showing that MRP4 is important for As efflux. MRP4 is a very high affinity, low capacity transporter of DMA^V ($K_{0.5}$ 0.22 μM and V_{max}, 32 $pmol^{-1}$ mg^{-1} protein min^{-1}) and $MMA(GS)_2$ ($K_{0.5}$ 0.7 μM and V_{max}, 112 $pmol^{-1}$ mg^{-1} protein min^{-1}) and so it is possible that at the concentrations the SCHH were exposed to resulted in saturation of MRP4. Saturation of MRP4 could result in cellular accumulation of DMA^V and end product inhibition of AS3MT with resultant increased levels of As^{III}. Therefore, saturation of MRP4 could result in an increased efflux of inorganic As by capable membrane transporters. Song *et al.,* reported that the K_m of AS3MT for As^{III} is 3.2 μM so it may be more likely that efflux of $MMA(GS)_2$ and DMA^V is rate limiting rather than methylation pathways when SCHH are dosed with 0.5 μM As [218]. It is possible that incubating SCHH at lower concentrations of As and thus a resultant increase in methylation of inorganic As, would reveal a more pronounced role for MRP4 in efflux of methylated As.

Preliminary studies in SCHH #23 do suggest that incubating SCHH with As at 0.1 -1.0 μM allows detection of similar amounts of methylated As species (Fig. 5.7). The K_m of AS3MT for MMA is not known and this information would be useful to determine whether or not MRP4 saturation could be a limiting factor in observing its role in DMA^V and $MMA(GS)_2$ efflux across the basolateral membrane of SCHH. A small sample size has also limited our ability to make conclusions and is another reason for further

investigation of the involvement of MRP4 in As efflux. Future studies using shRNA treated SCHH at a lower MOI and incubated with concentrations less than or equal to 0.1 μM As should be completed. This should maximize the production of methylated As and hopefully minimize non-specific viral effects in SCHH experiments, thus, allowing for proper interpretation of results about MRP4 and its role in As efflux using the SCHH model. Experiments should be conducted to determine the lowest dose of As treatment in SCHH that still allows detection of methylated As species using HPLC ICP-MS. One other question that still remains is whether the As species being effluxed into media are glutathione conjugates. This is difficult to determine because As-GSH conjugates are chemically unstable. The majority of As transported across the basolateral membrane of SCHH is inorganic and the ability to detect As-GSH conjugates would narrow the spectrum of transport proteins at the basolateral surface of hepatocytes that are imperative for As cellular detoxification.

Elucidation of specific transport proteins that are crucial for elimination of As from the liver to the blood will facilitate a better understanding of inter-individual susceptibility to As exposure. Understanding the cellular mechanisms underlying an individual's susceptibility to As is imperative for the development of more effective prevention and treatment methods to combat As exposure as well as provide information for more safe and individualized use of As in the clinic.

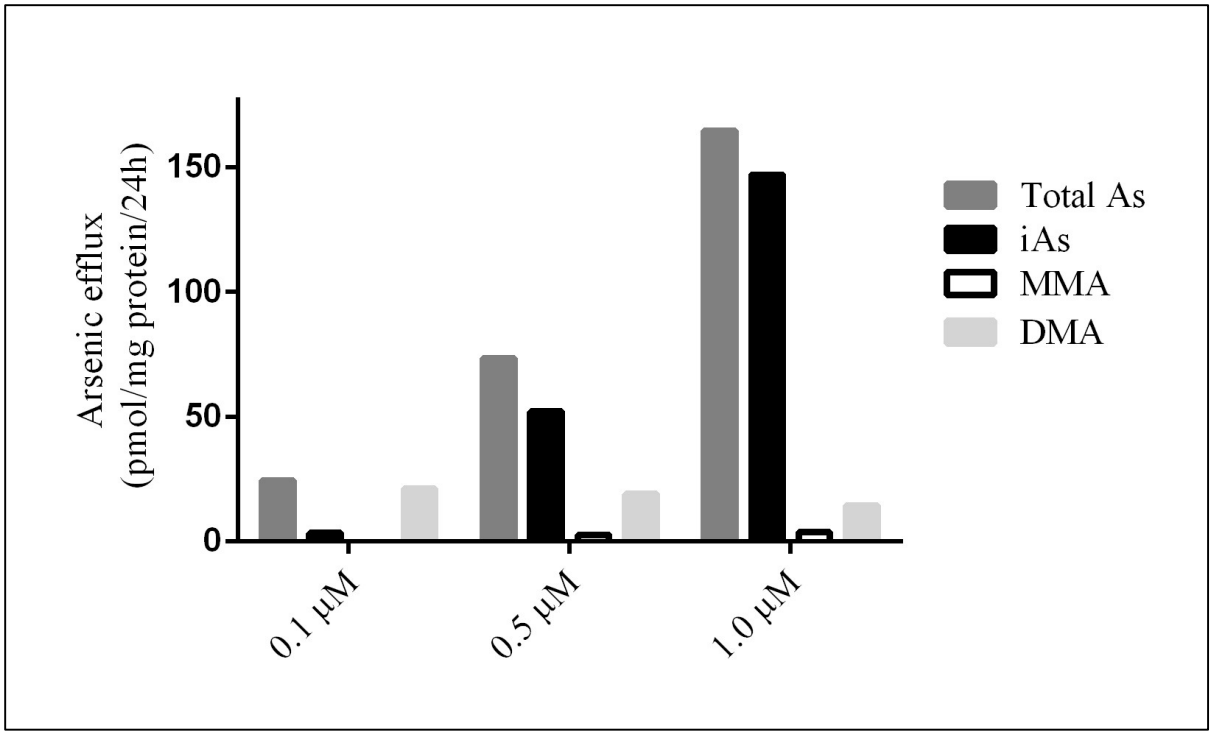

Fig. 5.7. Speciation analysis of SCHH treated with 0.1 -1.0 µM As^{III}. SCHH preparation # 23 was treated with As^{III} (0.1-1.0 µM) for 24 h and the media was collected and frozen at -80°C.

The media was collected and frozen at -80°C. Total As, inorganic As, monomethylated As, and dimethlyated As effluxed into media after 24 h were analyzed by HPLC-ICP-MS as described in the Materials and Methods (Section 2.2.9).

Chapter 6

General Discussion

6.1 Introduction

Arsenic is the 54th most abundant trace element in the earth's crust and a proven human carcinogen [1]. It naturally contaminates drinking water and causes skin, lung, and bladder cancer [3]. It has also been associated with kidney and liver tumors as well as a myriad of other health problems [3]. Despite this, the adverse health effects resulting from As exposure, and the complete pathways for elimination of As from the human body are not well understood. The liver is the main site of As metabolism and this involves methylation reactions that result in the formation of the trivalent more toxic methylated metabolites [195]. Therefore, in this thesis the hepatobiliary transport of As was characterized using physiologically relevant SCHH. The goals of this project were to address several objectives regarding As transport in the liver:

1. Characterize As transport in a human physiological model of the liver, sandwich cultured human hepatocytes.
2. Generate MRP3 and MRP5 stable cell lines and determine if MRP3 or MRP5 provide cellular protection against As^{III}, As^{V}, MMA^{III}, MMA^{v}, DMA^{III}, or DMA^{V}.
3. Optimize conditions for knockdown of MRP4 using shRNA lentiviral particles and determine the contribution MRP4 makes to As efflux from sandwich cultured human hepatocytes.

6.2 Summary

Arsenic transport was characterized in SCHH (Chapter 3). Transport occurred across only the basolateral membrane in nine SCHH preparations and across both the apical and basolateral membranes in five out of fourteen SCHH preparations. Further characterization of the basolateral transport revealed that an MRP was at least partially responsible for basolateral transport of As across the basolateral membrane of the hepatocyte, therefore, the role of candidate proteins MRP3, MRP4, and MRP5 was examined using multiple methods. MRP3 and MRP5 did not confer cellular protection against any of the As species tested (Chapter 4). Direct transport experiments using MRP3 or MRP5 enriched membrane vesicles showed that $As(GS)_3$ was not a substrate for either protein. It is unlikely that these proteins transport As across the basolateral membrane of hepatocytes. In contrast, evidence from cytotoxicity and MRP4-enriched membrane vesicle transport assays suggested that MRP4 plays an important role therefore, the contribution of MRP4 in As transport across the basolateral membrane of hepatocytes was investigated using RNA silencing (Chapter 5) [82]. The inter-individual differences in biliary excretion observed in the SCHH also initiated preliminary studies to characterize human MRP2 and rat Mrp2 transport of As and its GSH-conjugates using membrane-enriched vesicle transport assays and SCRH (Appendix 1).

6.2.1 Chapter 3: Characterization of arsenic using sandwich cultured human hepatocytes

Summary

Hepatobiliary transport of As was characterized for the first time in SCHH. Arsenic was transported across the basolateral membrane in nine out of fourteen SCHH preparations and across both the basolateral and canalicular membranes in five out of the fourteen SCHH preparations. The basolateral transport in SCHH was further characterized and shown to be temperature sensitive, partially GSH-dependent, and inhibited by the MRP inhibitor MK-571. Interestingly, the canalicular efflux of As was completely GSH- dependent. The influence of As and Nrf2 activators on MRP in SCHH was also investigated. Both As and oltipraz treatments upregulated MRP2 and MRP4 expression in SCHH but not other transporters such as MRP1, MRP6, or AQP9. These data suggested that there are inter-individual differences in As transport with basolateral being dominant and this transport appeared to be mediated at least in part by an MRP, likely MRP4.

Future Directions

The reasons for the differences in hepatobiliary transport of As between SCHH preparations are not clear and currently under investigation in our laboratory. It did not appear that MRP2 or MRP4 expression in whole cell lysates of SCHH preparations played a role in the differentially observed polarity of transport. Quantification of relative MRP2 levels in membrane fractions from the SCHHs might reveal a correlation between MRP2 levels and the BEI. Other proteins involved in transport pathways and methylation should be

investigated as potential reasons for the differences in biliary excretion between preparations. MRP2, MRP4 and AS3MT SNPs in the SCHH samples are currently under investigation in our lab. Also, a larger sample size and more cells per preparation would also be useful in the future. This smaller sample size may not be completely representative of an entire human population, however, sample acquisition and cell isolation and culture are somewhat challenging. The amount of cells per preparation was often a limiting factor in the number of experiments that could be performed.

6.2.2 Chapter 4: MRP3 and MRP5 do not protect HEK293 cells from inorganic, monomethylated, or dimethylated arsenic species

Summary

The specific roles of MRPs in As transport are currently being investigated in our lab. Glutathione levels in the liver are high and several of the MRPs are well known for their ability to efflux GSH conjugates. Studies have shown that As forms GSH conjugates and this is likely the predominant form effluxed from the liver into both blood and bile. Furthermore, the studies in Chapter 3 showed that basolateral transport was partially GSH - dependent and that an MRP was likely involved in the transport process. Prior to the start of my Ph.D. work the basolateral transport proteins responsible for As efflux had not been identified. The MRP candidates included MRP3, MRP4, MRP5, and MRP6. Michael W. Carew pursued the role of MRP4 in As detoxification and transport while I investigated

MRP3 and MRP5 as potential candidates. The role of MRP6 is still currently under investigation. Cytotoxicity assays were used to screen the ability of stable cell lines expressing MRP3 and MRP5 to confer cellular protection against As^{V}, As^{III}, MMA^{V}, MMA^{III}, DMA^{V}, and DMA^{III}. HEK293 cells stably expressing MRP3 or MRP5 did not provide cellular protection against any of the arsenicals tested. In parallel, MRP4 was found to confer cellular protection against several As species and direct transport studies found that MRP4 is a high affinity transporter of $MMA(GS)_2$ and DMA^{V} [82]. These findings led me to pursue experiments designed to determine the physiological relevance of MRP4 in the hepatobiliary transport of As using SCHH.

Future Directions

MRP4 appeared to be an ideal candidate for efflux of As across the basolateral membrane of hepatocytes while MRP3 and MRP5 did not (Chapter 4). Direct transport of $As(GS)_3$ was also tested in MRP3 and MRP5 membrane vesicles and was not shown to be a substrate for either protein. MRP6 is expressed at the basolateral membrane of the liver, however, its role in the transport of As has not been explored (Fig 6.1). Generation of an MRP6 stable cell line for use in cytotoxicity assays to test its ability to protect cells from As^{III}, As^{V}, MMA^{III}, MMA^{V}, DMA^{III}, and DMA^{V} would be very useful. In addition, MRP6-enriched membrane vesicles should be used to identify the specific As species transported.

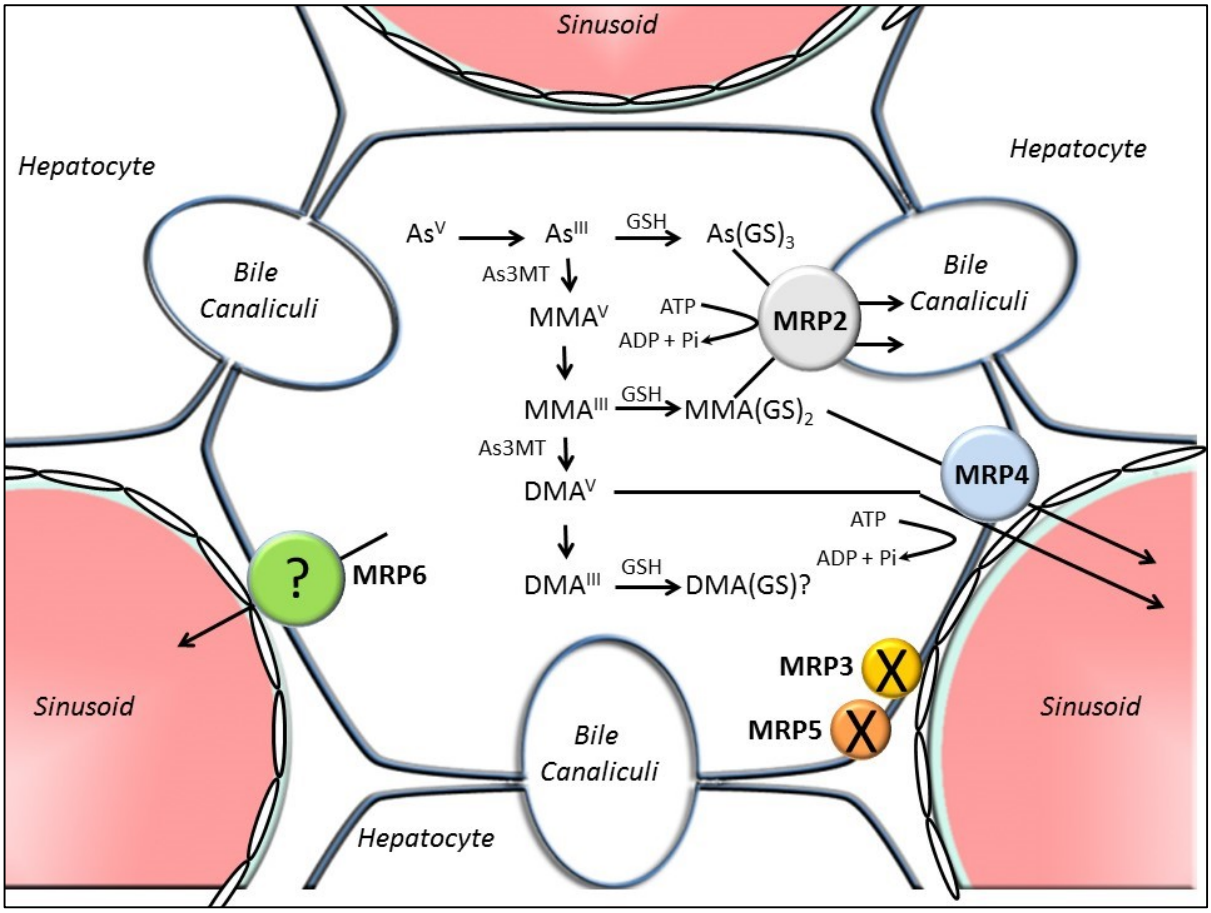

Adapted from: Mayukh Banerjee, Michael W. Carew, Barbara A. Roggenbeck, Brayden D. Whitlock, Hua Naranmandura, X. Chris Le, and Elaine M. Leslie, A Novel Pathway for Arsenic Elimination: Human Multidrug Resistance Protein 4 (MRP4/ *ABCC4*) Mediates Cellular Export of Dimethylarsinic Acid (DMA^V) and the Diglutathione Conjugate of Monomethylarsonous Acid (MMA^{III}), *Mol Pharmacol,* August 2014 86: 168-179 http://molpharm.aspetjournals.org/content/86/2/168.long. Modifications made to this figure include the addition of symbols to represent MRP3, MRP5, and MRP6.

Fig. 6.1. Cellular localization of MRPs in human hepatocytes.

The majority of arsenic is eliminated in urine and therefore must cross the basolateral surface of the hepatocyte into sinusoidal blood for entry into the systemic circulation. MRP3, MRP4, MRP5, and MRP6 are in the correct location for this function, but only MRP4 reduced the cytotoxicity of arsenic. MRP3 and MRP5 did not provide cellular protection against As^{III}, As^V, MMA^{III}, MMA^V, DMA^{III}, or DMA^V. MRP6 is denoted with a question mark because it is not known what role it plays in arsenic efflux from the hepatocyte.

6.2.3 Chapter 5: Knockdown of MRP4 in SCHH using shRNA

Summary

To determine the physiological relevance of MRP4 in SCHH the knockdown of MRP4 using lentiviral particles was first optimized using both HEK293T cells and SCHH. Greater than 90% knockdown of MRP4 was achieved in two SCHH preparations, #25 and #26. The knockdown did not result in any overall decrease in As efflux across the basolateral membrane. Furthermore, speciation analysis of efflux media did not reveal any decreases in DMA^V, a known MRP4 substrate, in the MRP4 knockdown condition compared to the control. It was difficult to draw meaningful conclusions from this work due to several non-specific effects of the lentivirus.

Future Directions

Characterization of MRP4 as a high affinity transporter of both $MMA(GS)_2$ and DMA^V initiated MRP4 knockdown studies using lentivirus containing MRP4-targeted shRNA. We were able to successfully knock down MRP4 in the SCHH, however, no functional effects were observed in the two preparations. We also observed non-specific effects on other membrane proteins due to the viral infection. Studies to optimize the maximum amount of knockdown while minimizing non-specific virus effects should be done. The other obvious weakness in these studies is the small sample size, therefore, these studies should be repeated using optimized conditions. Treating SCHH with lower concentrations of As might prevent saturation of methylation pathways. Furthermore, the use

of a lower MOI for a lower but still effective level of MRP4 knockdown might be a more representative way to determine the role of MRP4 as well as other potential As transport proteins using the SCHH model.

Speciation analysis of As efflux media revealed a high level of inorganic As in media. AQP9 is a well characterized transporter of As^{III} and could be responsible for efflux of As^{III} down its concentration gradient and out of the hepatocyte across the basolateral membrane. Other transport proteins that could be potentially involved in As uptake, such as AQP7, AQP9, GLUT2, GLUT5, and GLUT9 should also be screened for their ability to transport As^{III}, MMA^{III}, DMA^{III}, and DMA^{V}. Due to the high levels of GSH in the liver it seems likely that transport proteins capable of effluxing As^{III} in the form of an $As(GS)_3$ conjugate should also be studied further.

Transport of As-GSH conjugates by hepatocytes could also occur through OATP or MRP6 efflux. OATP1B1 is expressed at the basolateral surface of hepatocytes and although it is generally considered an uptake protein there is evidence that it is a bidirectional transporter which is why we checked expression in SCHH #25 and #26 [212]. Studies described above in the overexpressing OATP1B1- HEK293 cells do suggest that it could transport As-GSH conjugates. The non-specific effects observed due to lentivirus transduction made interpretation of those results inconclusive. Other OATPs at the basolateral surface of hepatocytes including OATP2B1 and OATP1B3 should also be tested for their ability to transport As. MRP6 was detected in the SCHH preparations, but, there also appeared to be non-specific effects due to the transduction that made interpretation difficult. None the less, MRP6 transport of As in currently underway in the laboratory.

The inability to detect As-GSH conjugates presents a major setback in elucidation of transport proteins involved in efflux. Efforts should be made in the development of a method for detection of As-GSH conjugates in the efflux media. This information would allow a more focused approach to identifying transport proteins that are involved in the hepatobiliary transport of As.

6.2.4 Overall Significance

These studies have provided a solid groundwork for the continuation of characterizing hepatobiliary transport of As in humans. Understanding how As is eliminated from the body is vital information for development of novel treatments for both acute and chronic As exposure. The use of As in the clinic for treatment of various cancers would also benefit from understanding human body elimination of this toxic and carcinogenic metalloid.

References

[1]S. Shen, X.F. Li, W.R. Cullen, M. Weinfeld, X.C. Le, Arsenic binding to proteins. Chem Rev 113 (2013) 7769-7792.

[2]H. Garelick, H. Jones, A. Dybowska, E. Valsami-Jones, Arsenic pollution sources. Rev Environ Contam Toxicol 197 (2008) 17-60.

[3]IARC, Arsenic, metals, fibres, and dusts. IARC Monogr Eval Carcinog Risks Hum 100 (2012) 11-465.

[4]A.H. Smith, E.O. Lingas, M. Rahman, Contamination of drinking-water by arsenic in Bangladesh: a public health emergency. Bull World Health Organ 78 (2000) 1093-1103.

[5]M.F. Naujokas, B. Anderson, H. Ahsan, H.V. Aposhian, J.H. Graziano, C. Thompson, W.A. Suk, The broad scope of health effects from chronic arsenic exposure: update on a worldwide public health problem. Environ Health Perspect 121 (2013) 295-302.

[6]S.V. Flanagan, R.B. Johnston, Y. Zheng, Arsenic in tube well water in Bangladesh: health and economic impacts and implications for arsenic mitigation. Bull World Health Organ 90 (2012) 839-846.

[7]S. Shankar, U. Shanker, Shikha, Arsenic contamination of groundwater: a review of sources, prevalence, health risks, and strategies for mitigation. ScientificWorldJournal 2014 (2014) 304524.

[8]J.S. Petrick, F. Ayala-Fierro, W.R. Cullen, D.E. Carter, H. Vasken Aposhian, Monomethylarsonous acid (MMA(III)) is more toxic than arsenite in Chang human hepatocytes. Toxicol Appl Pharmacol 163 (2000) 203-207.

[9]M.J. Mass, A. Tennant, B.C. Roop, W.R. Cullen, M. Styblo, D.J. Thomas, A.D. Kligerman, Methylated trivalent arsenic species are genotoxic. Chem Res Toxicol 14 (2001) 355-361.

[10]D.J. Thomas, M. Styblo, S. Lin, The cellular metabolism and systemic toxicity of arsenic. Toxicol Appl Pharmacol 176 (2001) 127-144.

[11]M.F. Hughes, Arsenic toxicity and potential mechanisms of action. Toxicol Lett 133 (2002) 1-16.

[12]M.J. Ellenhorn, Ellenhorn's Medical Toxicology: Diagnosis and Treatment of Human Poisoning. Williams & Wilkins, Baltimore (1997).

[13]K.M. Hunt, R.K. Srivastava, C.A. Elmets, M. Athar, The mechanistic basis of arsenicosis: pathogenesis of skin cancer. Cancer Lett 354 (2014) 211-219.

[14]I.C. Ch'i, R.Q. Blackwell, A controlled retrospective study of Blackfoot disease, an endemic peripheral gangrene disease in Taiwan. Am J Epidemiol 88 (1968) 7-24.

[15]S. De Chaudhuri, P. Ghosh, N. Sarma, P. Majumdar, T.J. Sau, S. Basu, S. Roychoudhury, K. Ray, A.K. Giri, Genetic variants associated with arsenic susceptibility: study of purine nucleoside phosphorylase, arsenic (+3) methyltransferase, and glutathione S-transferase omega genes. Environ Health Perspect 116 (2008) 501-505.

[16]H. Shi, X. Shi, K.J. Liu, Oxidative mechanism of arsenic toxicity and carcinogenesis. Mol Cell Biochem 255 (2004) 67-78.

[17]M. Delnomdedieu, M.M. Basti, J.D. Otvos, D.J. Thomas, Reduction and binding of arsenate and dimethylarsinate by glutathione: a magnetic resonance study. Chem Biol Interact 90 (1994) 139-155.

[18]M. Styblo, M.F. Hughes, D.J. Thomas, Liberation and analysis of protein-bound arsenicals. J Chromatogr B Biomed Appl 677 (1996) 161-166.

[19]D.C. Ellinsworth, Arsenic, reactive oxygen, and endothelial dysfunction. J Pharmacol Exp Ther 353 (2015) 458-464.

[20]J.R. Gurr, L.H. Yih, T. Samikkannu, D.T. Bau, S.Y. Lin, K.Y. Jan, Nitric oxide production by arsenite. Mutat Res 533 (2003) 173-182.

[21]M. Valko, D. Leibfritz, J. Moncol, M.T. Cronin, M. Mazur, J. Telser, Free radicals and antioxidants in normal physiological functions and human disease. Int J Biochem Cell Biol 39 (2007) 44-84.

[22]S.C. Chen, W.C. Chen, Vascular leakage induced by exposure to arsenic via increased production of NO, hydroxyl radical and peroxynitrite. Microvasc Res 75 (2008) 373-380.

[23]S.J. Flora, Arsenic-induced oxidative stress and its reversibility. Free Radic Biol Med 51 (2011) 257-281.

[24]E. Bustaffa, A. Stoccoro, F. Bianchi, L. Migliore, Genotoxic and epigenetic mechanisms in arsenic carcinogenicity. Arch Toxicol 88 (2014) 1043-1067.

[25]T.W. Gebel, Genotoxicity of arsenical compounds. Int J Hyg Environ Health 203 (2001) 249-262.

[26]K.T. Kitchin, Recent advances in arsenic carcinogenesis: modes of action, animal model systems, and methylated arsenic metabolites. Toxicol Appl Pharmacol 172 (2001) 249-261.

[27]P. Bhattacharjee, M. Banerjee, A.K. Giri, Role of genomic instability in arsenic-induced carcinogenicity. A review. Environ Int 53 (2013) 29-40.

[28]G. Lu, H. Xu, D. Chang, Z. Wu, X. Yao, S. Zhang, Z. Li, J. Bai, Q. Cai, W. Zhang, Arsenic exposure is associated with DNA hypermethylation of the tumor suppressor gene p16. J Occup Med Toxicol 9 (2014) 42.

[29]I.L. Druwe, R.R. Vaillancourt, Influence of arsenate and arsenite on signal transduction pathways: an update. Arch Toxicol 84 (2010) 585-596.

[30]Y. Huang, J. Zhang, K.T. McHenry, M.M. Kim, W. Zeng, V. Lopez-Pajares, C.C. Dibble, J.P. Mizgerd, Z.M. Yuan, Induction of cytoplasmic accumulation of p53: a mechanism for low levels of arsenic exposure to predispose cells for malignant transformation. Cancer Res 68 (2008) 9131-9136.

[31]I. Hertz-Picciotto, A.H. Smith, Observations on the dose-response curve for arsenic exposure and lung cancer. Scand J Work Environ Health 19 (1993) 217-226.

[32]I. Celik, L. Gallicchio, K. Boyd, T.K. Lam, G. Matanoski, X. Tao, M. Shiels, E. Hammond, L. Chen, K.A. Robinson, L.E. Caulfield, J.G. Herman, E. Guallar, A.J. Alberg, Arsenic in drinking water and lung cancer: a systematic review. Environ Res 108 (2008) 48-55.

[33]A. Lee-Feldstein, Cumulative exposure to arsenic and its relationship to respiratory cancer among copper smelter employees. J Occup Med 28 (1986) 296-302.

[34]J.H. Lubin, L.E. Moore, J.F. Fraumeni, Jr., K.P. Cantor, Respiratory cancer and inhaled inorganic arsenic in copper smelters workers: a linear relationship with cumulative exposure that increases with concentration. Environ Health Perspect 116 (2008) 1661-1665.

[35]H.R. Guo, Arsenic level in drinking water and mortality of lung cancer (Taiwan). Cancer Causes Control 15 (2004) 171-177.

[36]S.H. Lamm, S. Robbins, R. Chen, J. Lu, B. Goodrich, M. Feinleib, Discontinuity in the cancer slope factor as it passes from high to low exposure levels--arsenic in the BFD-endemic area. Toxicology 326 (2014) 25-35.

[37]S.R. Ostrowski, S. Wilbur, C.H. Chou, H.R. Pohl, Y.W. Stevens, P.M. Allred, N. Roney, M. Fay, C.A. Tylenda, Agency for Toxic Substances and Disease Registry's 1997 priority list of hazardous substances. Latent effects--carcinogenesis, neurotoxicology, and developmental deficits in humans and animals. Toxicol Ind Health 15 (1999) 602-644.

[38]C.M. Steinmaus, C. Ferreccio, J.A. Romo, Y. Yuan, S. Cortes, G. Marshall, L.E. Moore, J.R. Balmes, J. Liaw, T. Golden, A.H. Smith, Drinking water arsenic in northern chile: high cancer risks 40 years after exposure cessation. Cancer Epidemiol Biomarkers Prev 22 (2013) 623-630.

[39]C.J. Chen, T.L. Kuo, M.M. Wu, Arsenic and cancers. Lancet 1 (1988) 414-415.

[40]N. Saint-Jacques, L. Parker, P. Brown, T.J. Dummer, Arsenic in drinking water and urinary tract cancers: a systematic review of 30 years of epidemiological evidence. Environ Health 13 (2014) 44.

[41]W.P. Tseng, H.M. Chu, S.W. How, J.M. Fong, C.S. Lin, S. Yeh, Prevalence of skin cancer in an endemic area of chronic arsenicism in Taiwan. J Natl Cancer Inst 40 (1968) 453-463.

[42]M.R. Karagas, A. Gossai, B. Pierce, H. Ahsan, Drinking Water Arsenic Contamination, Skin Lesions, and Malignancies: A Systematic Review of the Global Evidence. Curr Environ Health Rep 2 (2015) 52-68.

[43]S.M. Cohen, T. Ohnishi, L.L. Arnold, X.C. Le, Arsenic-induced bladder cancer in an animal model. Toxicol Appl Pharmacol 222 (2007) 258-263.

[44]M.P. Waalkes, J.M. Ward, J. Liu, B.A. Diwan, Transplacental carcinogenicity of inorganic arsenic in the drinking water: induction of hepatic, ovarian, pulmonary, and adrenal tumors in mice. Toxicol Appl Pharmacol 186 (2003) 7-17.

[45]M. Vahter, Mechanisms of arsenic biotransformation. Toxicology 181-182 (2002) 211-217.

[46]M. Vahter, R. Couch, B. Nermell, R. Nilsson, Lack of methylation of inorganic arsenic in the chimpanzee. Toxicol Appl Pharmacol 133 (1995) 262-268.

[47]I. Csanaky, Z. Gregus, Species variations in the biliary and urinary excretion of arsenate, arsenite and their metabolites. Comp Biochem Physiol C Toxicol Pharmacol 131 (2002) 355-365.

[48]M. Vahter, E. Marafante, L. Dencker, Tissue distribution and retention of 74As-dimethylarsinic acid in mice and rats. Arch Environ Contam Toxicol 13 (1984) 259-264.

[49]M. Lu, H. Wang, X.F. Li, X. Lu, W.R. Cullen, L.L. Arnold, S.M. Cohen, X.C. Le, Evidence of hemoglobin binding to arsenic as a basis for the accumulation of arsenic in rat blood. Chem Res Toxicol 17 (2004) 1733-1742.

[50]M. Lu, H. Wang, X.F. Li, L.L. Arnold, S.M. Cohen, X.C. Le, Binding of dimethylarsinous acid to cys-13alpha of rat hemoglobin is responsible for the retention of arsenic in rat blood. Chem Res Toxicol 20 (2007) 27-37.

[51]M. Vahter, Methylation of inorganic arsenic in different mammalian species and population groups. Sci Prog 82 (Pt 1) (1999) 69-88.

[52]S.M. Cohen, L.L. Arnold, M. Eldan, A.S. Lewis, B.D. Beck, Methylated arsenicals: the implications of metabolism and carcinogenicity studies in rodents to human risk assessment. Crit Rev Toxicol 36 (2006) 99-133.

[53]M.P. Waalkes, J. Liu, B.A. Diwan, Transplacental arsenic carcinogenesis in mice. Toxicol Appl Pharmacol 222 (2007) 271-280.

[54]E.J. Tokar, L. Benbrahim-Tallaa, J.M. Ward, R. Lunn, R.L. Sams, 2nd, M.P. Waalkes, Cancer in experimental animals exposed to arsenic and arsenic compounds. Crit Rev Toxicol 40 (2010) 912-927.

[55]L.L. Arnold, M. Eldan, A. Nyska, M. van Gemert, S.M. Cohen, Dimethylarsinic acid: results of chronic toxicity/oncogenicity studies in F344 rats and in B6C3F1 mice. Toxicology 223 (2006) 82-100.

[56]M.P. Waalkes, W. Qu, E.J. Tokar, G.E. Kissling, D. Dixon, Lung tumors in mice induced by "whole-life" inorganic arsenic exposure at human-relevant doses. Arch Toxicol 88 (2014) 1619-1629.

[57]M.P. Waalkes, W. Qu, E.J. Tokar, G.E. Kissling, D. Dixon, Response to letter to the editor by Cohen et al. (2014) "Re: Waalkes et al.: Lung tumors in mice induced by "whole-life" inorganic arsenic exposure at human-relevant doses, Arch Toxicol, 2014". Arch Toxicol 88 (2014) 2063-2065.

[58]S.M. Cohen, L.L. Arnold, J.E. Klaunig, J.I. Goodman, Re: Waalkes et al.: Lung tumors in mice induced by "whole-life" inorganic arsenic exposure at human-relevant doses, Arch Toxicol, 2014. Arch Toxicol 88 (2014) 2061-2062.

[59]X. Cao, M.A. Surma, K. Simons, Polarized sorting and trafficking in epithelial cells. Cell Res 22 (2012) 793-805.

[60]D.A. Bow, J.L. Perry, D.S. Miller, J.B. Pritchard, K.L. Brouwer, Localization of P-gp (Abcb1) and Mrp2 (Abcc2) in freshly isolated rat hepatocytes. Drug Metab Dispos 36 (2008) 198-202.

[61]Z. Drobna, F.S. Walton, D.S. Paul, W. Xing, D.J. Thomas, M. Styblo, Metabolism of arsenic in human liver: the role of membrane transporters. Arch Toxicol 84 (2010) 3-16.

[62]E.L. LeCluyse, K.L. Audus, J.H. Hochman, Formation of extensive canalicular networks by rat hepatocytes cultured in collagen-sandwich configuration. Am J Physiol 266 (1994) C1764-1774.

[63]E. LeCluyse, A. Madan, G. Hamilton, K. Carroll, R. DeHaan, A. Parkinson, Expression and regulation of cytochrome P450 enzymes in primary cultures of human hepatocytes. J Biochem Mol Toxicol 14 (2000) 177-188.

[64]K.A. Hoffmaster, R.Z. Turncliff, E.L. LeCluyse, R.B. Kim, P.J. Meier, K.L. Brouwer, P-glycoprotein expression, localization, and function in sandwich-cultured primary rat and human hepatocytes: relevance to the hepatobiliary disposition of a model opioid peptide. Pharm Res 21 (2004) 1294-1302.

[65]X. Liu, E.L. LeCluyse, K.R. Brouwer, R.M. Lightfoot, J.I. Lee, K.L. Brouwer, Use of Ca2+ modulation to evaluate biliary excretion in sandwich-cultured rat hepatocytes. J Pharmacol Exp Ther 289 (1999) 1592-1599.

[66]X. Liu, E.L. LeCluyse, K.R. Brouwer, L.S. Gan, J.J. Lemasters, B. Stieger, P.J. Meier, K.L. Brouwer, Biliary excretion in primary rat hepatocytes cultured in a collagen-sandwich configuration. Am J Physiol 277 (1999) G12-21.

[67]G. Ghibellini, L.S. Vasist, E.M. Leslie, W.D. Heizer, R.J. Kowalsky, B.F. Calvo, K.L. Brouwer, In vitro-in vivo correlation of hepatobiliary drug clearance in humans. Clin Pharmacol Ther 81 (2007) 406-413.

[68]X. Liu, J.P. Chism, E.L. LeCluyse, K.R. Brouwer, K.L. Brouwer, Correlation of biliary excretion in sandwich-cultured rat hepatocytes and in vivo in rats. Drug Metab Dispos 27 (1999) 637-644.

[69]A. Hernandez, R. Marcos, Genetic variations associated with interindividual sensitivity in the response to arsenic exposure. Pharmacogenomics 9 (2008) 1113-1132.

[70]M. Vahter, Genetic polymorphism in the biotransformation of inorganic arsenic and its role in toxicity. Toxicol Lett 112-113 (2000) 209-217.

[71]D.J. Thomas, J. Li, S.B. Waters, W. Xing, B.M. Adair, Z. Drobna, V. Devesa, M. Styblo, Arsenic (+3 oxidation state) methyltransferase and the methylation of arsenicals. Exp Biol Med (Maywood) 232 (2007) 3-13.

[72]H. Naranmandura, N. Suzuki, K.T. Suzuki, Trivalent arsenicals are bound to proteins during reductive methylation. Chem Res Toxicol 19 (2006) 1010-1018.

[73]F. Challenger, Biological methylation. Adv Enzymol Relat Subj Biochem 12 (1951) 429-491.

[74]T. Hayakawa, Y. Kobayashi, X. Cui, S. Hirano, A new metabolic pathway of arsenite: arsenic-glutathione complexes are substrates for human arsenic methyltransferase Cyt19. Arch Toxicol 79 (2005) 183-191.

[75]R. Antonelli, K. Shao, D.J. Thomas, R. Sams, 2nd, J. Cowden, AS3MT, GSTO, and PNP polymorphisms: impact on arsenic methylation and implications for disease susceptibility. Environ Res 132 (2014) 156-167.

[76]B.L. Pierce, M.G. Kibriya, L. Tong, F. Jasmine, M. Argos, S. Roy, R. Paul-Brutus, R. Rahaman, M. Rakibuz-Zaman, F. Parvez, A. Ahmed, I. Quasem, S.K. Hore, S. Alam, T. Islam, V. Slavkovich, M.V. Gamble, M. Yunus, M. Rahman, J.A. Baron, J.H. Graziano, H. Ahsan, Genome-wide association study identifies chromosome 10q24.32 variants associated with arsenic metabolism and toxicity phenotypes in Bangladesh. PLoS Genet 8 (2012) e1002522.

[77]T. Agusa, J. Fujihara, H. Takeshita, H. Iwata, Individual variations in inorganic arsenic metabolism associated with AS3MT genetic polymorphisms. Int J Mol Sci 12 (2011) 2351-2382.

[78]A.L. Lindberg, R. Kumar, W. Goessler, R. Thirumaran, E. Gurzau, K. Koppova, P. Rudnai, G. Leonardi, T. Fletcher, M. Vahter, Metabolism of low-dose inorganic arsenic in a central European population: influence of sex and genetic polymorphisms. Environ Health Perspect 115 (2007) 1081-1086.

[79]A. Hernandez, L. Paiva, A. Creus, D. Quinteros, R. Marcos, Micronucleus frequency in copper-mine workers exposed to arsenic is modulated by the AS3MT Met287Thr polymorphism. Mutat Res Genet Toxicol Environ Mutagen 759 (2014) 51-55.

[80]Z. Drobna, S.B. Waters, F.S. Walton, E.L. LeCluyse, D.J. Thomas, M. Styblo, Interindividual variation in the metabolism of arsenic in cultured primary human hepatocytes. Toxicol Appl Pharmacol 201 (2004) 166-177.

[81]C.M. Schlebusch, L.M. Gattepaille, K. Engstrom, M. Vahter, M. Jakobsson, K. Broberg, Human adaptation to arsenic-rich environments. Mol Biol Evol 32 (2015) 1544-1555.

[82]M. Banerjee, M.W. Carew, B.A. Roggenbeck, B.D. Whitlock, H. Naranmandura, X.C. Le, E.M. Leslie, A novel pathway for arsenic elimination: human multidrug resistance protein 4 (MRP4/ABCC4) mediates cellular export of dimethylarsinic acid (DMAV) and the diglutathione conjugate of monomethylarsonous acid (MMAIII). Mol Pharmacol 86 (2014) 168-179.

[83]J.M. Carbrey, L. Song, Y. Zhou, M. Yoshinaga, A. Rojek, Y. Wang, Y. Liu, H.L. Lujan, S.E. DiCarlo, S. Nielsen, B.P. Rosen, P. Agre, R. Mukhopadhyay, Reduced arsenic clearance and increased toxicity in aquaglyceroporin-9-null mice. Proc Natl Acad Sci U S A 106 (2009) 15956-15960.

[84]M.W. Carew, E.M. Leslie, Selenium-dependent and -independent transport of arsenic by the human multidrug resistance protein 2 (MRP2/ABCC2): implications for the mutual detoxification of arsenic and selenium. Carcinogenesis 31 (2010) 1450-1455.

[85]X. Jiang, J.R. McDermott, A.A. Ajees, B.P. Rosen, Z. Liu, Trivalent arsenicals and glucose use different translocation pathways in mammalian GLUT1. Metallomics 2 (2010) 211-219.

[86]M. Calatayud, J.A. Barrios, D. Velez, V. Devesa, In vitro study of transporters involved in intestinal absorption of inorganic arsenic. Chem Res Toxicol 25 (2012) 446-453.

[87]A. Rojek, J. Praetorius, J. Frokiaer, S. Nielsen, R.A. Fenton, A current view of the mammalian aquaglyceroporins. Annu Rev Physiol 70 (2008) 301-327.

[88]Z. Liu, J.M. Carbrey, P. Agre, B.P. Rosen, Arsenic trioxide uptake by human and rat aquaglyceroporins. Biochem Biophys Res Commun 316 (2004) 1178-1185.

[89]J.R. McDermott, X. Jiang, L.C. Beene, B.P. Rosen, Z. Liu, Pentavalent methylated arsenicals are substrates of human AQP9. Biometals 23 (2010) 119-127.

[90]R. Mukhopadhyay, H. Bhattacharjee, B.P. Rosen, Aquaglyceroporins: generalized metalloid channels. Biochim Biophys Acta 1840 (2014) 1583-1591.

[91]M. Hamdi, M.A. Sanchez, L.C. Beene, Q. Liu, S.M. Landfear, B.P. Rosen, Z. Liu, Arsenic transport by zebrafish aquaglyceroporins. BMC Mol Biol 10 (2009) 104.

[92]D. Jung, M.A. Adamo, R.M. Lehman, R. Barnaby, C.E. Jackson, B.P. Jackson, J.R. Shaw, B.A. Stanton, A novel variant of aquaporin 3 is expressed in killifish (Fundulus heteroclitus) intestine. Comp Biochem Physiol C Toxicol Pharmacol 171 (2015) 1-7.

[93]B. Thorens, Glucose transporters in the regulation of intestinal, renal, and liver glucose fluxes. Am J Physiol 270 (1996) G541-553.

[94]Z. Liu, M.A. Sanchez, X. Jiang, E. Boles, S.M. Landfear, B.P. Rosen, Mammalian glucose permease GLUT1 facilitates transport of arsenic trioxide

and methylarsonous acid. Biochem Biophys Res Commun 351 (2006) 424-430.

[95]Q. Li, A. Manolescu, M. Ritzel, S. Yao, M. Slugoski, J.D. Young, X.Z. Chen, C.I. Cheeseman, Cloning and functional characterization of the human GLUT7 isoform SLC2A7 from the small intestine. Am J Physiol Gastrointest Liver Physiol 287 (2004) G236-242.

[96]G.W. Gould, G.D. Holman, The glucose transporter family: structure, function and tissue-specific expression. Biochem J 295 (Pt 2) (1993) 329-341.

[97]B. Hagenbuch, P.J. Meier, Organic anion transporting polypeptides of the OATP/ SLC21 family: phylogenetic classification as OATP/ SLCO superfamily, new nomenclature and molecular/functional properties. Pflugers Arch 447 (2004) 653-665.

[98]W.J. Lu, I. Tamai, J. Nezu, M.L. Lai, J.D. Huang, Organic anion transporting polypeptide-C mediates arsenic uptake in HEK-293 cells. J Biomed Sci 13 (2006) 525-533.

[99]L.V. Virkki, J. Biber, H. Murer, I.C. Forster, Phosphate transporters: a tale of two solute carrier families. Am J Physiol Renal Physiol 293 (2007) F643-654.

[100]R. Villa-Bellosta, V. Sorribas, Role of rat sodium/phosphate cotransporters in the cell membrane transport of arsenate. Toxicol Appl Pharmacol 232 (2008) 125-134.

[101]R. Villa-Bellosta, V. Sorribas, Arsenate transport by sodium/phosphate cotransporter type IIb. Toxicol Appl Pharmacol 247 (2010) 36-40.

[102]G. Englund, F. Rorsman, A. Ronnblom, U. Karlbom, L. Lazorova, J. Grasjo, A. Kindmark, P. Artursson, Regional levels of drug transporters along the human intestinal tract: co-expression of ABC and SLC transporters and comparison with Caco-2 cells. Eur J Pharm Sci 29 (2006) 269-277.

[103]H. Gutmann, P. Hruz, C. Zimmermann, C. Beglinger, J. Drewe, Distribution of breast cancer resistance protein (BCRP/ABCG2) mRNA expression along the human GI tract. Biochem Pharmacol 70 (2005) 695-699.

[104]Y. Shinkai, D. Sumi, T. Toyama, T. Kaji, Y. Kumagai, Role of aquaporin 9 in cellular accumulation of arsenic and its cytotoxicity in primary mouse hepatocytes. Toxicol Appl Pharmacol 237 (2009) 232-236.

[105]M. Doblado, K.H. Moley, Facilitative glucose transporter 9, a unique hexose and urate transporter. Am J Physiol Endocrinol Metab 297 (2009) E831-835.

[106]A.J. Percy, J. Gailer, Methylated trivalent arsenic-glutathione complexes are more stable than their arsenite analog. Bioinorg Chem Appl (2008) 539082.

[107]S.V. Kala, M.W. Neely, G. Kala, C.I. Prater, D.W. Atwood, J.S. Rice, M.W. Lieberman, The MRP2/cMOAT transporter and arsenic-glutathione complex formation are required for biliary excretion of arsenic. J Biol Chem 275 (2000) 33404-33408.

[108]L. Yehiayan, M. Pattabiraman, K. Kavallieratos, X. Wang, L.H. Boise, Y. Cai, Speciation, formation, stability and analytical challenges of human arsenic metabolites. J Anal At Spectrom 24 (2009) 1397-1405.

[109]E.M. Leslie, Arsenic-glutathione conjugate transport by the human multidrug resistance proteins (MRPs/ABCCs). J Inorg Biochem 108 (2012) 141-149.

[110]D.J. Thomas, S.B. Waters, M. Styblo, Elucidating the pathway for arsenic methylation. Toxicol Appl Pharmacol 198 (2004) 319-326.

[111]W.R. Cullen, Chemical mechanism of arsenic biomethylation. Chem Res Toxicol 27 (2014) 457-461.

[112]K. Moitra, M. Dean, Evolution of ABC transporters by gene duplication and their role in human disease. Biol Chem 392 (2011) 29-37.

[113]M. Dean, A. Rzhetsky, R. Allikmets, The human ATP-binding cassette (ABC) transporter superfamily. Genome Res 11 (2001) 1156-1166.

[114]R.G. Deeley, C. Westlake, S.P. Cole, Transmembrane transport of endo- and xenobiotics by mammalian ATP-binding cassette multidrug resistance proteins. Physiol Rev 86 (2006) 849-899.

[115]C.F. Higgins, ABC transporters: from microorganisms to man. Annu Rev Cell Biol 8 (1992) 67-113.

[116]J.E. Walker, M. Saraste, M.J. Runswick, N.J. Gay, Distantly related sequences in the alpha- and beta-subunits of ATP synthase, myosin, kinases and other ATP-requiring enzymes and a common nucleotide binding fold. EMBO J 1 (1982) 945-951.

[117]S.C. Hyde, P. Emsley, M.J. Hartshorn, M.M. Mimmack, U. Gileadi, S.R. Pearce, M.P. Gallagher, D.R. Gill, R.E. Hubbard, C.F. Higgins, Structural model of

ATP-binding proteins associated with cystic fibrosis, multidrug resistance and bacterial transport. Nature 346 (1990) 362-365.

[118]C.F. Higgins, K.J. Linton, The ATP switch model for ABC transporters. Nat Struct Mol Biol 11 (2004) 918-926.

[119]T.W. Loo, M.C. Bartlett, D.M. Clarke, The "LSGGQ" motif in each nucleotide-binding domain of human P-glycoprotein is adjacent to the opposing walker A sequence. J Biol Chem 277 (2002) 41303-41306.

[120]W. Mo, J.T. Zhang, Oligomerization of human ATP-binding cassette transporters and its potential significance in human disease. Expert Opin Drug Metab Toxicol 5 (2009) 1049-1063.

[121]E.M. Leslie, R.G. Deeley, S.P. Cole, Multidrug resistance proteins: role of P-glycoprotein, MRP1, MRP2, and BCRP (ABCG2) in tissue defense. Toxicol Appl Pharmacol 204 (2005) 216-237.

[122]Q. Mao, J.D. Unadkat, Role of the breast cancer resistance protein (BCRP/ABCG2) in drug transport--an update. AAPS J 17 (2015) 65-82.

[123]M. Maliepaard, G.L. Scheffer, I.F. Faneyte, M.A. van Gastelen, A.C. Pijnenborg, A.H. Schinkel, M.J. van De Vijver, R.J. Scheper, J.H. Schellens, Subcellular localization and distribution of the breast cancer resistance protein transporter in normal human tissues. Cancer Res 61 (2001) 3458-3464.

[124]S.B. Fernandez, Z. Hollo, A. Kern, E. Bakos, P.A. Fischer, P. Borst, R. Evers, Role of the N-terminal transmembrane region of the multidrug resistance protein MRP2 in routing to the apical membrane in MDCKII cells. J Biol Chem 277 (2002) 31048-31055.

[125]C.J. Westlake, S.P. Cole, R.G. Deeley, Role of the NH2-terminal membrane spanning domain of multidrug resistance protein 1/ABCC1 in protein processing and trafficking. Mol Biol Cell 16 (2005) 2483-2492.

[126]C.J. Westlake, L. Payen, M. Gao, S.P. Cole, R.G. Deeley, Identification and characterization of functionally important elements in the multidrug resistance protein 1 COOH-terminal region. J Biol Chem 279 (2004) 53571-53583.

[127]S.P. Cole, G. Bhardwaj, J.H. Gerlach, J.E. Mackie, C.E. Grant, K.C. Almquist, A.J. Stewart, E.U. Kurz, A.M. Duncan, R.G. Deeley, Overexpression of a

transporter gene in a multidrug-resistant human lung cancer cell line. Science 258 (1992) 1650-1654.

[128]H. Roelofsen, T.A. Vos, I.J. Schippers, F. Kuipers, H. Koning, H. Moshage, P.L. Jansen, M. Muller, Increased levels of the multidrug resistance protein in lateral membranes of proliferating hepatocyte-derived cells. Gastroenterology 112 (1997) 511-521.

[129]J.E. Ros, L. Libbrecht, M. Geuken, P.L. Jansen, T.A. Roskams, High expression of MDR1, MRP1, and MRP3 in the hepatic progenitor cell compartment and hepatocytes in severe human liver disease. J Pathol 200 (2003) 553-560.

[130]S.P. Cole, Multidrug resistance protein 1 (MRP1, ABCC1), a "multitasking" ATP-binding cassette (ABC) transporter. J Biol Chem 289 (2014) 30880-30888.

[131]S.P. Cole, Targeting multidrug resistance protein 1 (MRP1, ABCC1): past, present, and future. Annu Rev Pharmacol Toxicol 54 (2014) 95-117.

[132]D. Keppler, Multidrug resistance proteins (MRPs, ABCCs): importance for pathophysiology and drug therapy. Handb Exp Pharmacol (2011) 299-323.

[133]S.P. Cole, R.G. Deeley, Transport of glutathione and glutathione conjugates by MRP1. Trends Pharmacol Sci 27 (2006) 438-446.

[134]D.W. Loe, R.G. Deeley, S.P. Cole, Characterization of vincristine transport by the M(r) 190,000 multidrug resistance protein (MRP): evidence for cotransport with reduced glutathione. Cancer Res 58 (1998) 5130-5136.

[135]A. Rothnie, G. Conseil, A.Y. Lau, R.G. Deeley, S.P. Cole, Mechanistic differences between GSH transport by multidrug resistance protein 1 (MRP1/ABCC1) and GSH modulation of MRP1-mediated transport. Mol Pharmacol 74 (2008) 1630-1640.

[136]M.G. Belinsky, L.J. Bain, B.B. Balsara, J.R. Testa, G.D. Kruh, Characterization of MOAT-C and MOAT-D, new members of the MRP/cMOAT subfamily of transporter proteins. J Natl Cancer Inst 90 (1998) 1735-1741.

[137]D. Keppler, The roles of MRP2, MRP3, OATP1B1, and OATP1B3 in conjugated hyperbilirubinemia. Drug Metab Dispos 42 (2014) 561-565.

[138]M. Li, W. Wang, C.J. Soroka, A. Mennone, K. Harry, E.J. Weinman, J.L. Boyer, NHERF-1 binds to Mrp2 and regulates hepatic Mrp2 expression and function. J Biol Chem 285 (2010) 19299-19307.

[139]A.T. Nies, D. Keppler, The apical conjugate efflux pump ABCC2 (MRP2). Pflugers Arch 453 (2007) 643-659.

[140]C.C. Paulusma, M.A. van Geer, R. Evers, M. Heijn, R. Ottenhoff, P. Borst, R.P. Oude Elferink, Canalicular multispecific organic anion transporter/multidrug resistance protein 2 mediates low-affinity transport of reduced glutathione. Biochem J 338 (Pt 2) (1999) 393-401.

[141]Y. Cui, J. Konig, J.K. Buchholz, H. Spring, I. Leier, D. Keppler, Drug resistance and ATP-dependent conjugate transport mediated by the apical multidrug resistance protein, MRP2, permanently expressed in human and canine cells. Mol Pharmacol 55 (1999) 929-937.

[142]P. Borst, C. de Wolf, K. van de Wetering, Multidrug resistance-associated proteins 3, 4, and 5. Pflugers Arch 453 (2007) 661-673.

[143]M. Kool, M. van der Linden, M. de Haas, G.L. Scheffer, J.M. de Vree, A.J. Smith, G. Jansen, G.J. Peters, N. Ponne, R.J. Scheper, R.P. Elferink, F. Baas, P. Borst, MRP3, an organic anion transporter able to transport anti-cancer drugs. Proc Natl Acad Sci U S A 96 (1999) 6914-6919.

[144]P. Borst, N. Zelcer, K. van de Wetering, MRP2 and 3 in health and disease. Cancer Lett 234 (2006) 51-61.

[145]T. Hirohashi, H. Suzuki, K. Ito, K. Ogawa, K. Kume, T. Shimizu, Y. Sugiyama, Hepatic expression of multidrug resistance-associated protein-like proteins maintained in eisai hyperbilirubinemic rats. Mol Pharmacol 53 (1998) 1068-1075.

[146]J. Konig, D. Rost, Y. Cui, D. Keppler, Characterization of the human multidrug resistance protein isoform MRP3 localized to the basolateral hepatocyte membrane. Hepatology 29 (1999) 1156-1163.

[147]M.T. Hoque, S.P. Cole, Down-regulation of Na+/H+ exchanger regulatory factor 1 increases expression and function of multidrug resistance protein 4. Cancer Res 68 (2008) 4802-4809.

[148]M.T. Hoque, G. Conseil, S.P. Cole, Involvement of NHERF1 in apical membrane localization of MRP4 in polarized kidney cells. Biochem Biophys Res Commun 379 (2009) 60-64.

[149]Z.S. Chen, K. Lee, G.D. Kruh, Transport of cyclic nucleotides and estradiol 17-beta-D-glucuronide by multidrug resistance protein 4. Resistance to 6-mercaptopurine and 6-thioguanine. J Biol Chem 276 (2001) 33747-33754.

[150]C.A. Ritter, G. Jedlitschky, H. Meyer zu Schwabedissen, M. Grube, K. Kock, H.K. Kroemer, Cellular export of drugs and signaling molecules by the ATP-binding cassette transporters MRP4 (ABCC4) and MRP5 (ABCC5). Drug Metab Rev 37 (2005) 253-278.

[151]S.N. Barnes, L.M. Aleksunes, L. Augustine, G.L. Scheffer, M.J. Goedken, A.B. Jakowski, I.M. Pruimboom-Brees, N.J. Cherrington, J.E. Manautou, Induction of hepatobiliary efflux transporters in acetaminophen-induced acute liver failure cases. Drug Metab Dispos 35 (2007) 1963-1969.

[152]P. Wielinga, J.H. Hooijberg, S. Gunnarsdottir, I. Kathmann, G. Reid, N. Zelcer, K. van der Born, M. de Haas, I. van der Heijden, G. Kaspers, J. Wijnholds, G. Jansen, G. Peters, P. Borst, The human multidrug resistance protein MRP5 transports folates and can mediate cellular resistance against antifolates. Cancer Res 65 (2005) 4425-4430.

[153]G. Jedlitschky, B. Burchell, D. Keppler, The multidrug resistance protein 5 functions as an ATP-dependent export pump for cyclic nucleotides. J Biol Chem 275 (2000) 30069-30074.

[154]G.L. Scheffer, X. Hu, A.C. Pijnenborg, J. Wijnholds, A.A. Bergen, R.J. Scheper, MRP6 (ABCC6) detection in normal human tissues and tumors. Lab Invest 82 (2002) 515-518.

[155]O. Le Saux, L. Martin, Z. Aherrahrou, G. Leftheriotis, A. Varadi, C.N. Brampton, The molecular and physiological roles of ABCC6: more than meets the eye. Front Genet 3 (2012) 289.

[156]M.G. Belinsky, Z.S. Chen, I. Shchaveleva, H. Zeng, G.D. Kruh, Characterization of the drug resistance and transport properties of multidrug resistance protein 6 (MRP6, ABCC6). Cancer Res 62 (2002) 6172-6177.

[157]F. Ringpfeil, M.G. Lebwohl, A.M. Christiano, J. Uitto, Pseudoxanthoma elasticum: mutations in the MRP6 gene encoding a transmembrane ATP-binding cassette (ABC) transporter. Proc Natl Acad Sci U S A 97 (2000) 6001-6006.

[158]K.T. Suzuki, T. Tomita, Y. Ogra, M. Ohmichi, Glutathione-conjugated arsenics in the potential hepato-enteric circulation in rats. Chem Res Toxicol 14 (2001) 1604-1611.

[159]O.A. Levander, Metabolic interrelationships between arsenic and selenium. Environ Health Perspect 19 (1977) 159-164.

[160]J. Gailer, G.N. George, I.J. Pickering, R.C. Prince, H.S. Younis, J.J. Winzerling, Biliary excretion of [(GS)(2)AsSe](-) after intravenous injection of rabbits with arsenite and selenate. Chem Res Toxicol 15 (2002) 1466-1471.

[161]E.M. Leslie, A. Haimeur, M.P. Waalkes, Arsenic transport by the human multidrug resistance protein 1 (MRP1/ABCC1). Evidence that a tri-glutathione conjugate is required. J Biol Chem 279 (2004) 32700-32708.

[162]M.W. Carew, H. Naranmandura, C.B. Shukalek, X.C. Le, E.M. Leslie, Monomethylarsenic diglutathione transport by the human multidrug resistance protein 1 (MRP1/ABCC1). Drug Metab Dispos 39 (2011) 2298-2304.

[163]X.J. Wang, Z. Sun, W. Chen, Y. Li, N.F. Villeneuve, D.D. Zhang, Activation of Nrf2 by arsenite and monomethylarsonous acid is independent of Keap1-C151: enhanced Keap1-Cul3 interaction. Toxicol Appl Pharmacol 230 (2008) 383-389.

[164]A. Hayashi, H. Suzuki, K. Itoh, M. Yamamoto, Y. Sugiyama, Transcription factor Nrf2 is required for the constitutive and inducible expression of multidrug resistance-associated protein 1 in mouse embryo fibroblasts. Biochem Biophys Res Commun 310 (2003) 824-829.

[165]L. Ji, H. Li, P. Gao, G. Shang, D.D. Zhang, N. Zhang, T. Jiang, Nrf2 pathway regulates multidrug-resistance-associated protein 1 in small cell lung cancer. PLoS One 8 (2013) e63404.

[166]V. Vollrath, A.M. Wielandt, M. Iruretagoyena, J. Chianale, Role of Nrf2 in the regulation of the Mrp2 (ABCC2) gene. Biochem J 395 (2006) 599-609.

[167]C.I. Ghanem, S. Rudraiah, A.M. Bataille, M.B. Vigo, M.J. Goedken, J.E. Manautou, Role of nuclear factor-erythroid 2-related factor 2 (Nrf2) in the transcriptional regulation of brain ABC transporters during acute acetaminophen (APAP) intoxication in mice. Biochem Pharmacol 94 (2015) 203-211.

[168]S. Xu, J. Weerachayaphorn, S.Y. Cai, C.J. Soroka, J.L. Boyer, Aryl hydrocarbon receptor and NF-E2-related factor 2 are key regulators of human MRP4 expression. Am J Physiol Gastrointest Liver Physiol 299 (2010) G126-135.

[169]G.L. Scheffer, M. Kool, M. Heijn, M. de Haas, A.C. Pijnenborg, J. Wijnholds, A. van Helvoort, M.C. de Jong, J.H. Hooijberg, C.A. Mol, M. van der Linden, J.M. de Vree, P. van der Valk, R.P. Elferink, P. Borst, R.J. Scheper, Specific detection of multidrug resistance proteins MRP1, MRP2, MRP3, MRP5, and MDR3 P-glycoprotein with a panel of monoclonal antibodies. Cancer Res 60 (2000) 5269-5277.

[170]C.J. Oleschuk, R.G. Deeley, S.P. Cole, Substitution of Trp1242 of TM17 alters substrate specificity of human multidrug resistance protein 3. Am J Physiol Gastrointest Liver Physiol 284 (2003) G280-289.

[171]M. Rius, A.T. Nies, J. Hummel-Eisenbeiss, G. Jedlitschky, D. Keppler, Cotransport of reduced glutathione with bile salts by MRP4 (ABCC4) localized to the basolateral hepatocyte membrane. Hepatology 38 (2003) 374-384.

[172]M. Kool, M. de Haas, G.L. Scheffer, R.J. Scheper, M.J. van Eijk, J.A. Juijn, F. Baas, P. Borst, Analysis of expression of cMOAT (MRP2), MRP3, MRP4, and MRP5, homologues of the multidrug resistance-associated protein gene (MRP1), in human cancer cell lines. Cancer Res 57 (1997) 3537-3547.

[173]M. Buchler, J. Konig, M. Brom, J. Kartenbeck, H. Spring, T. Horie, D. Keppler, cDNA cloning of the hepatocyte canalicular isoform of the multidrug resistance protein, cMrp, reveals a novel conjugate export pump deficient in hyperbilirubinemic mutant rats. J Biol Chem 271 (1996) 15091-15098.

[174]N.J. Karin, Cloning of transfected cells without cloning rings. Biotechniques 27 (1999) 681-682.

[175]E.M. Leslie, I.J. Letourneau, R.G. Deeley, S.P. Cole, Functional and structural consequences of cysteine substitutions in the NH2 proximal region of the human multidrug resistance protein 1 (MRP1/ABCC1). Biochemistry 42 (2003) 5214-5224.

[176]G.A. Hamilton, S.L. Jolley, D. Gilbert, D.J. Coon, S. Barros, E.L. LeCluyse, Regulation of cell morphology and cytochrome P450 expression in human hepatocytes by extracellular matrix and cell-cell interactions. Cell Tissue Res 306 (2001) 85-99.

[177]D.F. Mercer, D.E. Schiller, J.F. Elliott, D.N. Douglas, C. Hao, A. Rinfret, W.R. Addison, K.P. Fischer, T.A. Churchill, J.R. Lakey, D.L. Tyrrell, N.M. Kneteman, Hepatitis C virus replication in mice with chimeric human livers. Nat Med 7 (2001) 927-933.

[178]G. Tiscornia, O. Singer, I.M. Verma, Production and purification of lentiviral vectors. Nat Protoc 1 (2006) 241-245.

[179]J.K. Lee, E.M. Leslie, M.J. Zamek-Gliszczynski, K.L. Brouwer, Modulation of trabectedin (ET-743) hepatobiliary disposition by multidrug resistance-associated proteins (Mrps) may prevent hepatotoxicity. Toxicol Appl Pharmacol 228 (2008) 17-23.

[180]D.W. Loe, K.C. Almquist, R.G. Deeley, S.P. Cole, Multidrug resistance protein (MRP)-mediated transport of leukotriene C4 and chemotherapeutic agents in membrane vesicles. Demonstration of glutathione-dependent vincristine transport. J Biol Chem 271 (1996) 9675-9682.

[181]P.F. Reay, C.J. Asher, Preparation and purification of 74As-labeled arsenate and arsenite for use in biological experiments. Anal Biochem 78 (1977) 557-560.

[182]J.H. Kalivas, Evaluation of volume and matrix effects for the generalized standard addition method. Talanta 34 (1987) 899-903.

[183]V.E. Kostrubsky, S.C. Strom, J. Hanson, E. Urda, K. Rose, J. Burliegh, P. Zocharski, H. Cai, J.F. Sinclair, J. Sahi, Evaluation of hepatotoxic potential of drugs by inhibition of bile-acid transport in cultured primary human hepatocytes and intact rats. Toxicol Sci 76 (2003) 220-228.

[184]D.R. Hipfner, S.D. Gauldie, R.G. Deeley, S.P. Cole, Detection of the M(r) 190,000 multidrug resistance protein, MRP, with monoclonal antibodies. Cancer Res 54 (1994) 5788-5792.

[185]T.L. Marion, E.M. Leslie, K.L. Brouwer, Use of sandwich-cultured hepatocytes to evaluate impaired bile acid transport as a mechanism of drug-induced hepatotoxicity. Mol Pharm 4 (2007) 911-918.

[186]S. Sharma, E.C. Ellis, R. Gramignoli, K. Dorko, V. Tahan, M. Hansel, D.R. Mattison, S.N. Caritis, R.N. Hines, R. Venkataramanan, S.C. Strom, Hepatobiliary disposition of 17-OHPC and taurocholate in fetal human hepatocytes: a comparison with adult human hepatocytes. Drug Metab Dispos 41 (2013) 296-304.

[187]Z. Drobna, S.B. Waters, V. Devesa, A.W. Harmon, D.J. Thomas, M. Styblo, Metabolism and toxicity of arsenic in human urothelial cells expressing rat arsenic (+3 oxidation state)-methyltransferase. Toxicol Appl Pharmacol 207 (2005) 147-159.

[188]M.J. Zamek-Gliszczynski, H. Xiong, N.J. Patel, R.Z. Turncliff, G.M. Pollack, K.L. Brouwer, Pharmacokinetics of 5 (and 6)-carboxy-2',7'-dichlorofluorescein and its diacetate promoiety in the liver. J Pharmacol Exp Ther 304 (2003) 801-809.

[189]L. Vernhet, M.P. Seite, N. Allain, A. Guillouzo, O. Fardel, Arsenic induces expression of the multidrug resistance-associated protein 2 (MRP2) gene in primary rat and human hepatocytes. J Pharmacol Exp Ther 298 (2001) 234-239.

[190]Y. Shirasaka, M. Shichiri, T. Mori, T. Nakanishi, I. Tamai, Major active components in grapefruit, orange, and apple juices responsible for OATP2B1-mediated drug interactions. J Pharm Sci 102 (2013) 280-288.

[191]R.M. Krupka, Asymmetrical binding of phloretin to the glucose transport system of human erythrocytes. J Membr Biol 83 (1985) 71-80.

[192]O. Kwon, P. Eck, S. Chen, C.P. Corpe, J.H. Lee, M. Kruhlak, M. Levine, Inhibition of the intestinal glucose transporter GLUT2 by flavonoids. FASEB J 21 (2007) 366-377.

[193]C.P. Wu, A.M. Calcagno, S.B. Hladky, S.V. Ambudkar, M.A. Barrand, Modulatory effects of plant phenols on human multidrug-resistance proteins 1, 4 and 5 (ABCC1, 4 and 5). FEBS J 272 (2005) 4725-4740.

[194]E. Jigorel, M. Le Vee, C. Boursier-Neyret, Y. Parmentier, O. Fardel, Differential regulation of sinusoidal and canalicular hepatic drug transporter expression by xenobiotics activating drug-sensing receptors in primary human hepatocytes. Drug Metab Dispos 34 (2006) 1756-1763.

[195]M. Styblo, L.M. Del Razo, E.L. LeCluyse, G.A. Hamilton, C. Wang, W.R. Cullen, D.J. Thomas, Metabolism of arsenic in primary cultures of human and rat hepatocytes. Chem Res Toxicol 12 (1999) 560-565.

[196]J. Lebeck, Metabolic impact of the glycerol channels AQP7 and AQP9 in adipose tissue and liver. J Mol Endocrinol 52 (2014) R165-178.

[197]X. Cui, Y. Kobayashi, T. Hayakawa, S. Hirano, Arsenic speciation in bile and urine following oral and intravenous exposure to inorganic and organic arsenics in rats. Toxicol Sci 82 (2004) 478-487.

[198]C.G. Dietrich, R. Ottenhoff, D.R. de Waart, R.P. Oude Elferink, Role of MRP2 and GSH in intrahepatic cycling of toxins. Toxicology 167 (2001) 73-81.

[199]N. Ishihara, T. Matsushiro, Biliary and urinary excretion of metals in humans. Arch Environ Health 41 (1986) 324-330.

[200]C. Pomroy, S.M. Charbonneau, R.S. McCullough, G.K. Tam, Human retention studies with 74As. Toxicol Appl Pharmacol 53 (1980) 550-556.

[201]C.A. Loffredo, H.V. Aposhian, M.E. Cebrian, H. Yamauchi, E.K. Silbergeld, Variability in human metabolism of arsenic. Environ Res 92 (2003) 85-91.

[202]X. Gu, J.E. Manautou, Regulation of hepatic ABCC transporters by xenobiotics and in disease states. Drug Metab Rev 42 (2010) 482-538.

[203]M.A. McAleer, M.A. Breen, N.L. White, N. Matthews, pABC11 (also known as MOAT-C and MRP5), a member of the ABC family of proteins, has anion transporter activity but does not confer multidrug resistance when overexpressed in human embryonic kidney 293 cells. J Biol Chem 274 (1999) 23541-23548.

[204]K. Lee, A.J. Klein-Szanto, G.D. Kruh, Analysis of the MRP4 drug resistance profile in transfected NIH3T3 cells. J Natl Cancer Inst 92 (2000) 1934-1940.

[205]J. Wijnholds, C.A. Mol, L. van Deemter, M. de Haas, G.L. Scheffer, F. Baas, J.H. Beijnen, R.J. Scheper, S. Hatse, E. De Clercq, J. Balzarini, P. Borst, Multidrug-resistance protein 5 is a multispecific organic anion transporter able to transport nucleotide analogs. Proc Natl Acad Sci U S A 97 (2000) 7476-7481.

[206]N. Zelcer, T. Saeki, G. Reid, J.H. Beijnen, P. Borst, Characterization of drug transport by the human multidrug resistance protein 3 (ABCC3). J Biol Chem 276 (2001) 46400-46407.

[207]G. Reid, P. Wielinga, N. Zelcer, M. De Haas, L. Van Deemter, J. Wijnholds, J. Balzarini, P. Borst, Characterization of the transport of nucleoside analog drugs by the human multidrug resistance proteins MRP4 and MRP5. Mol Pharmacol 63 (2003) 1094-1103.

[208]Y. Long, Q. Li, J. Li, Z. Cui, Molecular analysis, developmental function and heavy metal-induced expression of ABCC5 in zebrafish. Comp Biochem Physiol B Biochem Mol Biol 158 (2011) 46-55.

[209]U. Gradhand, T. Lang, E. Schaeffeler, H. Glaeser, H. Tegude, K. Klein, P. Fritz, G. Jedlitschky, H.K. Kroemer, I. Bachmakov, B. Anwald, R. Kerb, U.M. Zanger, M. Eichelbaum, M. Schwab, M.F. Fromm, Variability in human hepatic MRP4 expression: influence of cholestasis and genotype. Pharmacogenomics J 8 (2008) 42-52.

[210]K. Schlawicke Engstrom, B. Nermell, G. Concha, U. Stromberg, M. Vahter, K. Broberg, Arsenic metabolism is influenced by polymorphisms in genes involved in one-carbon metabolism and reduction reactions. Mutat Res 667 (2009) 4-14.

[211]M.O. Gribble, V.S. Voruganti, C.D. Cropp, K.A. Francesconi, W. Goessler, J.G. Umans, E.K. Silbergeld, S.L. Laston, K. Haack, W.H. Kao, M.D. Fallin, J.W. Maccluer, S.A. Cole, A. Navas-Acien, SLCO1B1 variants and urine arsenic metabolites in the Strong Heart Family Study. Toxicol Sci 136 (2013) 19-25.

[212]C. Mahagita, S.M. Grassl, P. Piyachaturawat, N. Ballatori, Human organic anion transporter 1B1 and 1B3 function as bidirectional carriers and do not mediate GSH-bile acid cotransport. Am J Physiol Gastrointest Liver Physiol 293 (2007) G271-278.

[213]M.K. DeGorter, R.H. Ho, B.F. Leake, R.G. Tirona, R.B. Kim, Interaction of three regiospecific amino acid residues is required for OATP1B1 gain of OATP1B3 substrate specificity. Mol Pharm 9 (2012) 986-995.

[214]J. Sampath, M. Adachi, S. Hatse, L. Naesens, J. Balzarini, R.M. Flatley, L.H. Matherly, J.D. Schuetz, Role of MRP4 and MRP5 in biology and chemotherapy. AAPS PharmSci 4 (2002) E14.

[215]T.K. Bera, S. Lee, G. Salvatore, B. Lee, I. Pastan, MRP8, a new member of ABC transporter superfamily, identified by EST database mining and gene prediction program, is highly expressed in breast cancer. Mol Med 7 (2001) 509-516.

[216]G.D. Kruh, Y. Guo, E. Hopper-Borge, M.G. Belinsky, Z.S. Chen, ABCC10, ABCC11, and ABCC12. Pflugers Arch 453 (2007) 675-684.

[217]S. Karim, D.H. Adams, P.F. Lalor, Hepatic expression and cellular distribution of the glucose transporter family. World J Gastroenterol 18 (2012) 6771-6781.

[218]X. Song, Z. Geng, X. Li, Q. Zhao, X. Hu, X. Zhang, Z. Wang, Functional and structural evaluation of cysteine residues in the human arsenic (+3 oxidation state) methyltransferase (hAS3MT). Biochimie 93 (2011) 369-375.

[219]S.V. Kala, G. Kala, C.I. Prater, A.C. Sartorelli, M.W. Lieberman, Formation and urinary excretion of arsenic triglutathione and methylarsenic diglutathione. Chem Res Toxicol 17 (2004) 243-249.

Appendix 1

Arsenic Transport by Human and Rat MRP2/Mrp2

A1.1 Introduction

The transport of As-GSH conjugates into the bile of rats has been demonstrated by several laboratories. Kala *et al.,* showed that both intravenous and oral administration of arsenite (0.1 mg/kg - 5 mg/kg) resulted in detection of $As(GS)_3$ and $MMA(GS)_2$, but not DMA(GS) in the bile of Wistar rats [107]. These GSH conjugates accounted for >90% of As in bile. Similar findings were made by Suzuki *et al*., after intravenous administration of As to Wistar rats [158]. Administration of As to Mrp2-deficient (TR^-) Wistar rats, resulted in a complete loss of As biliary excretion revealing a critical role for Mrp2 in this process [219] [198]. Interestingly, in Sprague Dawley rats Cui *et al.,* demonstrated that intravenous administration of As resulted in the detection of $As(GS)_3$ and $MMA(GS)_2$ in bile, whereas oral administration of As resulted in detection of $MMA(GS)_2$ and DMA^V in bile. DMA^V was not detected in bile by Kala *et al*., either after oral or iv administration [107,197]. The reason for this difference is not clear but some possible explanations are that different strains of rats were used and the amount of orally ingested As^{III} was likely variable between the two experiments. Overall, these studies showed that As undergoes extensive biliary excretion in rats and Mrp2 is a major player in this process.

In contrast with rats, our studies of As hepatobiliary transport using SCHH (Chapter 3) suggest that biliary excretion of As may be quite variable between humans. An unexplained difference in biliary excretion was observed in human hepatocytes as only five out of fourteen SCHH preparations transported As across the apical membrane. Based on the rat data this inter-human hepatocyte preparation variability was somewhat unexpected. These differences in biliary excretion could be explained by differences in Mrp2/MRP2

transport efficiencies between rats and some humans. It seemed plausible that maybe rat Mrp2 transported $As(GS)_3$ and $MMA(GS)_2$ with greater efficiency than (most) human MRP2 and is therefore, the dominant transport pathway in rats. Human MRP2 has been characterized as a high affinity transporter of both the seleno-bis(*S*-glutathionyl) arsinium ion $[(GS)_2AsSe]^-$ and $As(GS)_3$ with apparent K_m values of 1.7 μM and 4.2 μM, respectively. However, transport of DMA^V and $MMA(GS)_2$ by MRP2 has never been characterized. In addition, kinetic parameters for rat Mrp2 have not been determined and As hepatobiliary transport has not been determined in sandwich cultured rat hepatocytes (SCRH).

Studies in SCHH (Chapter 3) show that when biliary excretion of As occurred, it was completely GSH-dependent suggesting only GSH conjugates are transported across the canalicular surface. DMA^V does not form a GSH conjugate and determining if DMA^V is a substrate for MRP2 would provide some useful information. If DMA^V is not an MRP2 substrate or a poor substrate this could explain why GSH- independent biliary excretion of As is not observed. Furthermore, this would explain why basolateral transport pathways may prevail under conditions where DMA^V is extensively formed in the liver. The apparent affinity of human MRP2 for various arsenicals compared to the apparent affinity of rat Mrp2 may explain species specific differences in biliary excretion of As.

The results from a preliminary investigation of the species differences in As transport by Mrp2/MRP2 using plasma membrane vesicle transport assays and sandwich cultured rat hepatocytes (SCRH) are described below.

A1.2 Results and Discussion

A1.2.1 MRP2 transports $MMA(GS)_2$

To determine if $MMA(GS)_2$ is a substrate for human MRP2, ATP-dependent transport of $MMA(GS)_2$ by MRP2-enriched and vector control plasma membrane vesicles was measured. ATP-dependent transport of $MMA(GS)_2$ (10 μM) by MRP2 had an activity of 98 $pmol^{-1}$ mg^{-1} protein min^{-1} (Fig. A1-1A). To determine the linear range of $MMA(GS)_2$ (10 μM) uptake by MRP2, a time course was performed (Fig. A1-1B). Transport of $MMA(GS)_2$ by MRP2 was linear up to 1 min with maximal activity of 218 $pmol^{-1}$ mg^{-1} protein at 3 min (Fig. A1-1B). MRP2 transport of $MMA(GS)_2$ was further characterized by determining the initial rates of transport over several concentrations of $MMA(GS)_2$ (Fig. A1-1C). MRP2 transport of $MMA(GS)_2$ was not saturated at high (250 μM) concentrations of $MMA(GS)_2$, however, K_m and V_{max} values of 2759 μM and 17,296 $pmol^{-1}$ mg^{-1} protein min^{-1}, respectively, were estimated.

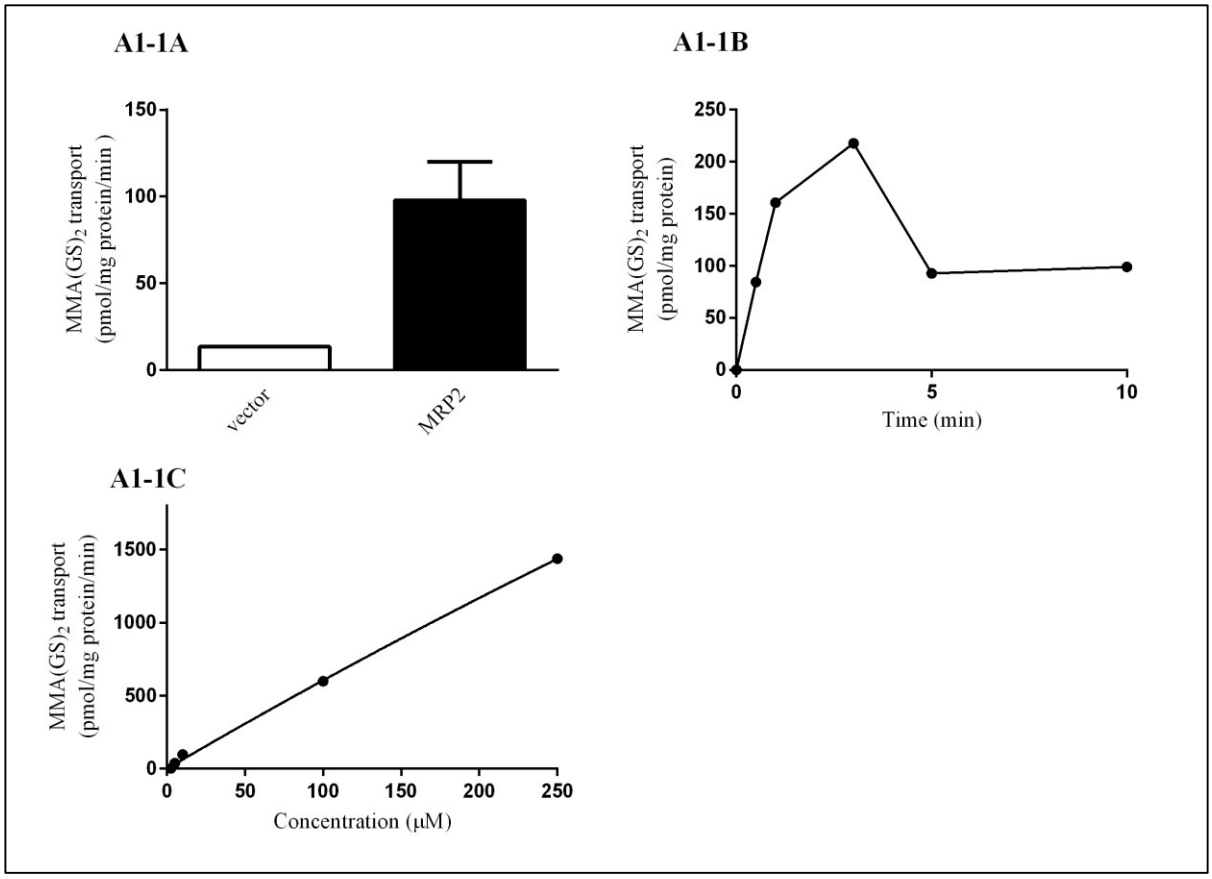

Fig. A1-1. ATP-dependent transport of $MMA(GS)_2$ by MRP2-enriched membrane vesicles.

Transport experiments were done with membrane vesicles (20 μg) prepared from HEK293T cells transiently transfected with pcDNA 3.1 (+) -MRP2 (closed bars or symbols) or empty pcDNA 3.1 (+) (open bars). (A) Vesicles were incubated for 3 minutes at 37°C in transport buffer with $MMA(GS)_2$ (10 μM). (B) Time course of ATP-dependent $MMA(GS)_2$ transport by MRP2 was determined by incubating MRP2-enriched membrane vesicles with $MMA(GS)_2$ (10 μM) in transport buffer at 37°C for the indicated time points. (C) MRP2-enriched membrane vesicles were incubated for 3 minutes at 37°C with increasing concentrations of $MMA(GS)_2$ (1-250 μM). Data were fit using a Michaelis-Menten kinetic model with GraphPad Prism 6. Bars and symbols represent the average of triplicate determinations from a single experiment except in (A) where the closed bar represents the mean (± S.D.) of three independent experiments.

A1.2.2 MRP2 does not transport DMA^V

To determine if DMA^V is a substrate for MRP2, ATP-dependent transport of DMA^V (10 μM) in MRP2-enriched and vector control plasma membrane vesicles was measured. Transport of DMA^V by MRP2 -enriched plasma membrane vesicles was not detected (i.e., it was similar to the AMP control) and was not different than transport of DMA^V by the empty vector control vesicles (Fig. A1-2).

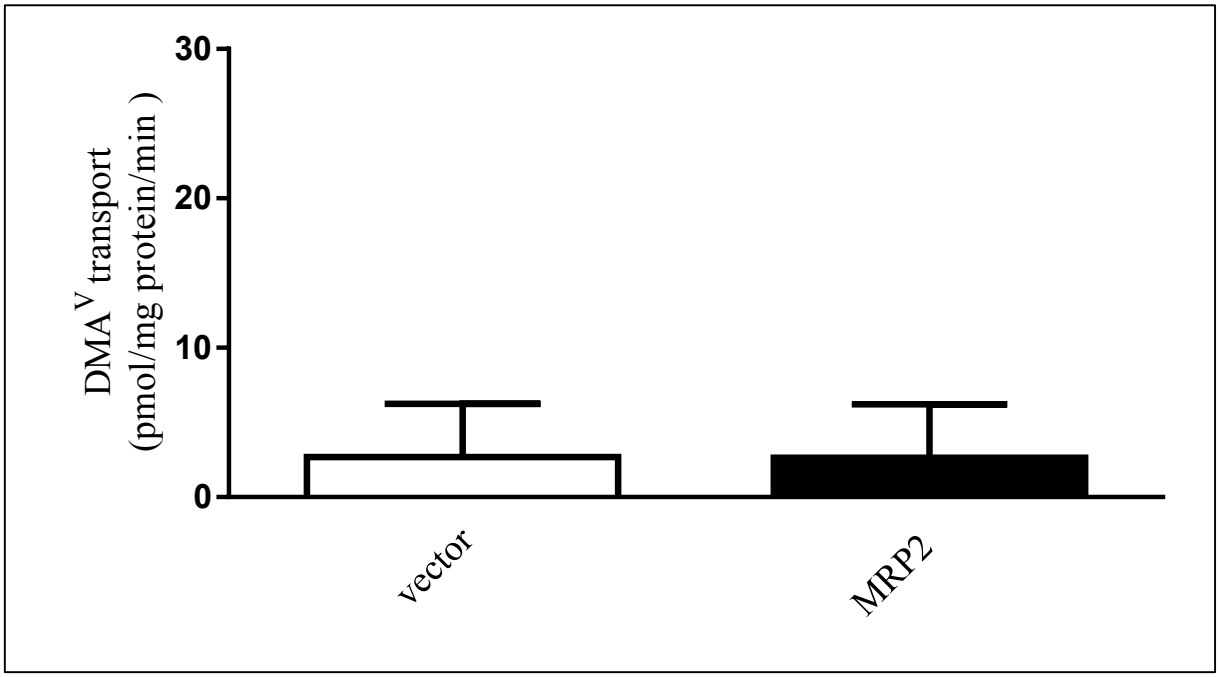

Fig. A1-2. ATP-dependent transport of DMA^V by MRP2-enriched membrane vesicles.

Transport experiments were done with membrane vesicles (20 μg) prepared from HEK293T cells transiently transfected with pcDNA 3.1 (+) -MRP2 (closed bars) or empty pcDNA 3.1 (+) (open bars). Vesicles were incubated for 3 minutes at 37°C in transport buffer with DMA^V (10 μM). Bars represent the average (± S.D.) of triplicate determinations from three independent experiments.

A1.2.3 Characterization of arsenic transport in SCRH and Mrp2-enriched plasma membrane vesicles

The *in vivo* hepatobiliary clearance of xenobiotics in humans and rats and the corresponding *in vitro* biliary clearance in SCH are highly correlated [67,68]. However, this relationship has never been tested for As. To determine if SCRH could model the extensive biliary excretion of As observed in intact Wistar and Sprague Dawley rats [107,197], pooled cryopreserved Wistar rat hepatocytes were cultured in a sandwich configuration and used in efflux experiments. SCRH were incubated with As^{III} (1 μM) and efflux was measured as described in the Materials and Methods (Section 2.2.2.6). Biliary excretion was observed in the SCRH with a calculated BEI of 43% (Fig. A1-3A). To test the functional activity of rat Mrp2 in plasma membrane vesicles, we incubated $^{73}As(GS)_3$ (1 μM, 100 nCi) with plasma membrane enriched vesicles prepared from vector, human MRP2, and rat Mrp2 transiently transfected HEK293T cells. There was no activity detectable in the vector control. The $As(GS)_3$ transport activity measured using human MRP2 and rat Mrp2-enriched membrane vesicles was 9 $pmol^{-1}$ mg^{-1} protein min^{-1} and 2 $pmol^{-1}$ mg^{-1} protein min^{-1}, respectively.

This preliminary data suggests that MRP2 is a very low affinity and high capacity transporter of $MMA(GS)_2$ (Fig. A1-1C). There are several experiments that must be performed in order to confirm that $MMA(GS)_2$ is a substrate for MRP2. First, kinetic characterization of $MMA(GS)_2$ transport should be repeated and at saturating concentrations in order to calculate more accurate apparent kinetic constants. Kinetic analysis of $MMA(GS)_2$ transport by vector membrane vesicles should also be performed to subtract

background $MMA(GS)_2$ transport. Lastly, osmotic sensitivity of transport should be tested to ensure that a true transport process is occurring for $MMA(GS)_2$ and not just binding.

Preliminary experiments suggest that DMA^V is not a substrate for MRP2. Future experiments should include a positive control such as MRP4-enriched membrane vesicles as well as tests for DMA^V transport in both the presence and absence of GSH. MRP2 transport of DMA^V might be GSH -dependent and this has not been tested yet.

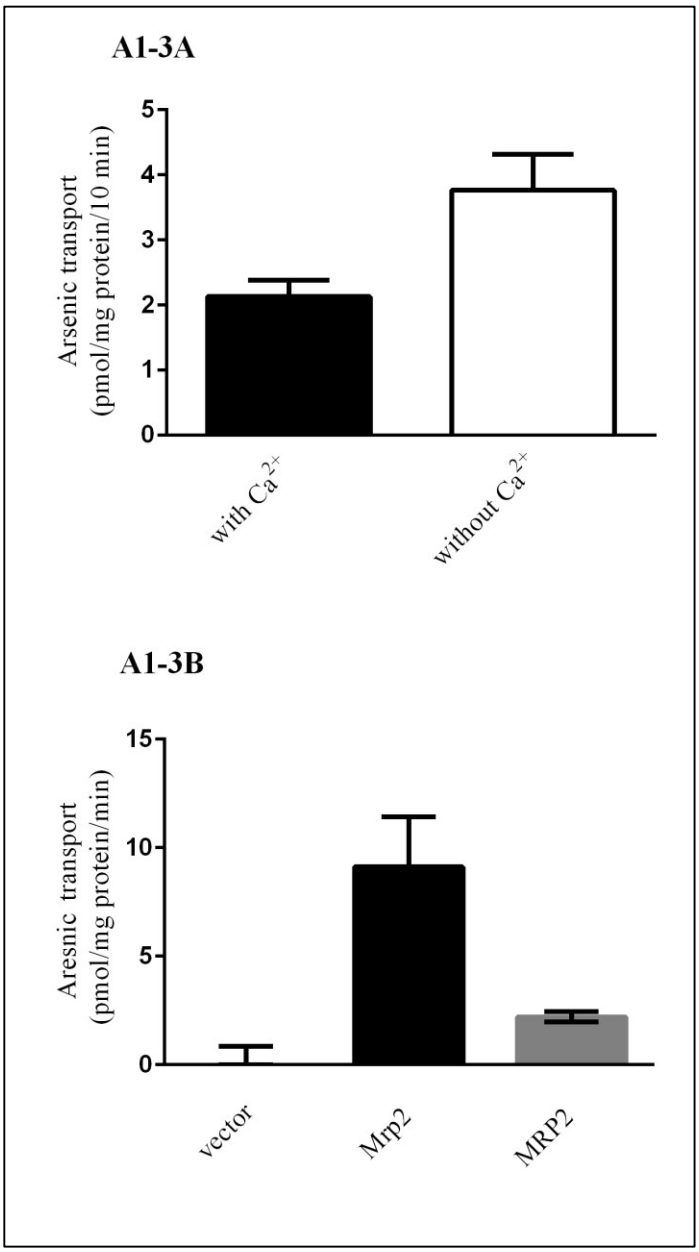

Fig. A1-3. Arsenic transport by SCRH and rat Mrp2-enriched membrane vesicles.

(A) SCRH were incubated with $^{73}As^{III}$ (1 μM, 100 nCi) for 24h; then incubation media was replaced with Ca^{2+}-containing (basolateral efflux, closed bars) or Ca^{2+}-free (basolateral + canalicular efflux, open bars) HBSS. Media was then sampled at a 10 min time point and total As efflux quantified by liquid scintillation counting. Bars represent the average of duplicate determinations in a single experiment. (B) ATP-dependent transport of $As(GS)_3$ was done with membrane vesicles (20 ug) prepared from HEK293T cells transiently transfected with empty pcDNA 3.1 (+) , pcDNA 3.1 (+) -rMrp2 or pcDNA 3.1 (+) -MRP2. Vesicles were incubated for 3 minutes at 37°C with 1 μM $^{73}As(GS)_3$. Bars represent the average (± S.D.) of triplicate determinations from a single experiment.

My studies described in Chapter 3 show that when biliary excretion is observed in SCHH, the biliary excretion is completely GSH-dependent. In contrast, DMA^V transport by the hepatic basolateral transporter MRP4 has been shown previously to be independent of GSH [82]. Thus, these preliminary experiments are consistent with the SCHH studies, however, further experiments must be done in order to form any meaningful conclusions regarding MRP2 transport of $MMA(GS)_2$ and DMA^V.

Arsenic transport was examined once in cryopreserved Wistar rat hepatocytes cultured in sandwich configuration. Biliary excretion was observed using this model, consistent with previously published studies using intact rats. Future experiments using this batch of cryopreserved rat hepatocytes will likely yield similar results. Future experiments should be performed under GSH-depleting conditions with BSO to determine if transport is fully GSH -dependent which would be expected because of the previously published data showing that rat Mrp2 is responsible for the biliary excretion of $As(GS)_3$ and $MMA(GS)_2$ [107].

A preliminary study using empty vector-, human MRP2-, or rat Mrp2-enriched membrane vesicles showed that human MRP2 and rat Mrp2 transport $As(GS)_3$. Studies must be repeated and normalized for protein expression in membrane vesicles. Future studies should also include characterizing kinetics of rat Mrp2 transport of other As metabolites including $MMA(GS)_2$ and DMA^V. Studies characterizing As transport in SCRH and membrane vesicles will provide useful information about the underlying mechanisms that account for species specific differences in susceptibility to As-induced toxicity and cancer. Furthermore, characterization of human MRP2 transport kinetics of $MMA(GS)_2$ and DMA^V will provide information that is useful to identify reasons for observing inter-individual

differences in the biliary excretion of As in SCHH. Subsequent identification of SNPs that alter transport kinetics of $MMA(GS)_2$ and DMA^V may also elucidate why we observed differences in hepatobiliary As efflux in the SCHH model and ultimately reasons for inter-individual susceptibility to As-induced toxicity and carcinogenesis.